MATHEMATISCH-NATURWISSENSCHAFTLICHE FAKULTÄT

INSTITUT FÜR BIOCHEMIE UND BIOLOGIE

DISSERTATION

zur Erlangung des akademischen Grades

doctor rerum naturalium

THE ROLES OF SECONDARY METABOLITES IN *MICROCYSTIS* INTER-STRAIN INTERACTIONS

vorgelegt von

A. Katharina Makower

Potsdam Golm, 02.02.2016

Published online at the
Institutional Repository of the University of Potsdam:
URN urn:nbn:de:kobv:517-opus4-93916
http://nbn-resolving.de/urn:nbn:de:kobv:517-opus4-93916

ABSTRACT

Among the bloom-forming and potentially harmful cyanobacteria, the genus *Microcystis* represents a most diverse taxon, on the genomic as well as on morphological and secondary metabolite levels. *Microcystis* communities are composed of a variety of diversified strains. The focus of this study lies on potential interactions between *Microcystis* representatives and the roles of secondary metabolites in these interaction processes.

The role of secondary metabolites functioning as signaling molecules in the investigated interactions is demonstrated exemplary for the prevalent hepatotoxin microcystin. The extracellular and intracellular roles of microcystin are tested in microarray-based transcriptomic approaches. While an extracellular effect of microcystin on *Microcystis* transcription is confirmed and connected to a specific gene cluster of another secondary metabolite in this study, the intracellularly occurring microcystin is related with several pathways of the primary metabolism. A clear correlation of a microcystin knockout and the SigE-mediated regulation of carbon metabolism is found. According to the acquired transcriptional data, a model is proposed that postulates the regulating effect of microcystin on transcriptional regulators such as the alternative sigma factor SigE, which in return captures an essential role in sugar catabolism and redox-state regulation.

For the purpose of simulating community conditions as found in the field, *Microcystis* colonies are isolated from the eutrophic

lakes near Potsdam, Germany and established as stably growing under laboratory conditions. In co-habitation simulations, the recently isolated field strain FS2 is shown to specifically induce nearly immediate aggregation reactions in the axenic lab strain *Microcystis aeruginosa* PCC 7806. In transcriptional studies via microarrays, the induced expression program in PCC 7806 after aggregation induction is shown to involve the reorganization of cell envelope structures, a highly altered nutrient uptake balance and the reorientation of the aggregating cells to a heterotrophic carbon utilization, e.g. via glycolysis. These transcriptional changes are discussed as mechanisms of niche adaptation and acclimation in order to prevent competition for resources.

ZUSAMMENFASSUNG

Die Gattung *Microcystis* stellt unter den blütenbildenden Cyanobakterien ein Taxon besonderer Diversität dar. Dies gilt sowohl für die Genomstruktur als auch für morphologische Charakteristika und Sekundärmetabolite. *Microcystis*-Communities weisen eine Zusammensetzung aus einer Vielzahl von diversifizierten Stämmen auf. Das Hauptaugenmerk dieser Arbeit lag darauf, potentielle Wechselwirkungen zwischen *Microcystis*-Vertretern zu charakterisieren und die Rolle von Sekundärmetaboliten in Interaktions-Prozessen zu untersuchen.

Die Rolle von Sekundärmetaboliten als Signalstoffe in *Microcystis*-Interaktionen wurde exemplarisch für das Hepatotoxin Microcystin demonstriert. Sowohl die extrazelluläre als auch die intrazellulare Funktion von Microcystin wurde anhand von Microarray-basierten Transkriptomstudien getestet. Dabei konnte eine extrazelluläre Wirkung von Microcystin bestätigt werden und mit der Transkription eines spezifischen anderen Sekundärmetaboliten in Verbindung gebracht werden. Intrazellulär vorkommendes Microcystin wurde hingegen mit verschiedenen Stoffwechselwegen des Primärstoffwechsels verknüpft. Es konnte ein deutlicher Zusammenhang zwischen einem Microcystin-Knockout und der SigE-vermittelten Regulation des Kohlenstoffmetabolismus festgestellt werden. Anhand der erworbenen Transkriptionsdaten wurde ein Modell vorgeschlagen, das eine regulierende Wirkung von Microcystin auf Transkriptionsfaktoren wie den alternativen Sigmafaktor

SigE postuliert, welcher seinerseits eine zentrale Rolle in Zuckerabbauprozessen und zellulärer Redoxregulation einnimmt.

Mit dem Ziel, Community-ähnliche Bedingungen zu simulieren, wurden *Microcystis*-Freiland-Kolonien aus eutrophen Gewässern in der Umgebung von Potsdam isoliert und ein stabiles Wachstum unter Laborbedingungen etabliert. Es konnte gezeigt werden, dass der frisch isolierte Freilandstamm FS2 spezifisch eine starke Zellaggregation in *Microcystis aeruginosa* PCC 7806 (einem axenischen Labortstamm) auslösen konnte. In Transkriptionsstudien mit Hilfe von Microarrays wurden Expressionsprogramme gefunden, die sowohl einen Umbau von Zellhüllstrukturen, als auch einen stark veränderten transmembranen Nährstofftransport beinhalteten. Darüber hinaus konnte in den aggregierenden PCC 7806-Zellen eine Verlagerung zu heterotrophen Kohlenstoffabbauprozessen wie der Glykolyse gefunden werden. Die transkriptionellen Veränderungen wurden als Akklimationsmechanismen zur Positionierung in ökologische Nischen diskutiert, um Konkurrenzen um Ressourcen zu vermeiden.

DECLARATION

This dissertation is the result of my own work. I assure I did not use any other resources that the ones identified or referenced.

A. Katharina Makower

2016, University of Potsdam, Germany

ABBREVIATIONS

Abbreviation	Denotation
ABC-transporters	ATP binding cassette transporters
AHL	N-acetyl-homeserine-lactone
ATP	Adenosine triphosphate
CAM	Crassulacean acid metabolism
CAS	Chrome Azurol S
CBB	Calvin-Benson-Bassham cycle
CCM	Carbon concentrating mechanism
cDNA	Complementary deoxyribonucleic acid
CHCA	α-cyano-4-hydroxycinnamic acid
COG	Cluster of Orthologous Groups
COG	Cluster of orthologous groups
CTAB	Cetyl trimethylammonium bromide
DHB	2,5-dihydroxybenzoic acid
dUTP	Deoxyuridine Tripphosphate
EPS	Extracellular polysaccharides
IPF	Individual protein file (term for gene/protein)
MC	Microcystin
MDS	Multidimensional scaling
NA	No information available
NADPH	Nicotinamide adenine dinucleotide phosphate
NIES	National Institute for Environmental Studies
NRPS	Nonribosomal peptide synthetase
OD	Optical density
OMV	Outer membrane vesicle
OUT	Operational taxonomic unit
PCC	Pasteur Culture Collection of Cyanobacteria
PCR	Polymerase chain reaction
PHA	Polyhydroxyalkanoate
PKS	Polyketide synthase
QS	Quorum sensing
Rpm	Rotations per minute
RubisCO	Ribulose-1,5-bisphosphate carboxylase/oxygenase
TCA	Tricarboxylic acid cycle

CONTENTS

1 Introduction

1.1 Relevance of Cyanobacteria in Global Patterns

As some of the oldest organisms in the earth's history cyanobacteria capture a vital role in geoecological equilibrium processes. Since the first occurrence of cyanobacteria over 2.7 billion years ago (Brocks, *et al.*, 1999; Rasmussen, *et al.*, 2008), these prokaryotic phototrophs have undergone an extensive period of evolutionary adaptation, coping with partly harsh environmental conditions and in turn shaping the face of the earth. The most critical example of this being the creation of an oxygenic atmosphere through O_2-accumulation emerging as byproduct from oxygenic photosynthesis (Berkner, *et al.*, 1965).

Beyond that, cyanobacteria account for considerable proportions of biomass in diverse ecosystems (Garcia-Pichel, *et al.*, 2003). In aquatic systems, where mass developments of single cyanobacterial representatives have been increasingly observed over recent decades (Carmichael, 2008), cyanobacteria influence nutrient cycles, as well as the ecological equilibrium and species composition (Paerl, 2014). Cyanobacterial toxin production, associated with so called cyanobacterial harmful algal blooms (CyanoHABs), poses a considerable threat to human and animal health. Ingestion of substantial doses of cyanobacterial toxins, for example through direct ingestion of contaminated drinking water resources potentially turns out fatal (Crush, *et al.*, 2008; Peuthert, *et al.*, 2007; Saqrane, *et al.*, 2009; Yoshida, *et al.*, 1997).

The ecological implications of mass cyanobacterial proliferation and the potential for toxin production have given rise to a series of comprehensive studies on bloom formation and correlated anthropogenic and natural impact factors (Paerl, *et al.*, 2013). While the role of abiotic factors such as high levels of nitrogen (N), phosphorous (P), high temperatures and light intensities where characterized as bloom-promoting in multiple studies (Elser, *et al.*, 2007; Foy,

et al., 1976; Robarts, *et al.*, 1987; Xu, *et al.*, 2010), evidence for the role of biotic factors is beginning to expand. Cyanobacterial blooms rarely represent a single cyanobacterial taxon (Woodhouse, *et al.*, 2015) and the production of signaling molecules and their role in inter-species interactions are only at the beginning to be understood (Briand, *et al.*, 2015; Kaplan, *et al.*, 2012). Understanding the interactions of co-occurring cyanobacteria in blooms and the involvement and interdependencies of cyanobacterial metabolites represents a novel strategy for advancing our understanding of the ecological success of cyanobacteria.

1.2 Cyanobacterial Diversity and Genomic & Ecological Plasticity

Over 2.7 billion years of evolution have enabled cyanobacteria to explore and adapt to almost any habitat on earth. Representatives of this diverse group of phototrophic gram negative bacteria can occur in aquatic as well as terrestrial habitats, from polar to tropical climatic regions, in acidic, saline and limnic waters and also in symbiotic life forms (Pankratova, *et al.*, 1969; Seckbach, 2007; Whitton, *et al.*, 2002), (Figure 1-1 a-c). Adaptations to harsh environmental conditions constitute a broad range of characteristics including protective cell envelope structures (Kehr, *et al.*, 2015), red-shift chlorophylls and other light harvesting pigments (Chen, *et al.*, 2010), UV-protective pigments (scytonemin, etc.) (Dillon, *et al.*, 2003), the production of secondary metabolites, and fine-tuned nutrient uptake systems (Sandrini, *et al.*, 2013). The morphological diversity of cyanobacteria is immense encompassing both, unicellular and multi-cellular filamentous forms (Figure 1-1 d, e). Additionally, differentiated motile (hormogonia) or dormant (akinetes) forms, floating colonies or sessile biofilms are frequently found in the field. Originally classified into five subsections, based on these gross morphological characteristics, phylogenetic analysis has since placed greater emphasis on sub-cellular characteristics (Giovannoni, *et al.*, 1988; Gugger, *et al.*, 2004).

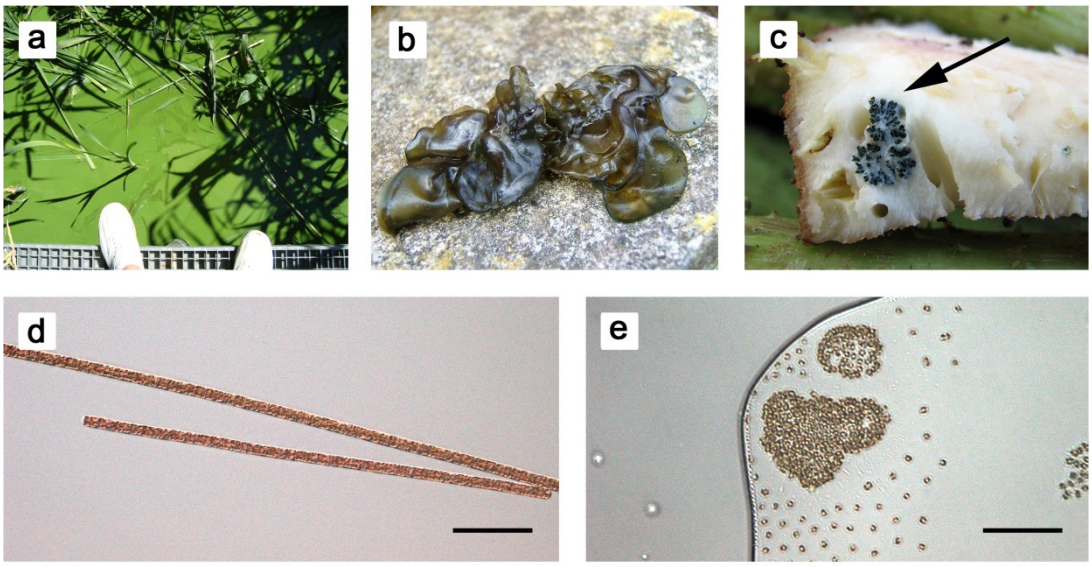

FIGURE 1-1: CYANOBACTERIAL DIVERSITY
a:*Microcystis* bloom in freshwater lake; **b**: cyanobacterium *Nostoc commune* occurring in terrestrial habitat; **c**: nitrogen fixing symbiotic *Nostoc* colonies (arrow) in the stem of the host plant *Gunnera*; **d**: micrograph of filamentous freshwater cyanobacterium *Planktothrix rubescens*, the typical reddish color originates from phycoerythrin, an additional photosynthesis pigment with an absorption maximum around 550 nm that is adapted for light absorption in deeper waters; **e**: micrograph of single cells and colonial shapes of *Microcystis*; scale bars: 100 µm; figures b and c obtained from web sources: http://www.aphotoflora.com/cyanobacteria_nostoc_commune_blue_green_algae.html (2015/09/17), http://www.srgc.org.uk/wisley/2007/061207/log.html (2015/09/17)

The genus *Microcystis*, which is phylogenetically well established within the order Chrooccocales, exemplifies how a strategy of diversification is deployed across many aspects of their life. The fact that *Microcystis* predominantly exhibits a seasonal life-style in freshwater ecosystems with largely fluctuating environmental conditions (light, temperature, oxygen) requires sophisticated acclimation and adaptation abilities. Most apparent is the expression of different morphospecies of *Microcystis* colonies that can vary in cell size, form, density and sheath characteristics (Figure 1-2). Even though clear distinctions between 21 morphotypes were defined (Komárek, 1998), the presence of transitional forms in the field raises questions as to what extent the formation of morphospecies results from genetic factors and/or from acclimation to environmental conditions (Otten, *et al.*, 2011).

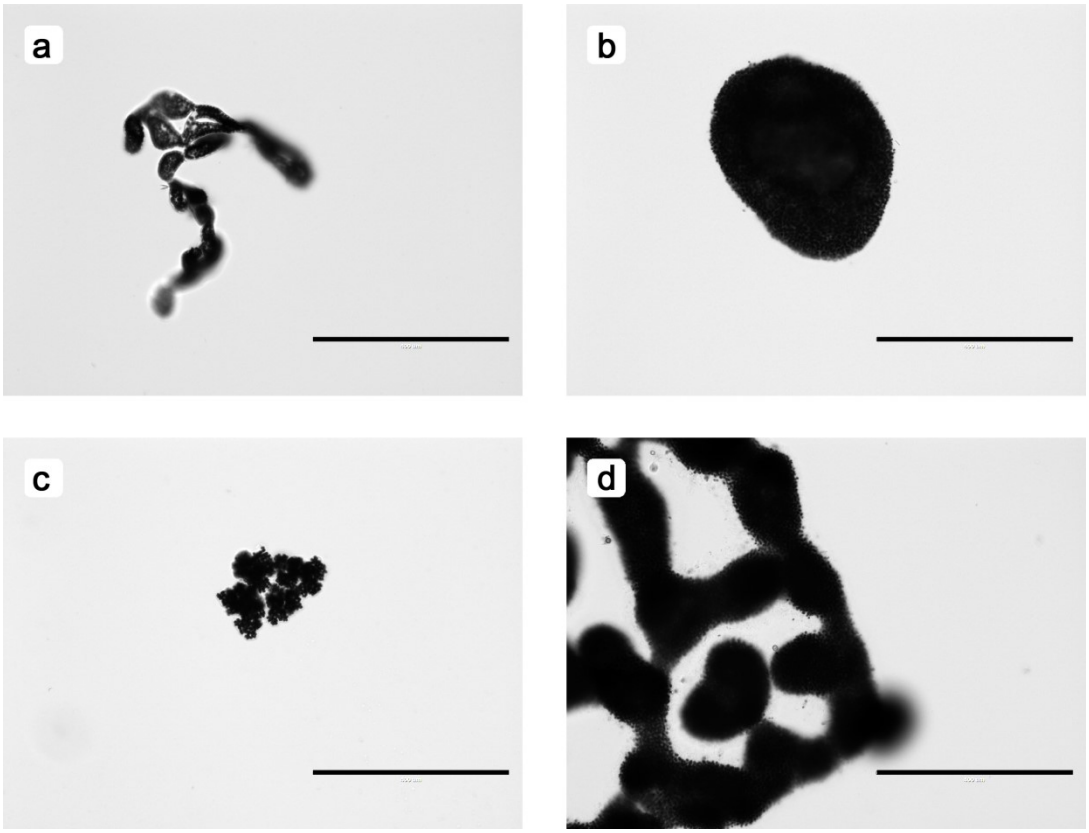

Figure 1-2: Selection of *Microcystis* Colonies Showing the Diversity of Morphotypes bright field micrographs of: **a:** *Microcystis wesenbergii* with typical coiled form and refractive mucilage margins, **b**: *Microcystis flos-aquae* showing solitary spheroidal, compact forms; **c**: *Microcystis viridis* with typical packet-like subcolonies, **d**: *Microcystis aeruginosa* lobate large compact colonies, scale bars: 400 µm

In addition to categorizing *Microcystis* by morphotype, there have also been attempts to classify *Microcystis* on the basis of the production of certain peptides (chemotypes). Despite this, attempts to equate either morphotypes or chemotypes with respective genotypes have been unsuccessful. (Otsuka, *et al.*, 2001; Welker, *et al.*, 2004). In fact, genome wide analyses of *Microcystis* strains revealed a high plasticity in genome organization arising as a consequence of horizontal gene transfer and intra-genomic recombination (Frangeul, *et al.*, 2008; Guljamow, *et al.*, 2007). As a result of the genome reorganization and the acquisition of new genes and gene clusters, *Microcystis* genomes have been shown to exhibit a very low synteny.

The comparison of genome data from 12 *Microcystis* strains was used to classify essential genes (found in all of the 12 sequenced *Microcystis* strains, such as certain genes from energy metabolism) into the "core genome". While the core represents ~2,500 genes (~50% of the genome) the remaining variable and strain specific genes are integrated in a large and open pan-genome numbered greater than 12,000 genes. In contrast to the core, the flexible genes include larger fractions of genes for DNA -replication, -modification and -repair (e.g. transposases, restriction enzymes, etc.), secondary metabolites as well as genes with predicted and unknown functions. The plasticity in the *Microcystis* genome is higher than in other cyanobacterial genomes and is facilitated by a huge number of transposases that are capable of mobilizing genomic regions and inevitably have led to a high percentage of large repeat sequences throughout the genome (Frangeul, *et al.*, 2008; Humbert, *et al.*, 2013). Even though, it prevented any attribution of phylogenetic *Microcystis* subclades to geographic regions, this plasticity and constant reorganization of the *Microcystis* genome has provided the genus with the means for diversification and niche adaptation and thus potentially for interactions between different genotypes.

1.3 Variable Aspects of Carbon Acquisition in *Microcystis*

A well-established example for variety in *Microcystis* genomes was found regarding the means of carbon acquisition. Recent genome comparisons revealed differences in inorganic carbon (C_i)-uptake systems among *Microcystis* strains (Sandrini, *et al.*, 2013). In principle, there are two CO_2-uptake systems and three HCO_3^--uptake systems found in *Microcystis* with different substrate affinities (Table 1-1) (Omata, *et al.*, 1999; Price, *et al.*, 2011; Price, *et al.*, 2004; Shibata, *et al.*, 2002; Shibata, *et al.*, 2001).

TABLE 1-1: SUMMARY OF C_i-UPTAKE SYSTEMS IN *MICROCYSTIS*

C_i-uptake system	Energetic drive	Substrate affinity	Flux rate	Remarks
NDH-1_3	NADPH	high (CO_2)	NA	converts passively diffused CO_2 into HCO_3^-
NDH-1_4	NADPH	low (CO_2)	NA	converts passively diffused CO_2 into HCO_3^-
BCT1	ATP	medium (HCO_3^-)	low	composed of subunits cmpABCD
BicA	Na-symport	low (HCO_3^-)	high	
SbtA	Na-symport	high (HCO_3^-)	low	in a dicistronic operon with sbtB (designated for periplasm)

Genomic analyses showed on the one hand that *Microcystis* genomes can be equipped with all of the aforementioned transporters or with just a selection including non-functional genes/ gene fragments of *bicA*. The synteny of the according genomic regions however, shows a stable pattern that always includes the flanking genes of the regulator *ccmR2* and the sodium/ proton antiporter *nhaS3* to the Na-dependent HCO_3^--transporter genes *bicA* and *sbtA/B* (Sandrini, *et al.*, 2013). It was speculated that the equipment with HCO_3^--importers of different affinities represents adaptations to varying CO_2-levels and partly characterizes different carbon uptake related ecotypes.

Efficient carbon uptake represents the first part in the phototrophic carbon concentrating mechanism (CCM), which is represented by adaptive measures to compartmentalize the bottleneck reaction of RubisCO-driven CO_2-fixation into a CO_2-elevated and O_2-reduced environment. In cyanobacteria the CCM includes compartment formation of polyhedral proteinaceous structures called carboxysomes, inorganic carbon uptake into the cells against concentration gradients, utilization of carbon in the form of bicarbonate HCO_3^- and conversion into CO_2 by carbonic anhydrases, and the exclusion of O_2 from RubisCO reaction sites (reviewed in (Burnap, *et al.*, 2015)).

In addition to the assortment of C_i-uptake systems and the CCM, *Microcystis* strains are furnished with gas vesicles as extra means to alter its depth in the water column by which a changing supply with CO_2 can be provided (Thomas, *et al.*, 1985; Walsby, 1972). This is accomplished by an accumulation of ballast carbohydrates to sink into deeper positions after saturation with light and CO_2 even to the point of light stress. On the other hand, increased buoyancy is achieved after metabolizing carbohydrate reserves, thus decreasing ballast and supplying gas fillings of CO_2 for the vesicles. This vertical migration was observed to occur in periodical rhythms to reach favorable light and CO_2 conditions either on the water surface or in deeper layers (Rabouille, *et al.*, 2003; Visser, *et al.*, 1997).

1.4 Variations in *Microcystis* Cell Envelope Components

Microcystis diversity was shown among other aspects, to manifest in the formation of different morphotypes (Figure 1-2, page 4). Extensive differences in these morphological shapes and sheath characteristics of *Microcystis* suggested an extensive variety in envelope structures, including proteinaceous, lipopolysaccharide and extracellular polysaccharide (EPS) components.

The high variety in EPS in different *Microcystis* strains was described from microscopic studies and is reflected in the genomic diversity of EPS biogenesis genes among these *Microcystis* strains as well (Karlsson, *et al.*, 1983; Kehr, *et al.*, 2015; Kessel, *et al.*, 1975). The specificity that can be accomplished through a diversity of monosaccharide components in polysaccharides, as well as bond positon, branching options, and modifications with chemical functional groups, is higher than in biological encoding of information by DNA or proteins (Werz, *et al.*, 2007).

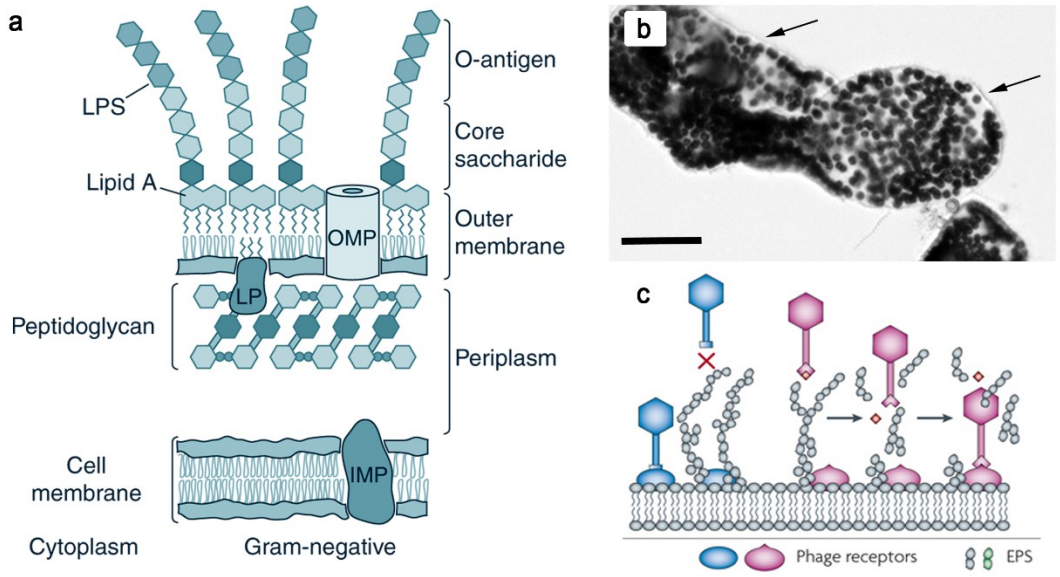

FIGURE 1-3: THE GRAM NEGATIVE *MICROCYSTIS* CELL ENVELOPE

a: principal structure of the gram negative cell envelope adapted from (Silhavy, *et al.*, 2010); an inner and an outer lipid bilayer membrane enclose the aqueous periplasm with peptidoglycan layer. Lipoproteins (LP) attach the peptidoglycan to the outer membrane. Outer and inner membrane proteins (OMPs, IMPs) and lipopolysaccharides (LPS) might facilitate cell-cell-interactions, **b:** micrograph of a *Microcystis wesenbergii* colony with the typical refractive margins of polysaccharide sheath (arrows), scale bar: 100 µm, **c:** phage interactions with cell surface structures adapted from (Labrie, *et al.*, 2010), polysaccharides can act to prevent infection through blocking binding to according receptors but can also be specifically bound.

Thus, versatile and highly specific interactions can occur via the binding between polysaccharide structures and proteins, and the involvement of EPS in intra- and interspecies interactions were documented for several processes, spanning defense against grazing predation through increased EPS production (Yang, *et al.*, 2008), the glycan mediated recognition of symbiosis partners, and the phage adhesion to bacterial host cells (Chaturongakul, *et al.*, 2014; Labrie, *et al.*, 2010).

The promoting effects of EPS on cell aggregation were also found by Xu (Xu, *et al.*, 2014) and correlated with the colonial life style of *Microcystis* morphotypes. Though many studies also tried to correlate specific morphotypes of *Microcystis* colonies with the production of typical cyanobacterial peptides, such as

microcystin (Fastner, *et al.*, 2001; Via-Ordorika, *et al.*, 2004), results were not hundred percent conclusive. Several studies however, showed that the hepatotoxic peptide microcystin can have an impact on the abundance of envelope proteins, which in turn can influence *Microcystis* cell aggregation patterns (Kehr, *et al.*, 2006; Zilliges, *et al.*, 2008). In correlation to an increased cell aggregation in cells with elevated expression of the O-glycosylated extracellular protein MrpC, an involvement of this non-essential protein in cell-cell-interactions and morphotype specification was suggested (Zilliges, *et al.*, 2008). Further evidence for protein-polysaccharide interactions in *Microcystis* cell envelopes with regard to microcystin production was found after the characterization of the lectin microvirin. This multivalent carbohydrate binding protein was shown to facilitate *Microcystis* cell aggregations, and its carbohydrate binding sites are believed to be responsible for this cross-linking between the polysaccharide structures of different *Microcystis* cells (Kehr, *et al.*, 2006).

These studies exemplify that the *Microcystis* envelope structures represent diversified reaction sites to the cell, encompassing varying protein and polysaccharide structures depending on the genomic facilities of the respective strain.

1.5 *Microcystis* Communities and Aspects of Communication

In contrast to *Microcystis* strains cultured under axenic conditions, in its natural environment *Microcystis* coexists with many other phototrophs (eukaryotes and prokaryotes) as well as with a variety of heterotrophic bacteria (Woodhouse, *et al.*, 2015). In fact, it has been proposed that the typical colonial morphology of *Microcystis* represents the community form of a floating biofilm (Zhai, *et al.*, 2012) with the characteristic assemblage of diverse organisms in a mucilaginous matrix analogous to the typical hydrogel matrix of a biofilm (Hall-

Stoodley, *et al.*, 2004). To heterotrophs the colonial polysaccharide sheath of *Microcystis* (see section 1.4) represents an attractive micro-environment presumably providing protection and supply with nutrients (Brunberg, 1999).

Since it was suspected that the heterotrophic community members might influence harmful bloom formation, more research has been focused on elucidating community structures as well as on interactions between the community-forming species. Several studies have reported competition between co-occurring bacteria with partly lethal effects such as lysing competitor cells (Harel, *et al.*, 2013; Ozaki, *et al.*, 2008). In contrast, other studies have uncovered tightly coupled population dynamics and mutually beneficial effects of the bacterial community life style (Parveen, *et al.*, 2013; Shen, *et al.*, 2011). Recent investigations comparing the community compositions of free-living versus *Microcystis*-attached heterotrophs and of different sampling sites from the Laurentian Lake Erie paint an interesting picture of principles underlying community organization. Taxonomic classification of community bacteria revealed a few very specific and individual interacting partners on the one hand and a variety of more generalist bacteria on the other. Furthermore, it could be deduced from deep sequencing data that irrespective of the contributing bacterial species the same functions of interacting partners were fulfilled in comparable communities by expression of the same genes (Parveen, *et al.*, 2013; Steffen, *et al.*, 2015). This stresses the point of dynamic community compositions with mutually benefitting roles of *Microcystis* and accompanied heterotrophs.

While a large share of the previous studies has concentrated on associated heterotrophic bacteria or interactions between two distinct species, like for instance between the green algae *Scenedesmus* and *Microcystis* (Harel, *et al.*, 2013) or between *Aphanizomenon* and *Microcystis* (Miller, *et al.*, 2013), recent studies on *Microcystis* specific interactions suggest multifaceted relations and emerging evidence for a role of secondary metabolites in them (Briand, *et al.*, 2015; Schatz, *et al.*, 2007). As pointed out before, within the *Microcystis* genome we find a huge potential for diversity, which may result for example from strain specific metabolic pathways, varying sets of transporters with different

affinities, or the strain specific equipment with secondary metabolites (Frangeul, *et al.*, 2008; Humbert, *et al.*, 2013). Interestingly, different *Microcystis* genotypes exhibit spatial and temporal patterns of co-occurrence with genomic diversity maintained over long periods of time. This level of diversity in the *Microcystis* community represents the basis for any possible interaction.

In terms of molecular communication, most attention has been paid to the broad variety of secondary metabolites in *Microcystis* as they are often found to be released from the cells providing a mechanism for how they might carry signals to surrounding organisms (Hudnell, *et al.*, 2008; Wiedner, *et al.*, 2003). Indeed, recent studies confirm that different *Microcystis* strains in co-cultivation (compartments separated by a membrane, thus sharing the same medium and released medium factors) can influence each other's growth rates, morphologies, and specifically the expression of secondary metabolites, partly by autoinduction processes (Briand, *et al.*, 2015; Gan, *et al.*, 2011; Schatz, *et al.*, 2007). Previous, co-cultivation experiments have demonstrated very strain specific effects and more general responses like enhanced production of extracellular polymeric substances (Shen, *et al.*, 2011).

The mechanism's underlying signal reception plus transduction are not yet known in detail and suggestions, that *Microcystis* uses some form of quorum sensing (QS) could not be fully confirmed, since typical QS signaling molecules (AHL-like molecules: N-acetyl-homoserine-lactones) were identified but the full signaling and subsequent processes of coordinated gene expression/ repression were not elucidated (Zhai, *et al.*, 2012). Although the evidence for specific interactions and communication pathways among *Microcystis* strains is accumulating, a comprehensive view on the organisms' reactions and affected cellular processes is missing to date.

1.6 Secondary Metabolites

Beyond the scope of sole survival and nutrition, organisms of all kingdoms of life have developed the production of compounds, which would equip them with evolutionary advantages. In general, these originally termed secondary metabolites were defined as small molecules that do not belong to the primary metabolisms and are not essential to the organism's development, reproduction and growth (Fraenkel, 1959). This notion has been reassessed with a stronger focus on the role as supportive means in primary and secondary metabolism to cope with challenging environmental conditions in the long run (Davies, 2013). The denomination of this group of compounds as *natural products* or *specialized metabolites* reflects the fields of interests in medical research and investigations of their mechanisms of action.

Secondary metabolites have long since been recognized as promising source of bioactive compounds with particular application in pharmaceuticals due to their versatile activities, among others as antibiotic, antifungal, antiviral, anticancer, or protease inhibitory agents. (Edelman*, et al.*, 2003; Ishida*, et al.*, 1997; Larsen*, et al.*, 1994; Neuhof*, et al.*, 2005; Shin*, et al.*, 1997)

Cyanobacteria have emerged as surprisingly resourceful with over 1,100 reported secondary metabolites from 39 genera. Of these 216 compounds alone are attributed to *Microcystis* strains. These numbers already imply a high diversity and indeed, the so far elucidated secondary metabolite structures include e.g., intricate multicyclic structures, highly modified peptides or alkaloids and terpenes (Dittmann*, et al.*, 2015). *Microcystis* was shown to mainly produce peptidic secondary metabolites, which were classified into six families (aeruginosins, anabaenopeptins, cyanobactins, cyanopeptolins, microgininins, and microviridins; (Welker*, et al.*, 2006)) primarily according to their structure.

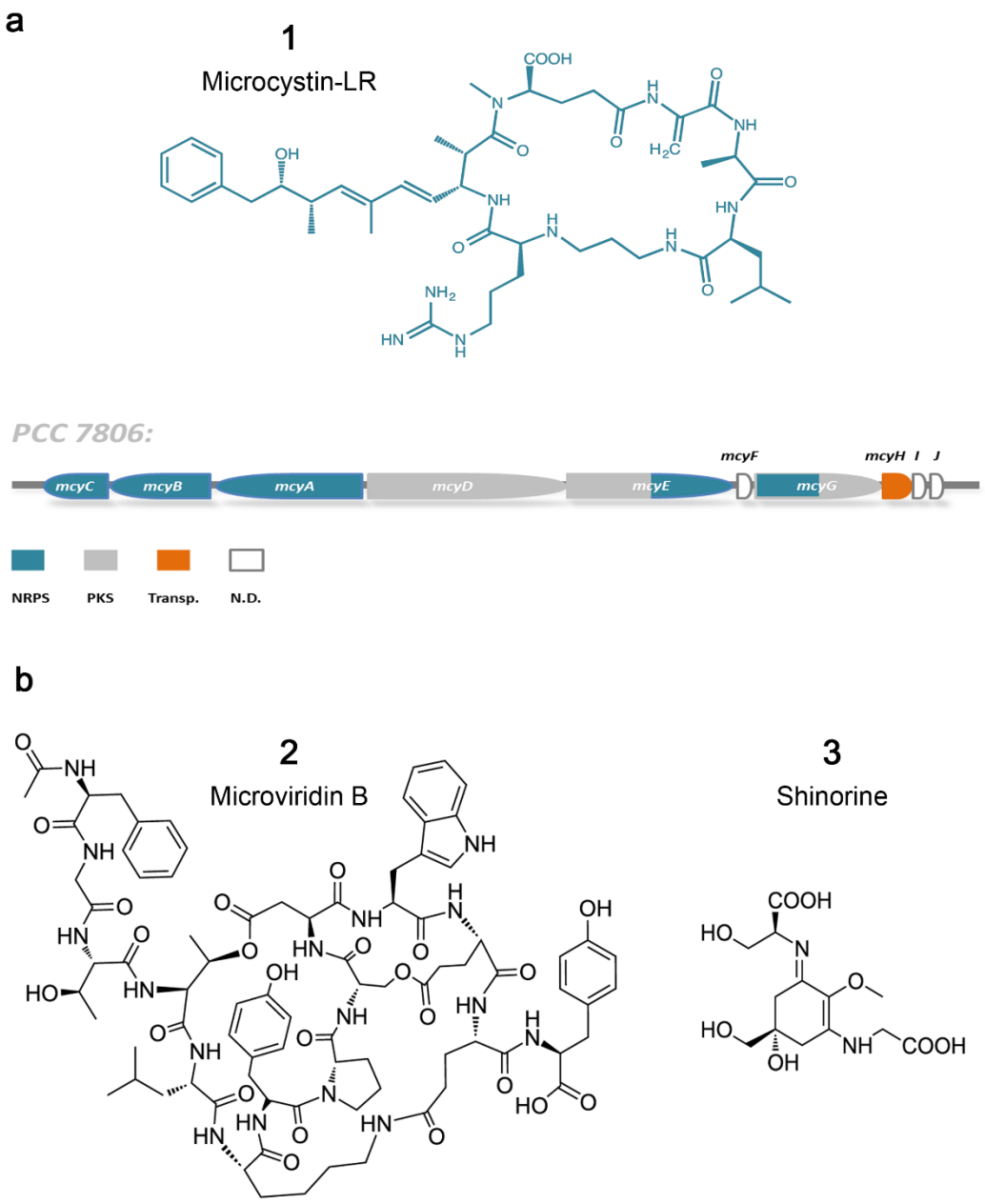

Figure 1-4: Secondary Metabolite Structures and Diversity

a: Structure of microcystin-LR **(1)**, produced by PCC 7806 is one of over 90 reported isoforms of microcystin; the biosynthesis cluster includes NRPS (blue) and PKS (grey) genes, as well as a transporter homologue (*mcyH*, orange) and undefined gene/protein types (white); **b:** examples for *Microcystis* secondary metabolites; **(2)** ribosomally produced tricyclic microviridin; **(3)** mycosporine-like amino acid shinorine

In addition, secondary metabolite peptides can be classified according to the mechanisms behind their biosynthesis. Predominantly they are categorized into two types of biosynthesis mechanism. This includes a non-ribosomal production of peptides (incorporation of proteinogenic and non-proteinogenic amino acids) and a second mechanism, which is considered ribosome-dependent with genomically encoded precursor peptides, that are restricted to the proteinogenic amino acids as building blocks (Kehr, *et al.*, 2011). Metabolites from ribosome-dependent peptide biosynthesis show a high diversity that derives from a multitude of post-translational modifications, including methylation, oxidation, heterocyclization, or prenylation (Sivonen, *et al.*, 2010). One of the larger and more complex structures is found in microviridin (**2**), a tricyclic depsipeptide featuring lactam and lactone rings (Ishitsuka, *et al.*, 1990)(Figure 1-4). Nonribosomal peptide synthesis on the other hand, introduces tremendous diversity to the produced peptides by admitting about 300 different amino acids as components and being combined with additional modifications, such as amino acid epimerization or tailoring enzymes (Grunewald, *et al.*, 2006). Furthermore, the synthesizing multi-domain enzymes designated nonribosomal peptide synthetases (NRPS) can cooperate with polyketide synthases (PKS) that utilize various carboxylic acids for incorporation into the particular secondary metabolite (Kehr, *et al.*, 2011). Another example that demonstrates diversity in structure and biosynthesis of cyanobacterial secondary metabolites is shinorine (**3**) an UV-light absorbing mycosporine-like amino acid (Figure 1-4).

Within the genomes of cyanobacteria and numerous other bacterial and fungal taxa the genes involved in the biosynthesis of secondary metabolites are organized in coherent gene clusters. Recent genome analyses and genome mining approaches describe that most cyanobacteria and *Microcystis* in particular dedicate approximately 4-5 % (2-9 gene clusters) of their genome to the encoding of secondary metabolite synthesis (Calteau, *et al.*, 2014; Humbert, *et al.*, 2013). Considering the extent to which recombination occurs within the genomes of *Microcystis* species (see section 1.2) in correlation with the nonessential character, secondary metabolite gene clusters are subject to a vivid

evolutionary progression and we find almost every *Microcystis* subspecies equipped with a unique combination of potentially very diverse secondary metabolites and according biosynthesis gene clusters.

The quest for the biological role of secondary metabolites has proven to be challenging and so far could place them in many different aspects of cyanobacterial physiology. Most studies were focused on the heptapeptidic microcystin (Figure 1-5) as its hepatotoxicity represents a considerable risk to human health in drinking water reservoirs with potentially lethal effects. Microcystin (MC) is produced among others by the cyanobacterial genera of *Microcystis*, *Planktothrix*, and *Anabaena* by an NRPS/PKS hybrid system, which is encoded in the ~ 54.6 kb spanning *mcy* gene cluster (Dittmann, *et al.*, 1997; Tillett, *et al.*, 2000).

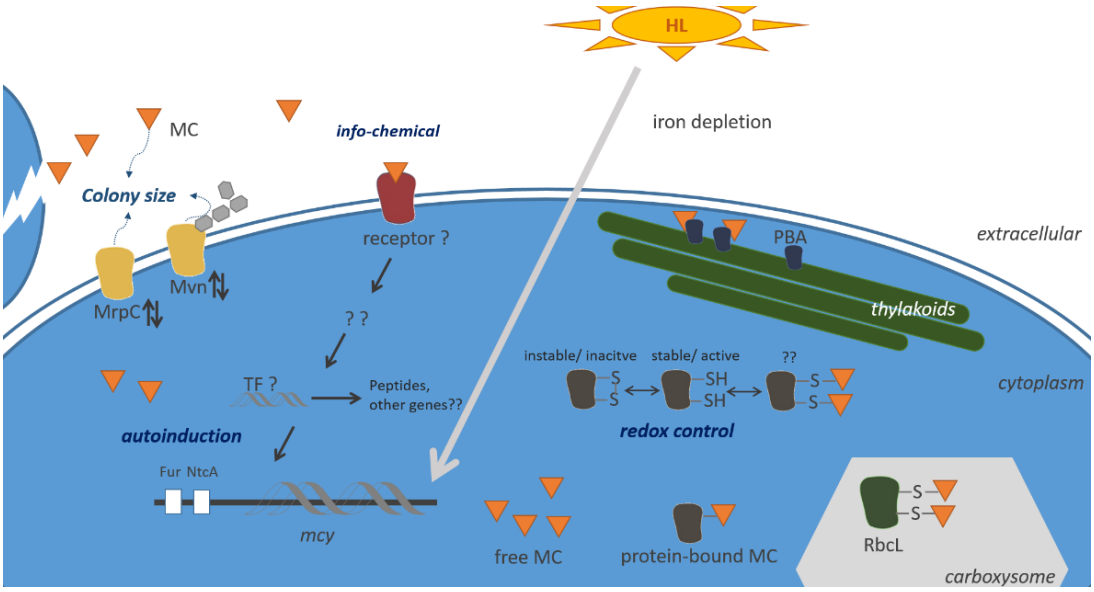

Figure 1-5: Model for Diverse Roles of Microcystin in *Microcystis aeruginosa*, adapted from (Neilan, *et al.*, 2012)

MC biosynthesis: up-regulated under high light (HL) and iron deficiency. Two transcriptional regulators (NtcA, Fur) bind to the bidirectional promoter region of the mcy operon. Release of MC from lysing cells may act as info-chemical (e.g., leading to an autoinduction of MC biosynthesis, receptor not known yet, regulatory cascade and transcription factors (TF) not known yet). The abundance of the lectin MVN and the glycoprotein MrpC in dependency of MC influence cell aggregations/colony size. Intracellular MC either free or protein-bound, e.g. to large RubisCO subunit RbcL and phycobilisome antennas (PBA). Redox control via covalent binding to cysteines, thus regulating stable and instable protein forms.

Targeted sequencing of the ten *mcy* genes (*mcyA-J,* see Figure 1-4) provided the basis for transcriptional and related expression and functional studies of microcystin. The presence of DNA binding motifs for the ferric iron uptake transcriptional regulator FurA and the global nitrogen regulator NtcA in the promoter region of the *mcy* cluster resulted in many studies examining the role of microcystin production in responding to changes in the availability of nutrients, including Fe and N. Studies on nutrient dependent microcystin production as well as circadian studies however provided conflicting outcomes (Harke, *et al.*, 2013; Penn, *et al.*, 2014; Sevilla, *et al.*, 2010; Straub, *et al.*, 2011). Promising leads to its biological function emerged after showing that microcystin was involved in protein protection through covalent binding to RubisCO after high light stress and might also play a role in oxidative stress responses (Zilliges, *et al.*, 2011). The presumption that microcystin might directly or indirectly affect CO_2-fixation was reinforced by competition experiments of microcystin producing and nonproducing strains, which uncovered growth advantages of toxic strains under CO_2-limited conditions (Van de Waal, *et al.*, 2011). While these cues to the microcystin function concern intracellular processes, the frequently detected amounts of microcystin in the surrounding extracellular medium point towards a potential role as extracellular signal. Studies examining the extracellular functions of secondary metabolites show influences on the production of a whole network of metabolites (Briand, *et al.*, 2015; Schatz, *et al.*, 2007). Other studies have proposed a signaling function of the toxin cylindrospermopsin that would induce the production and excretion of alkaline phosphatase in other phytoplankton species and thus increase phosphate levels under limited conditions (Bar-Yosef, *et al.*, 2010; Kaplan, *et al.*, 2012). The mechanisms behind intra- and extracellular secondary metabolite effects are only beginning to be explored and comprehensive insights concerning which aspects of cyanobacterial physiology and affected metabolite patterns are missing to date.

1.7 Aims of This Study

Recent genome sequencing projects of several *Microcystis* strains have attributed approximately 50 % of the genome to flexible and strain specific genes. The genomic and morphological diversity of this cyanobacterial genus has been known for decades. The co-occurrence and annual persistence of diverse strains within the same habitat has provoked the question, if and to what outcome diverse *Microcystis* strains can interact. The characterization of inter-strain interactions among the *Microcystis* genus is intended to obtain a deeper understanding of the ecological and physiological principles of the potentially harmful and mass proliferating cyanobacterium. In this respect, it shall be focused on the role of *Microcystis*-derived info-chemicals as interaction mediators. In particular, comprehensive comparative transcriptomic studies are intended to correlate the intra- and extracellular role of the toxic secondary metabolite microcystin to metabolic processes. The experimental design to answer these questions includes the simulated co-habitation of *Microcystis* field strains and axenic lab strains with subsequent transcriptomic and physiological investigations (displayed below, section 2.1).

2 Materials and Methods

2.1 Experimental Design

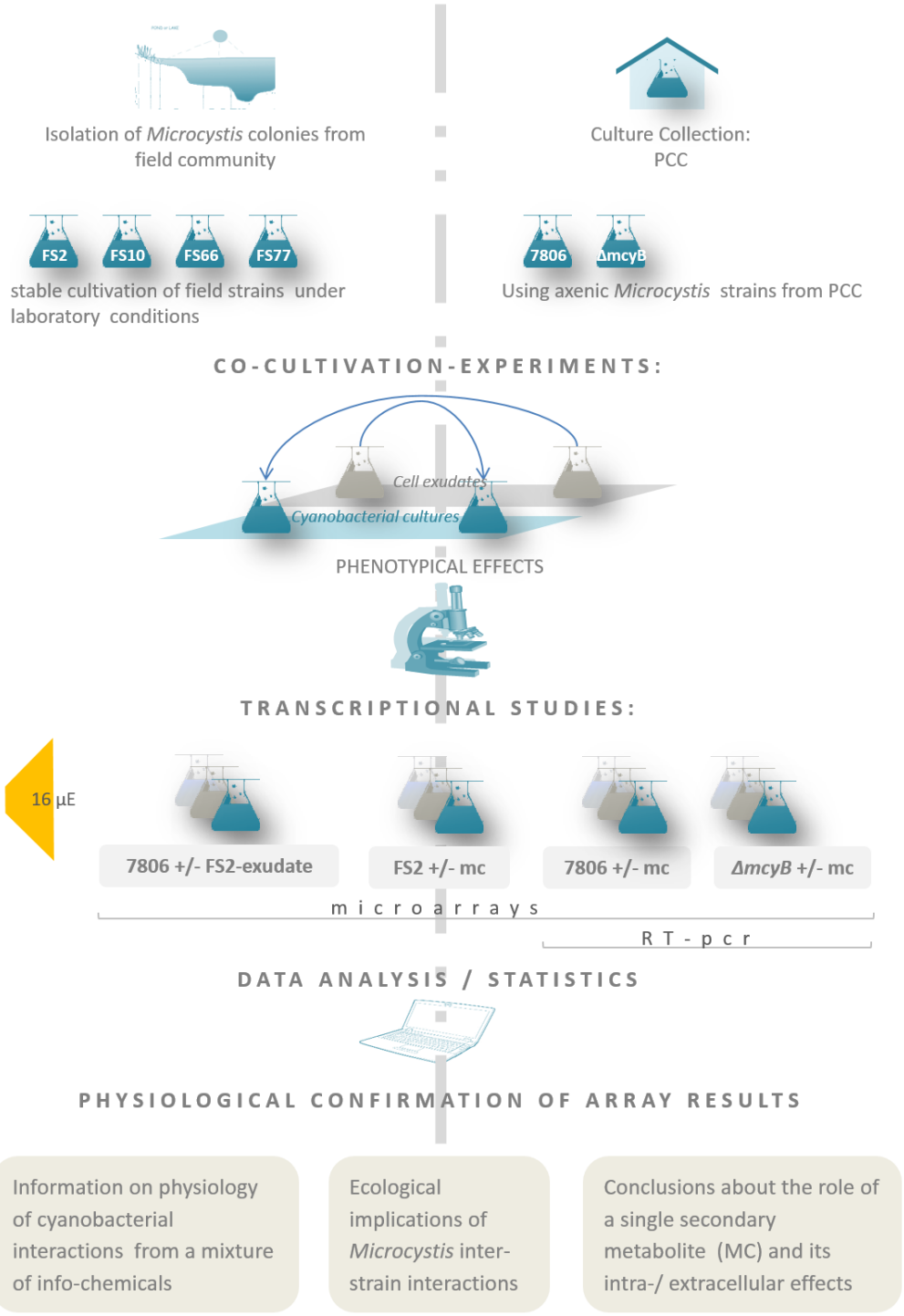

Figure 2-1: Experimental Design and Workflow

2.2 Materials

2.2.1 Biological Materials

Table 2-1: Biological Materials

Bacterial Strain	Source
Axenic cyanobacterial strains:	
Microcystis aeruginosa PCC 7806	Institute Pasteur, France
Microcystis aeruginosa ΔmcyB	Institute Pasteur, France
Microcystis aeruginosa PCC7005	Institute Pasteur, France
Microcystis aeruginosa NIES 843	National Institute for Environmental Studies, Tsukuba, Japan
Recently isolated cyanobacterial field strains:	
Microcystis spec. FS2	Lake Zernsee, Potsdam, Germany
Microcystis botrys FS10	Lake Zernsee, Potsdam, Germany
Microcystis spec. FS66	Lake Wannsee, Potsdam, Germany
Microcystis aeruginosa FS77	Lake Wannsee, Potsdam, Germany

2.2.2 Primers

Table 2-2: Primers Used in this Study

Name	Original organism	5'-3'-sequence	T_m	Application
RT-mcyA-fw	PCC 7806	tgggttgatagggtgccaat	59	RT-qPCR
RT-mcyA-rv	PCC 7806	cctcaatctcagcaagggga	59	RT-qPCR
RT-aerJ-fw	PCC 7806	caacggttgattctcccact	58	RT-qPCR
RT-aerJ-rv	PCC 7806	atttgtggcggtggattagc	59	RT-qPCR
RT-mcnB-fw	PCC 7806	tttgccgctacagatgcttg	59	RT-qPCR
RT-mcnB-rv	PCC 7806	taggggacaactaccaagcg	59	RT-qPCR
RT-IPF47-fw	PCC 7806	aaactgccggtcaaaatccc	59	RT-qPCR
RT-IPF47-rv	PCC 7806	gccgctcaaaattgctttcc	59	RT-qPCR

RT-mcaE-fw	PCC 7806	gccacttagctgaactctctg	59	RT-qPCR
RT-mcyA-rv	PCC 7806	cgaaagcgcagatactaacagt	59	RT-qPCR
RT-rnpB-fw	PCC 7806	ggggtaagggtgcaaaggt	60	RT-qPCR
RT-rnpB-rv	PCC 7806	agaccaacctttgtccctcc	59	RT-qPCR
P1: bic-clust-fw	PCC 7806	tccaggtttagctcttgggg	59	PCR/ sequencing
P4: bic-clust-rv	PCC 7806	accgatactggttgctgtca	59	PCR/ sequencing
P3: sbtA-fw	NIES 843	aggggaggcttaaggaggta	59	PCR/ sequencing
P2: sbtA-rv	NIES 843	gtcggaactagaggaagcga	59	PCR/ sequencing
P5: bic-clust-fw2	FS2	cagctgccatcgtttctctc	59	sequencing
P6: bic-clust-rv2	FS2	ccgattttggtcagcagcat	59	sequencing
P7: SbtA-fw2	FS2	ggcggataatcgggtcaaga	59	sequencing
515F_01	prokaryote	acgta-gt-gtgccagcmgccgcggtaa		Illumina
806R_01	prokaryote	acgta-cc-ggactachvgggtwtctaat		Illumina
FWmicroginin	PCC 9432	cgttggttacaggccctttct	60	PCR
RVmicroginin	PCC 9432	ccgacctgtgataaacaattc	60	PCR
FW-AGD	NIES98	GGATCCatgactaacaacatctctact	50	PCR
RV-AGD	NIES98	CTGCAG-G-ctattttccaaagcgacgct	50	PCR
FW-anabaenopeptin	PCC 9432	agtgcctacgttcccattga	59	PCR
RV-anabaenopeptin	PCC 9432	tttgctcagtatccagggca	59	PCR
FW-microviridinA	NIES298	GGATCC-G-atggcatatcccaacgatca	50	PCR
RV-microviridinA	NIES298	GAATTC-ttaatactcttcccagtcagaagg	50	PCR

2.2.3 Chemicals

Substance	Provider
Acetic acid	Carl Roth, Karlsruhe, Germany
Agarose LE	Biozym Scientific, Oldendorf, Germany
Bacto™ Agar	Becton-Dickson, Sparks, MD, USA
Boric acid	Carl Roth, Karlsruhe, Germany
Bromophenol blue	Carl Roth, Karlsruhe, Germany
Calcium chloride x2H_2O	Serva, Heidelberg, Germany
Cetyl trimethylammonium bromide	Carl Roth, Karlsruhe, Germany
Chloroform	Carl Roth, Karlsruhe, Germany
Chrome azurol S	Fluka, Buchs, Switzerland
Citric acid	Carl Roth, Karlsruhe, Germany
Cobalt(II) chloride	Carl Roth, Karlsruhe, Germany
Copper(II) sulphatex5H_2O	Sigma-Aldrich, Munich, Germany
Cycloheximide	Carl Roth, Karlsruhe, Germany
Dipotassium hydrogen phosphate x3H_2O	Carl Roth, Karlsruhe, Germany
Disodium carbonate	Carl Roth, Karlsruhe, Germany
EDTA disoidum salt	Carl Roth, Karlsruhe, Germany
Ethanol	Carl Roth, Karlsruhe, Germany
Ethidium bromide	Carl Roth, Karlsruhe, Germany
Ferric ammonium citrate	Fluka, Buchs, Switzerland
Ferric (III) chloride	Merck, Darmstadt, Germany
Ficoll	Carl Roth, Karlsruhe, Germany
Formaldehyde	Sigma-Aldrich, Munich, Germany
HCl	Carl Roth, Karlsruhe, Germany
Isopropanol	Carl Roth, Karlsruhe, Germany
Magnesium sulphate x7H_2O	Carl Roth, Karlsruhe, Germany
Manganes chloride x2H_2O	Carl Roth, Karlsruhe, Germany
MC-LR	Katrin Hinrichs University of Potsdam

Methanol, HPLC grade	Carl Roth, Karlsruhe, Germany
MOPS	Carl Roth, Karlsruhe, Germany
Phenole	Carl Roth, Karlsruhe, Germany
SDS	Carl Roth, Karlsruhe, Germany
Sodium acetate	Fluka, Buchs, Switzerland
Sodium molybdate x2H_2O	ICN Biomedicals, Aurora, Ohio, USA
Sodium nitrate	Carl Roth, Karlsruhe, Germany
Sucrose	Merck, Darmstadt, Germany
Tris	Carl Roth, Karlsruhe, Germany
Universal MALDI Matrix	Sigma Aldrich, Munich, Germany
Xylene cyanol	Carl Roth, Karlsruhe, Germany
Zinc sulphate H2O	Merck, Darmstadt, Germany

2.2.4 Enzymes, Markers, Kits

Item	**Provider**
Custom *Microcystis* PCC 7806 microarrays	Agilent Technologies Inc., Santa Clara, CA, USA
Cy3/5 dUTPs	Sigma Aldrich, Munich, Germany
E.Z.N.A. MicroElute cleanup kit	Omega Bio-tek, Norcross, GA, USA
Lysozyme from chicken egg white	Serva, Heidelberg, Germany
Maxima reverse transcriptase	Thermo Fisher Scientific Inc. Waltham, MA, USA
ProteinaseK	Thermo Fisher Scientific Inc. Waltham, MA, USA
Qiaquick PCR Purification Kit	Qiagen, Düsseldorf, Germany
Random hexamer primers	Thermo Fisher Scientific Inc. Waltham, MA, USA
RNA Gel Loading Dye	Thermo Fisher Scientific Inc. Waltham, MA, USA

RNase A/T1 mix	Thermo Fisher Scientific Inc. Waltham, MA, USA
RNeasy® Mini Kit 50	Qiagen, Düsseldorf, Germany
SensiMix SYBR Low-ROX kit	Bioline, Luckenwalde, Germany
Superscript II RT,	Life Technologies, Carlsbad, CA, USA
Taq DNA Polymerase	Qiagen, Düsseldorf, Germany
TRIzol	Thermo Fisher Scientific Inc. Waltham, MA, USA
TURBO DNase	Thermo Fisher Scientific Inc. Waltham, MA, USA

2.2.5 Miscellaneous

Item	**Provider**
Syringes 1, 5, 20, 30 mL Omnifix	B Braun, Melsungen, Germany
Sterile polypropylene tubes, 15 and 50 mL	Greiner Bio-One, Frickenhausen, Germany
Pipettes 0.01-2, 0.5-10, 2-20, 10-200, 100-1000 µL	PeqLab Biotechnology GmbH, Germany
Petri dishes 92 x 16 mm w/o	Sarstedt, Nümbrecht, Germany
Glass sample slides 76x26x1 mm	Carl Roth, Karlsruhe, Germany
Cover slips 40x25x0.13-0.16 mm	Carl Roth, Karlsruhe, Germany
Pipettor	BrandTech® Scientific INC., Essex, CT, USA
Polypropylene centrifuge tubes 15, 50 mL	Greiner Bio-One, Frickenhausen
Plastibrand® Cuvettes PS, 1.5-3 mL	Carl Roth, Karlsruhe, Germany
Rotiprotect® Nitril gloves	Carl Roth, Karlsruhe, Germany
PARAFilm "M" Distensible plastic sealing film	Pechiney Plastic Packaging, Chicago, Il, USA

Pipette tips, TipOne® 0.1-10, 1-200, 101-1250 µL natural tips	Starlab, Ahrensburg, Germany
Safe Lock Tubes Polypropylene reaction tubes, 500 µL, 1500 µL	Eppendorf AG, Hamburg, Germany Carl Roth, Karlsruhe, Germany
Serological Pipettes 2 mL, 10 mL, 25 mL, sterile	Greiner Bio-One, Frickenhausen
Syringe filter 4 mm, Acrodisc®, 0.45 µm nylon membrane	PALL Life Sciences, USA
Syringe filter Whatman®, 0.2 µm sterile	Whatman®, Maidstone, UK
Sep-Pak Plus C18 cartridge 55-105 µm	Waters GmbH, Eschborn, Germany

2.2.6 Technical Appliances

Item	**Provider**
Master TL-D 58W/865 (Lamps)	Philips, Eindhoven, Netherlands
KM-2-SWIP-VARIO Shaker	Edmund Buhler, Germany
DOS-10L Shaker	NeoLab, Migge, Heidelberg, Germany
Multicultivator MC1000	Photon Systems Instruments, Czech Republic
LI-193 Spherical Quantum Sensor	LI-COR Biosciences, Lincoln, NE, USA
LI-250A Light Meter	LI-COR Biosciences, Lincoln, NE, USA
PCE-PHD 1 mobile pH-meter	PCE Instruments, Meschede, Germany
Evos fl, Digital Inverted Microscope	AMG of Thermo Fisher Scientific Inc. Waltham, MA, USA
Stereomicroscope stemiDV4	Zeiss, Jena, Germany

Milli-Q Reference A+	Merck Millipore, Darmstadt, Germany
Haereus Pico 21 Microcentrifuge	Thermo Fisher Scientific Inc. Waltham, MA, USA
Perfect Spin 24R Microcentrifuge	PeqLab Biotechnology GmbH, Germany
200R 21 Microcentrifuge	Hettich, Tuttlingen, Germany
Heraeus Multifuge 1S-R	Thermo Fisher Scientific Inc. Waltham, MA, USA
Sigma 6-16K	Sartorius AG, Göttingen, Germany
Vortex Genie 2™, G560E	Scientific Industries, Bohemia N.Y., USA
IKAMAG®RET Magnetic stirrer	IKA GmbH & Co. Kg, Staufen, Germany
Variomag mono	Thermo Fisher Scientific Inc. Waltham, MA, USA
Stirring bars	Carl Roth, Karlsruhe, Germany
Thriller Thermo-shaker block	PeqLab Biotechnology GmbH, Germany
Heat block	PeqLab Biotechnology GmbH, Germany
Microwave NN-E209W	Panasonic, Osaka, Japan
Sartorius Basic Balance	Sartorius AG, Göttingen, Germany
Kern 572-37 Balance	Kern & Sohn GmbH, Balingen, Germany
FiveEasy™ FE 20 pH Meter	Mettler Toledo AG, Schwerzenbach, Switzerland
LE 409 pH electrode	Mettler Toledo AG, Schwerzenbach, Switzerland
UV-1800 Spectrophotometer	Shimadzu, Japan
SpeedVac Vacuum concentrator	Eppendorf, Hamburg, Germany

MZ 2C Vacuum Pump	Vacuubrand, Wertheim, Germany
PC 2004 Vario Vacuum Pump	Vacuubrand, Wertheim, Germany
NanoDrop 2000 Spectrophotometer	PeqLab Biotechnology GmbH, Germany
C1000™ ThermoCycler	Biorad, USA
Light Cycler C480	Roche, Basel, Switzerland
PowerPac Basic	Biorad, USA
Electrophoresis chambers, combs and accessories	PeqLab Biotechnology GmbH, Germany
ChemiDoc™ XRS+ Imager	BioRad, USA
2100 Bioanalyzer	Agilent Technologies Inc., Santa Clara, CA, USA
DNA microarray scanner G2565CA	Agilent Technologies Inc., Santa Clara, CA, USA
NimbleGen hybridization system 4	NimbleGen Roche Madison, WI, USA
MALDI LTQ Orbitrap mass spectrometer	

2.3 Methods

2.3.1 Cultivation of Cyanobacteria

Standard cultivation of cyanobacteria was arranged in semi continuous liquid cultures in 500 mL Erlenmeyer flasks provided with BG-11 medium (Rippka, *et al.*, 1979) and constant illumination of 16 µmol photons $* m^{-2} * s^{-1}$ (Philips Master TL-D 58W/865) at 25 °C.

During the course of this study nutrient deficient and replete modifications to the original BG-11 medium were used. In iron depleted medium ferric ammonium citrate was entirely omitted from BG-11. Residual iron from cultivation vessels was removed by acid washing with 10 % HCl thrice followed by thorough rinsing until pH tests turned out neutral.

A different supply of carbon sources in BG-11 was arranged. That included carbonate depleted medium and a tenfold increased carbon concentration. Due to the close coupling of Na^+/ HCO^- import into cyanobacterial cells, sodium sources were reduced in the C-depleted medium, as well (Table 2-3). These adapted media were applied in plate cultivation on 0.7 % agar /BG-11.

Table 2-3: Changes in Nutrient Supply for Carbon Source Adapted BG-11

Nutrient changed	BG-11 medium	CO_3 depleted BG-11	10 x CO_3 BG-11
Na_2CO_3	0.189 mM	0.0 mM	1.89 mM
$NaNO_3$	17.6 mM	17.6 mM KNO_3	176 mM

2.3.2 Isolation of Cyanobacterial Field Strains

Havel water bodies around Potsdam, Germany were chosen during mid-bloom event in August 2011 as sampling sites to isolate *Microcystis* colonies from the field, which exhibit the original colonial morphology. *Microcystis* colonies were isolated either via scoop sampling from the water surface or with the help of a plankton net from depths down to 2 m. The subsequent separation of single colonies from further biological material by stepwise dilution within BG-11 medium was followed by determining the colony's morphotype after (Komárek, 1998).

In order to establish stable laboratory cultures, *Microcystis* field strains were ensured to be uni-algal and free of contaminating eukaryotes by filtering and re-selection/separation of *Microcystis* colonies and additionally, by temporary addition of the eukaryote specific antibiotic cycloheximide to the cultivation medium to a final concentration of 100 mg/L.

2.3.3 Bioactivity Assays Of Extracellular Bacterial Compounds

Several compounds that accumulate in cyanobacterial growth medium during cultivation or during bloom formation in the field were tested for bioactivity and their respective effects on different *Microcystis* strains (Figure 2-1, page 18).

Two strategies for testing were applied. On the one hand, mixtures of undifferentiated bacterial compounds from spent media were tested. *Microcystis* strains (Table 2-1) were cultivated under standard conditions until late exponential growth phase (OD_{750}: 1.75) to allow for compound accumulation. Subsequently, cell exudates were acquired by centrifuging cultures (4,500 x g; 10 min) and removing residual cells from the obtained supernatant by filtration through 0.45 µm pore sized PVDF syringe filters. Cell-free *Microcystis* cell exudates were added promptly to other *Microcystis* strains

in equal volumes. In contrast to a compound mixture, the effects of extracellular microcystin as single metabolite were similarly tested. Microcystin-LR was added to PCC 7806 and *ΔmcyB* cultures to a final concentration of 50 ng/mL.

The cultivation setup for *Microcystis* cultures to be treated with cell exudates/ microcystin comprised independent biological triplicate cultivation of the respective strains under meticulously equal growth conditions. That was achieved by the cultivation in a multicultivator (16 µmol photons $* m^{-2} * s^{-1}$ constant illumination, 28 °C, light aeration) unto the exponential growth phase (OD_{750}: 0.75), when test substances (spent medium, microcystin) were applied. Phenotypical changes were examined macro- and microscopically during an incubation time of 1-120 h. The sampling of treated cell material for diverse analyses was performed as described in the respective sections. The described experimental setup was used for different downstream experiments, i.e. a time course experiment, determination of growth rates and transcriptional analyses in microarrays and RT-PCR.

2.3.4 Time Course of Bioactive Cell Exudate Effects

Recording of the effects of *Microcystis* cell exudates in a time dependent manner was performed using the above described cultivation set up and exudate preparation (2.3.3). Samples for image documentation of phenotypes, chlorophyll-a quantification, and recording of absorption spectra were taken each at 0; 0.5; 1; 2; 3; 4; 24; 48; and 96 hours.

2.3.5 Chlorophyll-a Quantification

Chlorophyll-a amounts were considered as measure for cell counts and chlorophyll-a differences for cyanobacterial growth, respectively. A primary methanol extraction was performed by centrifugation of 5 mL culture volume (4,500 x g; 10 min) and dissolving the resulting pellet in 90 % methanol. After pipette mixing and vortexing the cell material was allowed to extract in the dark overnight. Subsequently, the extracts were briefly centrifuged to pellet cellular debris. Spectrophotometric absorption measurements of the resulting supernatant at λ = 665 nm were used to calculate chlorophyll-a concentrations based on the Beer-Lambert law (Beer, 1852) considering an absorption coefficient of 78.74 $L * g^{-1} * cm^{-1}$ for chlorophyll- a in 90 % methanol (Meeks, *et al.*, 1971).

2.3.6 Absorption Spectra of *Microcystis* cultures

In order to compare cellular contents of light absorbing components like chlorophyll and other chromophores, absorption spectra were recorded between 300-800 nm with the help of a SHIMADZU UV spectrophotometer (UV-1800). *Microcystis* cultures in BG-11 were used without further processing with cell densities between (OD_{750} = 0.5-0.8).

2.3.7 Determining *Microcystis* Growth Rates

Microcystis growth rates were determined in order to check for growth influencing effects of the FS2 field strain exudate. The cultivation setup for PCC 7806 and the microcystin deficient *ΔmcyB* mutant was arranged as

described in section 2.3.3 with a few alterations. Instead of cultivation in aerated multicultivator vessels, independent biological triplicate cultures with exactly equal starting cell densities of OD_{750} = 0.35 were grown in Erlenmeyer flasks at 25 °C and 16 µmol photons * m^{-2} * s^{-1}. After the treatment of cultures with FS2 exudate or BG-11 in control cultures, chlorophyll-a amounts were quantified each day over a period of ten days. After five days the treatment was repeated in order to keep the stimulus at sufficient levels. The calculation of growth rates (µ) was based on the daily chlorophyll-a increase and followed the equation below with successive sampling times t_1, t_2, etc.

$$\mu = \frac{\ln(chl_{a2}) - \ln(chl_{a1})}{t_2 - t_1}$$

2.3.8 Microscopic Documentation

The visual documentation of cyanobacterial phenotypes in various experiments combined microscopic and photographic means. Cyanobacterial morphotypes and pictures of cells and aggregates, respectively, were acquired with a digital inverted fluorescence Microscope (Evos fl, Digital Inverted Microscope, AMG). For the applications in this study bright field transmitted light images were recorded using the integrated microscope imaging software giving monochromatic digital image output. Samples comprised *Microcystis* material in their original growth medium without further preparation or fixation steps. In order to document realistic morphological colony/ cell aggregate features, microscopic examinations were conducted without cover slip, thereby avoiding distortion.

Plate cultivation of *Microcystis* was documented photographically using up to 32-fold magnification of a stereomicroscope (stemiDV4, Zeiss) combined with a digital camera (Panasonic DMC-FZ45 Lumix) attached to one ocular.

2.3.9 CAS-Assay

In order to test for siderophore production of *Microcystis* field strain FS2 the universal CAS (Chrome Azurol S) Assay developed by Schwyn and Neilands (Schwyn, *et al.*, 1987) was applied to FS2-exudates. Colorimetric changes of the CAS dye from blue to orange due to the removal of iron from the dye-Fe-complex by a strong chelator/ siderophore were measured in liquid media via absorption values at 630 nm. The CAS dye solution (final concentrations: 40 µM CAS; 0.18 µM $Fe(III)Cl_3 6H_2O$; 1.8 mM HCl; 4 mM CTAB) was prepared according to the following instructions:

- Stock A: 0.06 g CAS in 50 mL H_2O
- Stock B: 0.0027 g $FeCl_3\ 6H_2O$ in 10 mL 10 mM HCl
- Stock C: 0.073 g CTAB in 40 mL H_2O

1 mL of stock A was combined with 9 mL of stock B before adding 40 mL of stock C. The Dye solution was autoclaved and stored in the dark. Colorimetric assays were performed by adding one volume of dye solution to the test medium and spectrophotometric measurements at 630 nm after an incubation of 20 minutes. Test solutions were measured at their original pH and at an adjusted pH of 5.6.

2.3.10 DNA-Preparation

DNA preparation was conducted as published by Hisbergues (Hisbergues, *et al.*, 2003). The preparation of genomic DNA of *Microcystis* strains after harvesting the cell material (centrifugation: 10 min, 4,500 x g) followed the steps of washing the pellet twice in TE-buffer (10 mM Tris-HCl, 1 mM EDTA), resuspension and incubation in TES-buffer (25 % (w/v) sucrose, 50 mM Tris-HCl, 100 mM EDTA, pH 8.0) on ice for 1 hour. The subsequent incubation with

added lysozyme to a final concentration of 2 mg/ml for 1 hour at 37 °C was followed by a proteinaseK digest plus the addition of 2 % SDS at 50 °C for 2-3 hours. Separation of nucleic acid molecules from proteins and other cellular debris was achieved by a phenol chloroform extraction after Chomczynski and Sacchi (Chomczynski, *et al.*, 1987). After the precipitation of the yielded DNA from an aqueous solution in 40 % final isopropanol concentration, and a washing step in 70 % ethanol, DNA was resuspended in water for further utilization and finally, residual RNA contaminations were removed by RNase mix addition and incubation at 37 °C for 1 hour.

2.3.11 Sequencing of Genomic DNA From Field Strain FS2

In order to determine the *Microcystis* genotype of field strain FS2 concerning carbon uptake systems, genomic DNA was used for PCR amplification and its products subsequently send for sequencing at GATC Biotech, Konstanz.

According to Sandrini (Sandrini, *et al.*, 2013) the genomic region of bicarbonate uptake transporters *bicA* and/or *sbtA, sbtB* in *Microcystis* was expected to be flanked by a transcriptional regulator gene *ccmR2* and the sodium/proton antiporter gene *NhaS3,* which surround varying forms and combinations of *bicA* and *sbtA*. To cover the genomic region for sequencing, PCRs were designed to yield overlapping products and sequencing primers were deduced considering a sequence overlap of at least 100 base pairs (Figure 2-2). The primer design was based on PCC 7806 sequences for primers: P1: bic-clust-fw; P4: bic-clust-rv and on NIES 843 sequences in case of primers P2: sbtA-rv, P3: sbtA-fw using the online tool Primer3web (Koressaar, *et al.*, 2007; Untergasser, *et al.*). PCRs were conducted using the Qiagen Taq-polymerase and according buffer systems after the manufacturer's instructions. Subsequently, PCR products were purified with the Quiaquick PCR Purification Kit (Qiagen) and assessed concerning their concentrations (specific absorption measurements on a nanodrop).

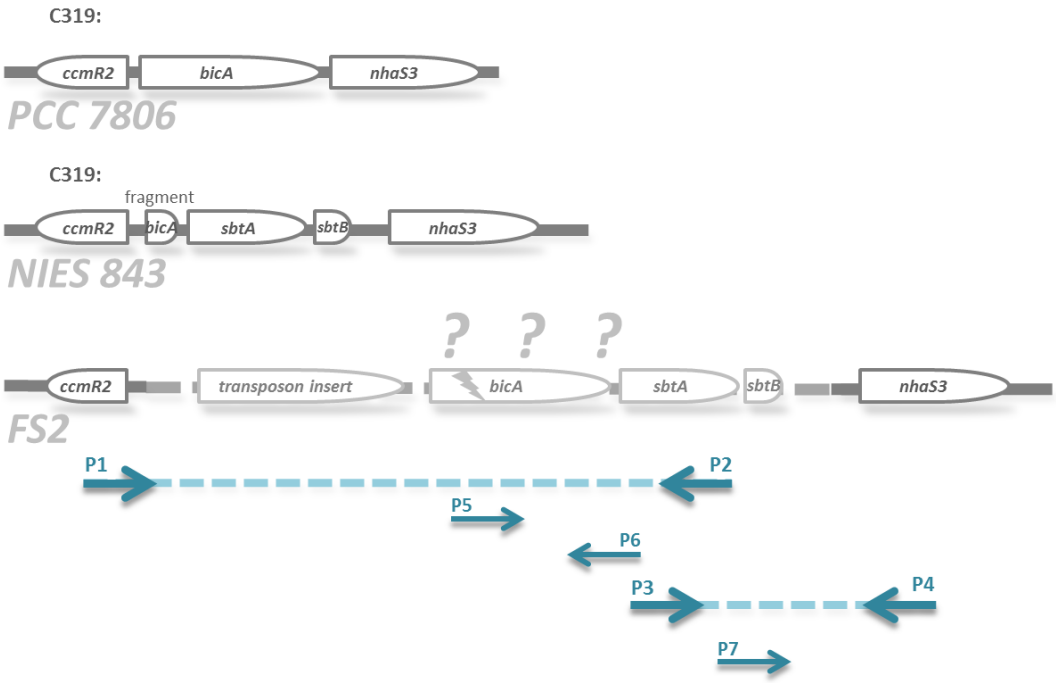

FIGURE 2-2: SEQUENCING STRATEGY FOR FS2 GENOTYPE OF BICARBONATE TRANSPORTERS
Genome Sequences of FS2 were determined using *Microcystis* PCC 7806 and NIES 843 genome sequences as template for the primer design of primers P1, P2, P3, P4, which served in PCRs and subsequent amplicon (blue dashed lines) sequencing. The unknown FS2 sequence is shown with all potentially comprised genes, like the c_i-uptake systems *bicA* (complete, as a fragment, or split into two parts), *sbtA*, *sbtB* and a transposon insert. Additionally, primers P5, P6 and P7 were deduced from first sequencing results and used for further sequencing. For primer specifications see **TABLE 2-2**.

Size and specificity of the products were checked by size-wise DNA fragment separation in agarose gel-electrophoresis (Sambrook, 1989) using TAE running buffer (40 mM Tris; 20 mM acetic acid; 1 mM EDTA) and the following loading dye (50 % Ficoll; 1 mM EDTA; pH 8.0; 0.05 % (w/v); Bromophenol blue; 0,05 % (w/v) Xylene cyanol. UV-visualization of ethidium bromid intercalating in DNA-molecules occurred on a ChemiDoc™XRS+ Imager (BioRad, USA). Finally, purified PCR products were sent to GATC Konstanz for successive sequencing with several primers (Figure 2-2, Table 2-2, page 19). The obtained genomic FS2 DNA sequences were assembled with the help of the online tool CAP3 Sequence Assembly Program (Huang, *et al.*, 1999).

2.3.12 Illumina Sequencing of Cyanobacterial Field Strains

The established uni-algal cyanobacterial field strain FS2 was analyzed for potentially associated heterotrophic bacteria. Based on the Illumina MiSeq technology, the hypervariable regions V4 of the 16 S rRNA were sequenced from a DNA-mix of isolated field strains (isolation described in section 2.3.10). Primer specifications are listed below comprising a 5 bp tag, a 2 bp linker and a 20 bp primer sequence spanning a region of 291 bp (*E. coli* reference sequence). After the sequencing was conducted by GATC Biotech, Konstanz, Germany, the acquired raw data was analyzed by Dr. Fabian Horn from the section Geomicrobiology of the GFZ German Research Centre for Geosciences, Potsdam, Germany. The bioinformatics approach started with the quality control of the sequencing library using the fastqc tool. (FastQC A Quality Control tool for High Throughput Sequence Data http://www.bioinformatics.babraham.ac.uk/projects/fastqc/ by S. Andrews). Sequence reads were sorted according to their identifying barcodes, which were detected and removed with the CutAdapt tool (Martin, 2011). The subsequent steps included merging of reads using overlapping sequence regions (PEAR, (Zhang, *et al.*, 2014)), standardizing the nucleotide sequence orientation, and trimming and filtering of low quality sequences (Trimmomatic, (Bolger, *et al.*, 2014)). After chimera removal, sequences were clustered into OTUs and taxonomically assigned, employing the GreenGenes database with a cutoff of 97 % using the QIIME pipeline (Caporaso, *et al.*, 2010). Resulting graphics were created with the help of the open source krona toolkit (http://sourceforge.net/projects/krona/).

Forward:	515F_01	ACGTA-GT-GTGCCAGCMGCCGCGGTAA
Reverse:	806R_01	ACGTA-CC-GGACTACHVGGGTWTCTAAT

2.3.13 Transcriptional Studies

The effects of extracellular *Microcystis* compounds (undifferentiated cell exudates and 50 ng/mL microcystin-LR) on the physiological state of treated *Microcystis* cultures (PCC 7806, *ΔmcyB*, FS2) were investigated on the transcriptional level via microarrays and quantitative real time PCR (for detailed experimental setup see Figure 2-1, page 18). Additionally, the microarray studies allowed for a transcriptional comparison of the microcystin deficient mutant *ΔmcyB* and the wild type PCC 7806.

The experimental and cultivation set up was conducted as described in section 2.3.3, using three biologically independent replicates of each test condition. To provide robust transcriptional data, potential deviation in mRNA contents due to technical mishandling was minimized by meticulously equal, as well as fast and cool treatment of the samples.

2.3.13.1 RNA Preparation

Cell pellets of 40 mL cell culture obtained after the centrifugation (4,500 x g; 10 min) in ice-filled tubes were used for the preparation of total RNA according to the single step method (Chomczynski, *et al.*, 1987). Immediate fixation of cell pellets in 1 mL of the phenol based TRIzol agent was followed by snap freezing in liquid nitrogen. The RNA preparation was performed after TRIzol manufacturer's protocol including heating to 65 °C for 20 minutes while shaking at 400 rpm. After addition of 200 µL chloroform, phase separation was achieved through centrifugation (11,000 x g; 15 min) and the aqueous upper phase was further used. This chloroform extraction step was repeated before nucleic acid precipitation with 0.7 volumes of isopropanol for 5-30 minutes and a following centrifugation at 11,000 x g for 10 minutes. After a wash step in 75 % ethanol (1 mL; 7,500 x g; 5 min) the resulting RNA pellet was dried and dissolved in 30 µL H_2O. Residual DNA was removed by TURBO DNase digest

after the manufacturer's protocol. An RNA clean up with RNeasy® Mini Kit 50 followed. RNA quality assessment included the determination of concentrations, as well as protein and phenol contents based on nanodrop absorption measurements at 230/260/280 nm, RNA agarose gel electrophoresis for RNA degradation check, PCR giving negative results after complete DNA digest, and in case of further use in microarrays an RNA integrity check with an RNA 6000 Nano chip on a 2100 Bioanalyzer (Agilent Technologies). RNA Samples were stored at -80 °C.

2.3.13.2 RNA Agarose Gel-Electrophoresis

Agarose gel-electrophoresis for RNA samples was conducted using a 1.5 % agarose matrix in a MEN-buffer system. Agarose was melted in water by microwave heating and allowed to cool down to approximately 50 °C before adding 10 % of the final volume of 10 x MEN-buffer. Furthermore, formaldehyde was added to a final concentration of 10 % vol. to reduce secondary structures in nucleic acids. RNA samples were supplied with loading buffer containing ethidium bromide for UV-visualization and denatured at 65 °C for 10 minutes before loading and running the agarose gel at 50 V for 15 minutes and finally at 80 V for final size separation. Visualization was performed on a ChemiDoc™XRS+ Imager (BioRad, USA).

MEN-buffer: 20 mM Mops; 1 mM EDTA; 5 mM sodium acetate; pH 8.0

2.3.13.3 Quantitative Real Time PCR

Transcription levels of the *Microcystis* PCC 7806 genes *rnpB*, *mcyA*, *mcnB*, *mcaA*, *aerJ*, and IPF_47 (see Table 2-2) were determined in PCC 7806 wild type cultures as well as *ΔmcyB* cultures with and without the application of external

microcystin (50 ng/mL final concentration). Cultivation occurred at three different light conditions (high light: 70 µmol photons * m^{-2} * s^{-1}; low light: 16 µmol photons * m^{-2} * s^{-1}; darkness: 0 µmol photons * m^{-2} * s^{-1}) for biologically independent triplicate batch cultures.

After RNA preparation and RNA quality assessment of these cultures as described in 2.3.13.1 first strand cDNA was generated with random primers and MAXIMA RT (Thermo Fisher Scientific Inc.) according to the manual instructions and tested in technical triplicates of 100 ng template each, plus non transcription control. RT-qPCR was conducted based on a SYBR green system (SensiMix SYBR Low-ROX kit; Bioline) on the Light Cycler C480 (Roche) with the following specifications: (95 °C: 10 min; 45 x [95 °C: 15 sec; 60 °C: 1 min]; melting curve: [95 °C: 5 sec; 65 °C: 1min; 97 °C: 1 sec]; 40 °C ∞).

Data analysis including baseline correction, linear regression, and threshold cycle calculation, was performed by the LC480Conversion and LinRegPCR software provided by the Heart Failure Research Centre (HFRC) in Amsterdam, Netherlands.

Relative expression levels were determined according to (Pfaffl, 2001) including corrections for the particular PCR efficiency and normalizing to the expression of the housekeeping gene *rnpB*, a constitutively expressed component of RNaseP.

Statistical significance was determined with the two tailed t-test after standard error calculation of replicate groups and subsequent error propagation.

2.3.13.4 Microarray Conduction

The microarray hybridization was performed with the support and in the facilities of the Microarray Department of the University of Amsterdam.

The RNA samples were reversely transcribed (Superscript II RT, Life Technologies) into cDNA using random primers and incorporating Cy3- and

Cy5-labelled dUTPs into control and treatment samples, respectively (Table 2-4). Protocols were conducted after the manufacturer's manuals. After cDNA clean up (E.Z.N.A. MicroElute cleanup kit), samples were tested for Cy-dye incorporation (via nanodrop) and subsequently hybridized to two slides of 8 x 60K custom *Microcystis* PCC 7806 microarrays for 20 h at 65 °C with a NimbleGen hybridization system 4 NimbleGen/Roche). Hybridization signals were recorded with the help of the DNA microarray scanner G2565CA.

Table 2-4: Microarray Hybridization Scheme

***Microcystis* strain**	**Treatment**	**Sample Type**	**Dye**	**Array Slide**	**Array No**
PCC 7806-I	+ FS2-exudate	treat	Cy3	1	1.1
PCC 7806-I	- FS2-exudate	Co	Cy5	1	1.1
PCC 7806-II	+ FS2-exudate	treat	Cy5	1	1.2
PCC 7806-II	- FS2-exudate	Co	Cy3	1	1.2
ΔmcyB-I	+MC	treat	Cy5	1	1.3
ΔmcyB-I	-MC	Co	Cy3	1	1.3
ΔmcyB-II	+MC	treat	Cy3	1	1.4
ΔmcyB-II	-MC	Co	Cy5	1	1.4
FS2-I	+MC	treat	Cy3	1	2.1
FS2-I	-MC	Co	Cy5	1	2.1
FS2-II	+MC	treat	Cy5	1	2.2
FS2-II	-MC	Co	Cy3	1	2.2
PCC 7806-I	+MC	treat	Cy5	1	2.3
PCC 7806-I	-MC	Co	Cy3	1	2.3
PCC 7806-II	+MC	treat	Cy3	1	2.4
PCC 7806-II	-MC	Co	Cy5	1	2.4
PCC 7806-III	+ FS2-exudate	treat	Cy3	2	1.1
PCC 7806-III	- FS2-exudate	Co	Cy5	2	1.1
ΔmcyB-III	+MC	treat	Cy5	2	1.2
ΔmcyB-III	-MC	Co	Cy3	2	1.2
FS2-III	+MC	treat	Cy3	2	1.3
FS2-III	-MC	Co	Cy5	2	1.3
PCC 7806-III	+MC	treat	Cy5	2	1.4
PCC 7806-III	-MC	Co	Cy3	2	1.4

A hybridization scheme was developed that would account for impacts of dye bias as well as for deviations in array quality. This was accomplished by avoiding grouping samples of the same test conditions on the same array slides or using the same dye for it. Intended for two-channel-detection per array, a control sample and its treatment counterpart were labeled with Cy3 and Cy5, respectively and hybridized to the same array. Triplicates were distributed over 2 slides of 8 arrays each with dye swaps for each genotype (Table 2-4).

2.3.13.5 Microarray Design

In this study custom *Microcystis* PCC 7806 oligonucleotide microarrays provided by Agilent Technologies were used that were based on arrays of earlier publications (Straub, *et al.*, 2011) and modified by the Microarray Department of the University of Amsterdam. 4,691 genes of the PCC 7806 genome (88.6 %) were mapped on 60,000 spot arrays with an average of 5 probes per gene, while each of the 60-mer oligonucleotides was printed in duplicate across one array, thereby ensuring within-array replication and statistical computability. For detailed probe information see data-set 1 in supplementary disc.

2.3.14 Data Analysis[1]

The data processing and statistical analysis of the microarray data was computed in the R environment (version R3.0.2 (R Core Team, 2013)), utilizing the freely available Bioconductor software (Gentleman, *et al.*, 2004), with the limma package (Smyth, *et al.*, 2003) for normalization. Statistical calculus was performed in four groups of microarrays combining 1) WT samples treated with

[1] This section is based on the Materials and Methods paragraph of the Publication Makower, et al. (see List of Publications) and might bear some identical text segments.

FS2-supernatant; 2) FS2 samples treated with MC-LR; 3) WT and MT (mutant) samples treated with MC-LR, and 4) DNA-microarrays of PCC 7806, *ΔmcyB*, and FS2. Normalization employed within-array-normalization (loess method, normexp background correction; offset: 50) and between-array-normalization (aquantile method), followed by the separation of the two color channels. Due to technical failure, one of the WT array triplicates, WT (± MC-LR), was omitted from the statistical analysis. Reduced statistical power due to one missing replicate was carefully considered during the interpretation of the data and might have led to an overestimation of p-values in a few cases. Accordingly, some genes just below the thresholds of differential expression were discussed, nonetheless. Based on the obtained intensity lists for red (Cy5) and green (Cy3) channels after normalization, hierarchical clustering (Euclidian), multidimensional scaling (Cox, 2001), and principal component analysis (PCA) (Groth, *et al.*, 2012) were performed.

An analysis of variance (ANOVA) calculation provided probe-specific values of fold changes, log2-scaled absolute expression, and p-values. In order to assess differential gene expression, p-values for each of the 2 to 7 probes per gene had to be combined into a single value that could be evaluated as being clearly below or above the threshold of differential gene expression. This was achieved by applying Fisher's method (Mosteller, 1948), which considers each probe of a gene as a replicate and additionally takes into account that similarly low p-values of all probes per gene are not likely to occur due to chance but reflect a more significant expression value than one value alone would show. Following this, lists of differentially expressed genes were extracted, setting thresholds to $p \leq 0.1$ and log2-fold changes of ≥ 1 and ≤ -1 (see data-sets 2 and 3 in supplementary disc). For physiological interpretation of the array results, assignments of functional gene categories (Table 2-5) to each gene were conducted using both a *Microcystis* sp. strain PCC 7806 annotation and Synechocystis sp. strain PCC 6803 annotation obtained from CyanoBase (Kazusa genome resources; http://genome.microbedb.jp/cyanobase/).

TABLE 2-5: FUNCTIONAL GENE CATEGORIES IN RELATION TO COG (CLUSTER OF ORTHOLOGOUS GROUPS)- CATEGORIES

	Cyanobacterial functional Category		COG category
1	Amino acid biosynthesis	E	Amino acid transport and metabolism
2	Biosynthesis of cofactors	H	Coenzyme transport and metabolism
3	Cell envelope	M	Cell-wall/membrane/envelope biogenesis
4	Cellular processes	D	Cell cycle control, cell division, chromosome partitioning
		N	
		O	Posttranslational modification, protein turnover, chaperones
5	Central intermediary metabolism		
6	Energy metabolism	C	Energy production and conversion
		G	Carbohydrate transport and metabolism
7	Fatty acid, P-lipid and sterol metabolism	I	Lipid transport and metabolism
8	Photosynthesis and respiration		
9	Nucleotide bases, nucleosides, nucleotides	F	Nucleotide transport and metabolism
10	Regulatory functions		
11	DNA replication, DNA processing	B	Chromatin structure and dynamics
		L	Replication, recombination and repair
12	Transcription	A	RNA processing and modification
		K	Transcription
13	Translation	J	Translation, ribosomal structure and Biogenesis
14	Transport and binding proteins	P	Inorganic ion transport and metabolism
15	Other categories		
16	Hypothetical	R	General function prediction only
17	Unknown	S	Function unknown
18	Secondaty metabolites		
	No assignment	U	Intracellular trafficking, secretion, and vesicular transport
		W	Extracellular structures
		Z	Cytoskeleton

T	Signal transduction mechanism
V	Defense mechanisms
Y	Nuclear structure

2.3.15 DNA-DNA-Microarrays

Genomic DNA of the *Microcystis* strains PCC 7806, *ΔmcyB* and FS2 was used for random DNA fragment amplification and subsequent fluorescent cyanine dye labelling before the labelled fragments were hybridized to PCC 7806 custom microarrays that are described in detail in section 2.3.13.5. The hybridization scheme is displayed in Table 2-4, page 39. Statistical evaluation followed the same bioinformatics pipeline developed for the transcriptional studies of this project.

Table 2-6: Hybridization Scheme of DNA-Microarrays

***Microcystis* strain**	**Dye**	**Array Slide**	**Array No**
PCC 7806-I	Cy3	2	2.1
PCC 7806-I	Cy5	2	2.1
ΔmcyB-I	Cy3	2	2.2
ΔmcyB-I	Cy5	2	2.2
FS2-I	Cy3	2	2.3
FS2-I	Cy5	2	2.3

2.3.16 MALDI Imaging

Thin-layer BG-11 agar plates of *Microcystis aeruginosa* PCC 7806 and FS2 field strain mono- or co-cultures to study bacterial interactions were inoculated as drop spots from fresh liquid cultures and incubated for 20 days. Further sample processing and data-acquisition was carried out by Eric Helfrich at the ETH Zurich, Switzerland. Sample preparation, matrix application, and dehydration

were conducted as described previously (Yang, *et al.*, 2012). Agar pieces with mono- or co-cultures were carefully transferred onto stainless steel MALDI target plates and covered with a 1:1 mixture of 2,5-dihydroxybenzoic acid (DHB) and α-cyano-4-hydroxycinnamic acid (CHCA), provided as Universal MALDI Matrix (Sigma-Aldrich). The samples were dehydrated by incubation at 37 °C overnight and subsequently stored in a desiccator. The data was acquired on a MALDI LTQ Orbitrap mass spectrometer in positive mode with a resolution of 60.000, a laser energy of 35 µJ and a scan range between 100-2000 *m/z*. In order to increase sensitivity, the scan range was split into two (100-950 and 900-2000 *m/z*). The spatial resolution was set to 350 µm. Method optimization was conducted using Thermo Tune Plus and Xcalibur. The data analysis was performed with ImageQuest1.1. False colors were assigned to masses of interest and superimposed onto an optical picture taken before matrix application. Single spectra analysis on different spatial localizations for spectral comparison was performed using ImageQuest.

2.3.17 Analyzing the Exudate of *Microcystis* FS2

Spent media of *Microcystis* cultures were analyzed. Measurements of pH values, and electric conductivity were conducted with a mobile pH-meter without further preparation of the media. For mass spectrometer analysis FS2 exudates were desiccated and sent to Eric Helfrich, ETH Zurich for testing.

For solid phase extraction, Sep-Pak Plus C18 cartridges were equilibrated with 2 mL methanol, and rinsed with 2 mL H_2O. Subsequently cell exudates were transferred to cartridges and the flow-through was kept for activity tests. 2 mL of 5 % methanol solution were applied on the cartridge, before dissolving bound compounds with 2 mL 100 % methanol. The solvent methanol was entirely evaporated in a vacuum concentrator. For bioactivity tests the precipitate was solved in 200 µL of 100 % methanol and diluted by additional 200 µL H_2O. Additional dilution to 50 mL was conducted with BG-11 for application in *Microcystis* cultures.

3 Results

3.1 Transcriptomics-aided analysis of the intracellular and extracellular roles of microcystin[2]

In this first chapter of the experimental results, investigations regarding the role of one distinct secondary metabolite, the heptapeptide microcystin, are described. Microcystin, which is produced by only a fraction of *Microcystis* strains, can be found in considerable amounts in the waters of *Microcystis* habitats during mass proliferation events (Dittmann*, et al.*, 2006). The potential function of microcystin in the extracellular environment is under debate (Kaplan*, et al.*, 2012). Additionally, the physiological role of intracellular microcystin is of great interest (D'Agostino*, et al.*, 2015) and previous studies have connected microcystin production to a broad range of physiological aspects, including nutrient availability, light intensity and oxidative stress (Jähnichen*, et al.*, 2007; Kaebernick*, et al.*, 2000; Zilliges*, et al.*, 2011).

In order to investigate both, a potential extracellular function and the intracellular role of microcystin, a comprehensive study was undertaken concerning the transcriptomic states of the microcystin producer *Microcystis aeruginosa* PCC 7806 and its *ΔmcyB* mutant, which is deficient in microcystin production. This transcriptomic comparison enabled the identification of physiological processes that were strongly influenced by the lack of microcystin in the mutant. Furthermore, both strains were evaluated at the transcriptional level in response to the presence of extracellular microcystin (50 ng/mL MC-LR).

[2] The data of this chapter was in large parts published in the journal of *Applied and Environmental Microbiology* in 2014 (see List of Publications).

3.1.1 Array statistics

The obtained microarray datasets for *Microcystis* wild type PCC 7806 (WT) and microcystin deficient mutant *ΔmcyB* (MU) samples with their respective treatments (BG-11 control and MC-LR addition) were assessed regarding the quality of the output data. Normalized data exhibited comparable medium log2-expression values, which were found to be in the same range among all tested sample sets (Figure 3-1 a). The similarity between the complete datasets of each replicate (characterized by the specific tested genotype, treatment and array-chip number) was visualized by hierarchical clustering based on the Euclidian distance matrix and by a multidimensional scaling (MDS) approach (Figure 3-1 b, c). Both plots indicate that the overall similarity of transcriptional datasets is very high within the same genotype and that in return, we find pronounced expression differences between these two genotypes of the microcystin producer and the non-producer. In the comparison of the complete datasets however, the influence of extracellularly applied microcystin on gene expression does not show in global similarity of the investigated transcriptomes. However, this does not exclude a specific impact of extracellular microcystin on individual genes and gene clusters.

Statistical robustness was demonstrated by the distribution of p-values that assembles the majority of p-values for each gene/expression change within the range of 0.0-0.1 (Figure 3-1 d). These preliminary results were used to define thresholds for differential gene expression, which then were set to a log2-fold change (lfc) of $1 \leq lfc \leq -1$ and p-values ≤ 0.1. Median log2-transformed expression changes in the microcystin deficient mutant compared to the wild type exhibited a Gaussian distribution (Figure 3-1 e) with a slight shift to the negative values. This suggested that in the mutant more downregulated genes are found relative to the wild type.

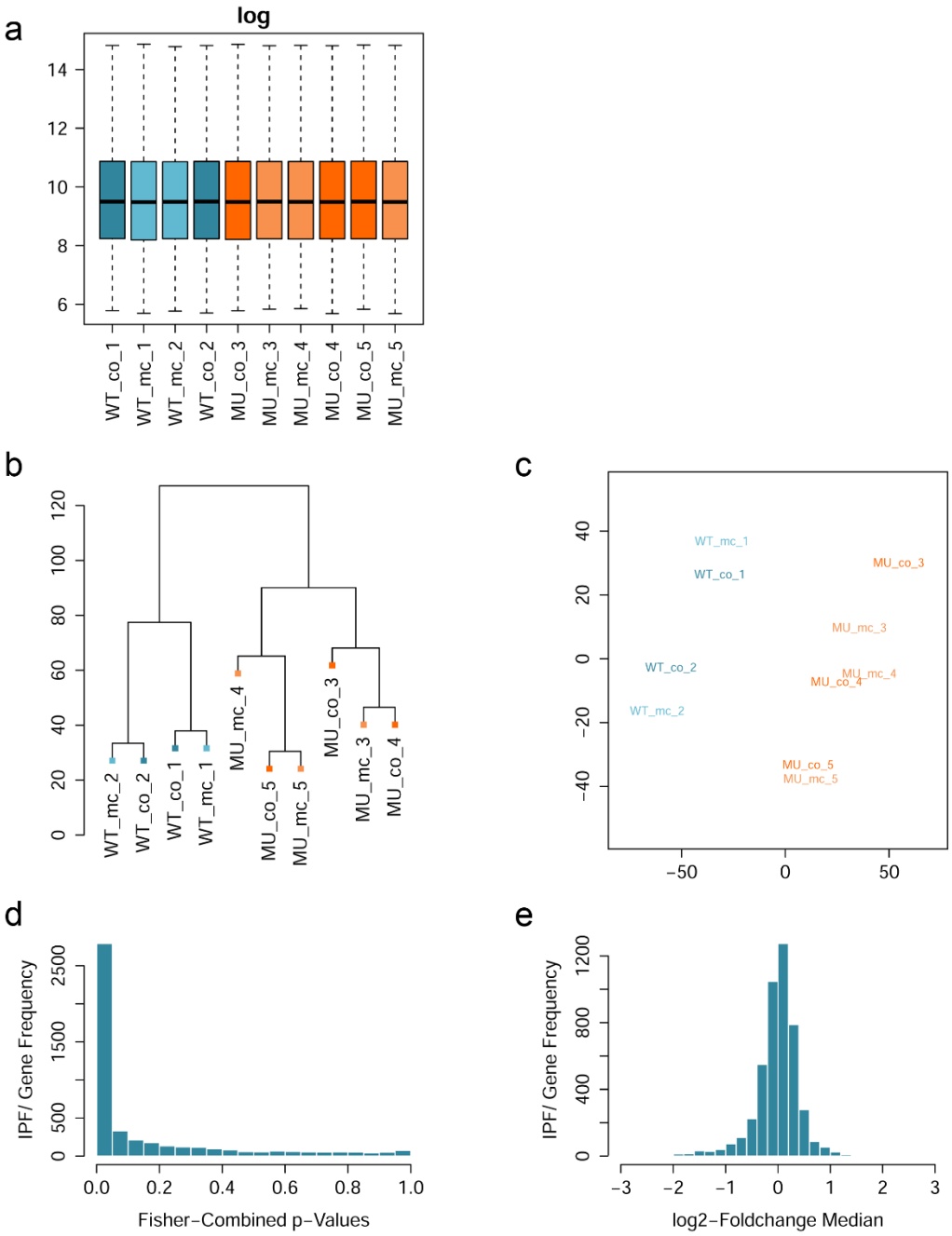

FIGURE 3-1: EVALUATION OF THE MICROARRAY DATASETS

a: log2-expression values of the replicate datasets of *Microcystis aeruginosa* PCC 7806 control and MC-LR-treatment samples (WT_co_1-2/WT_mc_1-2) and *Microcystis aeruginosa ΔmcyB* samples with control and MC-treatment (MU_co_3-5/MU_mc_3-5); **b**/**c**: similarities between the considered datasets, dendrogram of hierarchical clustering using the Euclidian distance matrix (**b**), Multidimensional scaling (MDS) (**c**) calculated from the results of the hierarchical clustering in (**b**). **d**: p-value distribution for the numbers of genes regarding genotype comparison, **e**: distribution of log2-fold changes for according gene numbers regarding genotype comparison+

3.1.2 PCA and MC-complementation

Since several parameters and influence factors (genotype and extracellular microcystin) were tested simultaneously in this experimental setup, a principle component analysis (PCA) was performed to further evaluate the influence and significance of each parameter on the global expression patterns. The largest fraction of the variance between the transcriptomic datasets is harbored by PC1 (41.6 %) and was considered as genotype influence factor. The MC-LR-treated samples however, did not separate from the control samples (Figure 3-2 a), which was evaluated as indication for a less global but more specific influence of the extracellular microcystin-LR to *Microcystis* gene expression. The principle components PC2-PC11 might represent technical influence parameters like Cy-dye bias or chip specifics and will not be further discussed regarding the biological context (Figure 3-2 b).

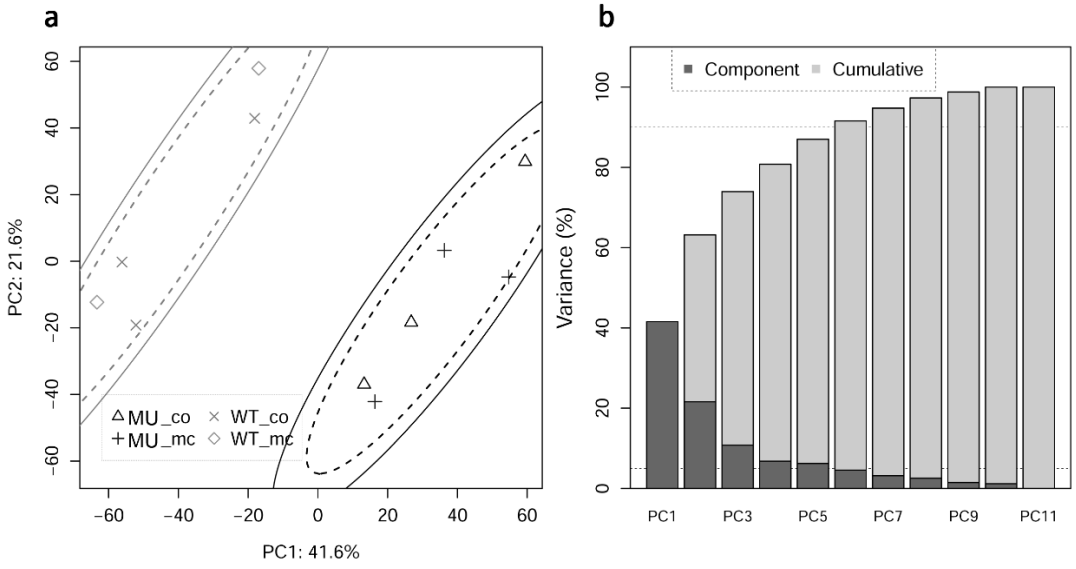

Figure 3-2: Principle Component analysis and Confidence Display

a: PCA of log2-normalized gene expression data for *M. aeruginosa* (WT) and *ΔmcyB* mutant (MU) cells. Confidence ellipses of 85 % (dashed line) and 95 % (solid line) for PC1 (41.6 % of overall variance) and PC2 (21.6 % variance) clearly separate genotypes, indicating highly significant cluster separation for the genotypes. **b**: shares of principle components of variance in single and cumulative display

3.1.3 Overview transcriptional differences + DNA-DNA arrays

After the statistical calculus and applying significance filters to the expression data, 213 genes were identified as differentially expressed in the microcystin deficient *ΔmcyB* mutant relative to the PCC 7806 wild type (data-set 3 of the supplementary disc). The majority (78 %) of differentially expressed genes (DEGs) was downregulated while the remaining 22 % were upregulated in *ΔmcyB* (Figure 3-3).

In order to confirm that these broad changes are indeed the result of the sole microcystin knockout, and that additional natural mutations could be excluded as impacting factors, the *ΔmcyB* genome was tested via microarray hybridization. Hybridization efficiencies were compared between *ΔmcyB* DNA and PCC 7806 DNA. 16 out of the 30,066 tested probes from the array showed more than 5 % difference in hybridization efficiency (see data-set 4 ins supplementary disc). Whereas nine of the 16 genes were localized to intergenic spacers, the remaining seven could be attributed to coding sequences of identified genes. Only one gene that exhibited sequence similarity to a predicted nucleoside-diphosphate sugar epimerase, was considered as potentially affected. The other candidates of the *ΔmcyB* genome were neglected either due to an even higher hybridization efficiency than PCC 7806 probes or due to the identification as transposase or hypothetical proteins. In summary, the comparison of the mutant and wild type genomes showed only minor differences and exclude global expression differences as a result from major genome reorganization in the mutant.

The expression differences in the *ΔmcyB* cultures were considered substantial and the role of microcystin was further investigated. With the addition of extracellular MC-LR to the *ΔmcyB* mutant it was tested, if and to what extend the lack of intracellular MC can be complemented. In this regard, one specific gene cluster of 12 genes, coding for the biosynthesis enzymes of a putative PKS

metabolite was responding strongly. It showed a downregulation in *ΔmcyB* after the extracellular MC-LR stimulus. Thus the elevated expression of this cluster in the mutant was reversed (Figure 3-3).

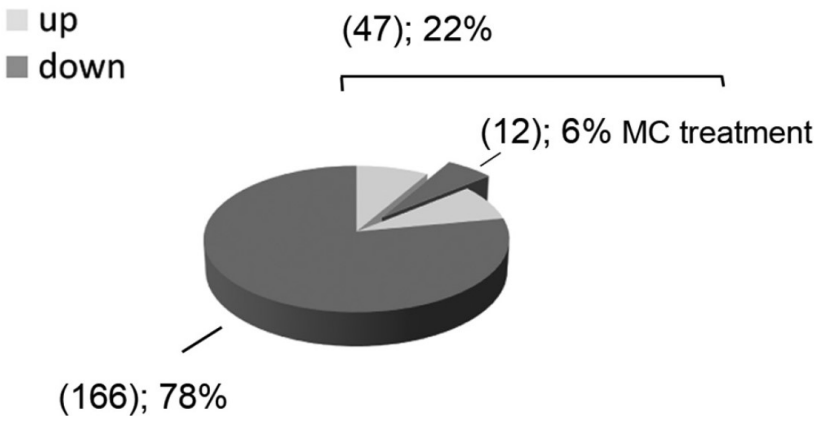

FIGURE 3-3: TOTAL OVERVIEW OF DIFFERENTIALLY EXPRESSED GENES
Number of differentially up- and downregulated genes in the *ΔmcyB* mutant compared to the wild type. For 6 % of the differentially upregulated genes in the mutant, these effects could be reversed by external MC-LR addition

The set of DEGs was annotated to functional gene categories as defined on the online platform CyanoBase (Kazusa genome resources; http://genome.microbedb.jp/cyanobase/) (Figure 3-4). The most pronounced differences were found in the functional categories of the central intermediary metabolism, secondary metabolism and in unknown genes. Central categories of the primary metabolism, such as energy metabolism, fatty acid metabolism and photosynthesis are considerably changed in the mutant with the major percentage of downregulated genes. Nevertheless, the fraction of DEGs that belong to the core genome makes up for only 30 %. Notably, the downregulation of numerable genes of the primary metabolism was not accompanied by a lower growth of the mutant.

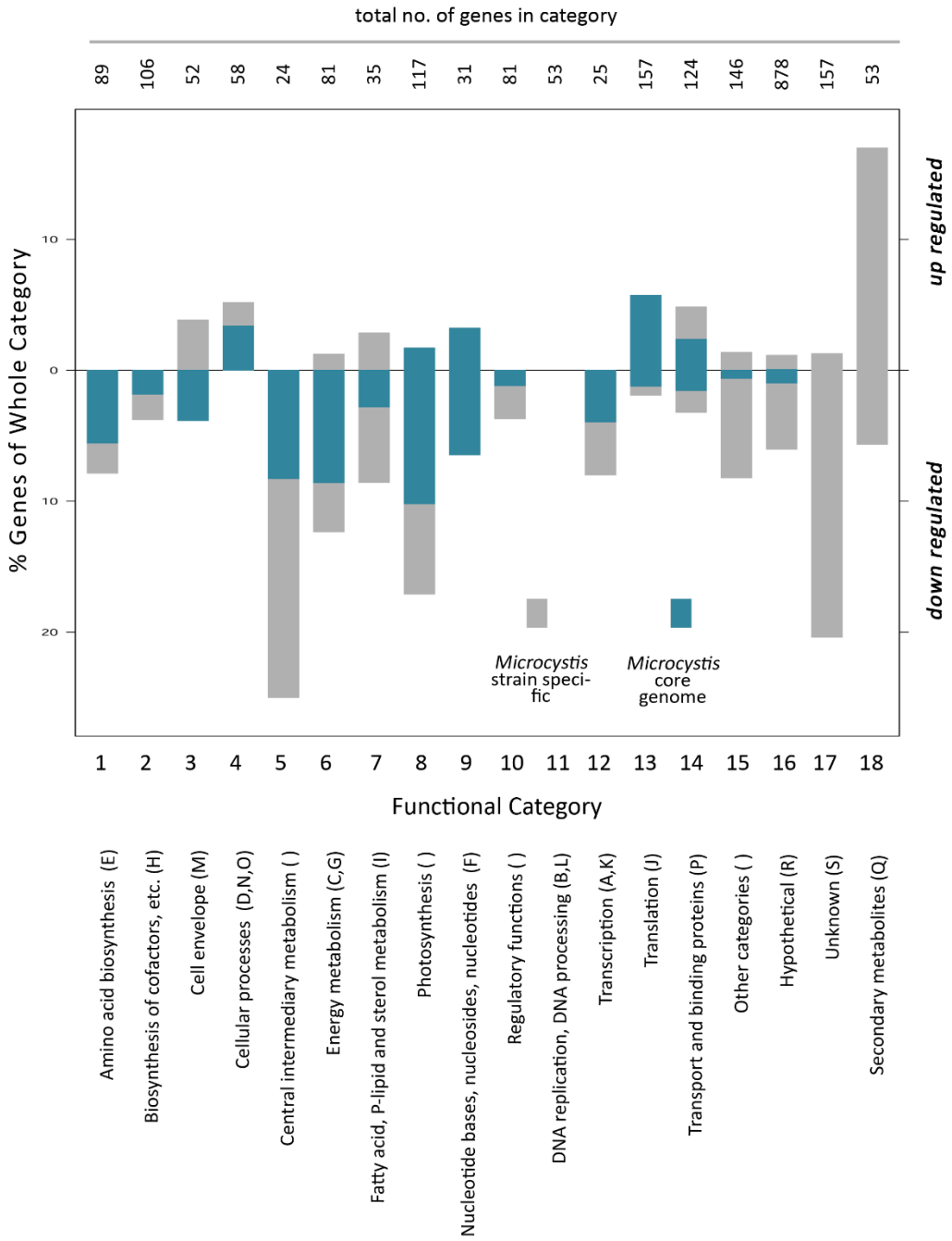

Figure 3-4: Differential Gene Expression According to Functional Gene Categories
The percentage of functional gene categories showing differential up- or downregulation with separation into genes belonging to the core genome of *Microcystis* (blue) and into strain specific genes (grey). Gene categories are obtained from CyanoBase (Kazusa genome resources; http://genome.microbedb.jp/cyanobase/) and listed with their according COG-categories (**Table 2-5**, page 42). The total number of genes belonging to one category is given on top of the bars.

Since the transcriptional changes were spanning a broad set of genes from all categories of primary and secondary metabolism, it was focused on differentially expressed regulators and their potential to alter comprehensive transcriptional programs. A promising candidate was found in IPF_1434, an HTH-type transcriptional regulator that was more than tenfold downregulated in the mutant (lfc=-3.2). The function of this regulator has not been confirmed yet. However, considering that it is not present in a number of toxic *Microcystis* strain, speaks against a direct involvement with microcystin. A regulator, conserved across *Microcystis* strains that was considerably downregulated in the MC-deficient mutant, was identified as alternative circadian clock regulator *kaiB1*. It acts in an opposing manner to the original *kaiB* gene from PCC 7806 and opens up speculation about the influence of MC on processes determined by the circadian rhythm. Another lead to a correlation of the MC-knockout to light related processes was found in the downregulation of the essential response regulator Ycf27, which has been implicated in the transfer of excitation energy from the phycobilisome to PSI (Ashby, *et al.*, 2002). Additional DEGs with regulating functions are mentioned in later sections in respect to their biological contexts.

3.1.4 Transcriptional Changes in the *ΔmcyB* Mutant in the Cellular Context

The transcriptional changes in the *ΔmcyB* mutant compared to the PCC 7806 wild type were analyzed in regard to their implications in metabolic and cellular processes. An overview is displayed below (Figure 3-5, page 53). In the following sections, differentially expressed genes are discussed in detail concerning their involvement in photosynthesis, energy metabolism and secondary metabolites.

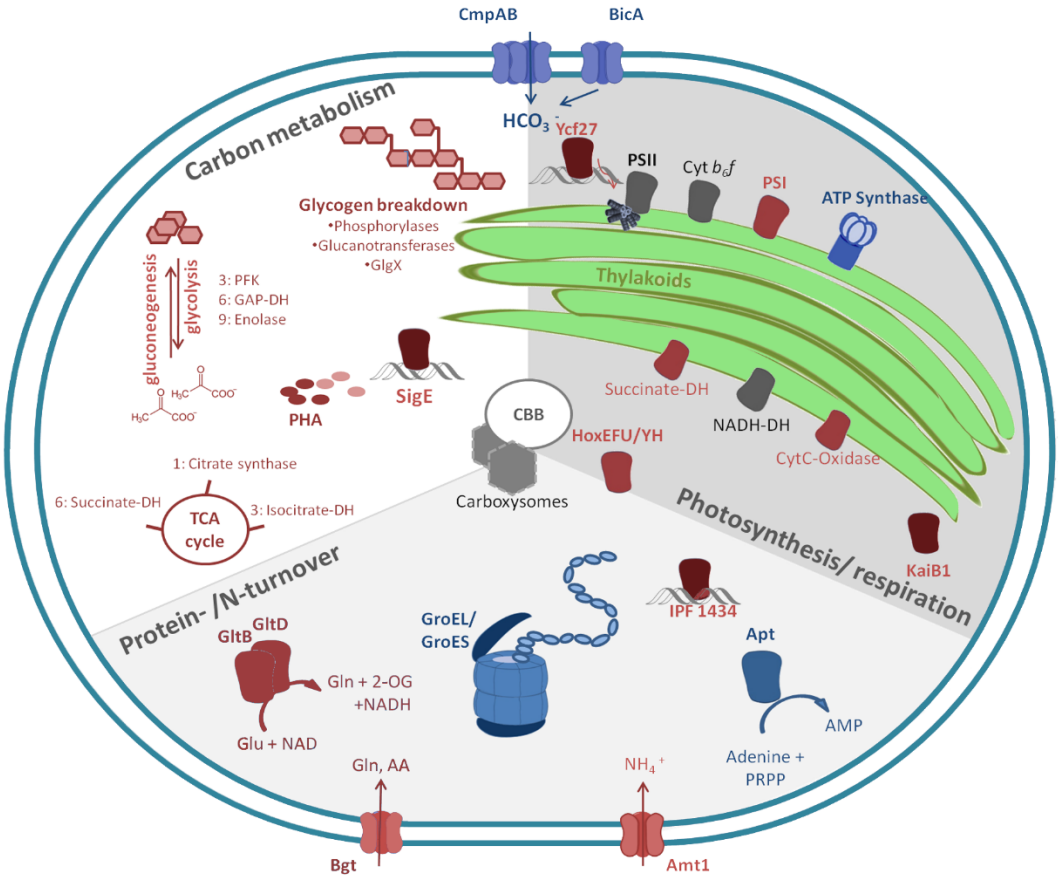

FIGURE 3-5: OVERVIEW OF THE TRANSCRIPTIONAL DIFFERENCES IN THE *ΔMCYB* MUTANT COMPARED TO THE PCC 7806 WILDE TYPE

Differential gene expression of cell components and proteins is displayed in a color coded manner. Red components were found downregulated in *ΔmcyB* mutant cells while blue components showed upregulation and grey components were found unchanged. Thylakoids are displayed in green. Abbreviations: Cyt, cytochrome; DH, dehydrogenase; PRPP, phosphoribosyl pyrophosphate; AA, amino acid; 2-OG, 2-oxoglutarate=α-ketoglutarate; PHA, polyhydroxyalkanoate; CBB, Calvin-Benson-Bassham cycle.

3.1.5 PHOTOSYNTHESIS AND RESPIRATION GENES

The transcriptional alterations to the photosynthetic and respirational apparatus in the Δ*mcyB* mutant occurred in different measures to the single components. While photosystem I (PSI) was downregulated in the mutant in all of its components except for *psaA*, the core components of photosystem II

(PSII) were not differentially expressed with only *psbO, psbU, psbV* downregulated in *ΔmcyB*. This supports an altered ratio of PSI:PSII in the mutant compared to the wild type, which has implications for the balancing of the photosynthetic and respirational electron flow (reviewed in (Vermaas, 2001)). Further photosynthesis components were hardly affected except for a slight upregulation of the ATP synthase.

TABLE 3-1: DIFFERENTIALLY EXPRESSED GENES OF THE *ΔMCYB* MUTANT REGARDING PHOTOSYNTHESIS AND RESPIRATIONAL GENES

Photosynthesis and Respiration components	**Upregulated genes**	**Downregulated genes**
Photosystem II		*psbO, psbU, psbV*
Phycobilisomes		*apcE*
Cytochrome b_6f complex		*petM*
Photosystem I		*psaB, psaC, psaI, psaK1, psaK2, psaK, psaL*
ATP synthase	*atpF, atpG*	
Soluble electron carriers		*petF, pyruvate flavodoxin, oxidoreductase, probable ferredoxin*
NADH-dehydrogenase		*ndhD1*
Terminal oxidases		*ctaB, ctaEI*

Genes encoding components of respiration complexes showed a downregulation of terminal oxidases (cytochrome c oxidase as well as quinol oxidase) with the strongest expression decrease of the cytochrome oxidase folding protein (*ctaB:* lfc=-2.4). In contrast, genes including the NADH-dehydrogenase did not show demonstrable expression changes in the *ΔmcyB* mutant. The observed downregulation of soluble electron carriers might be attributed to both processes, photosynthesis as well as respiration.

3.1.6 Energy- & Central Intermediary Metabolism

Consistent with the identification of considerable expression changes in genes belonging to the central intermediary and energy metabolism found in the *ΔmcyB* mutant (Figure 3-4, page 51), central metabolic processes such as glycolysis, the TCA-cycle, and carbon storage and uptake routes were affected by the loss of microcystin (Table 3-2).

Table 3-2: Differentially Expressed Genes of the Functional Category of Central intermediary and Energy Metabolism in the *ΔmcyB* mutant Compared to the PCC 7806 Wild Type

Gene	PCC 6803 homologe	lfc	Metabolic process
glgX	slr0237	-1.66	Glycogen degradation
glgP	slr1367	-1.45	
IPF_5378	sll1356	-1.54	
phaA	slr1993	-1.91	PHA synthesis
phaB	slr1994	-1.78	
phaC	slr1830	-1.52	
phaE	slr1829	-1.67	
pfkA1	sll1196	-1.41	Glycolysis
gap1	slr0884	-1.99	
IPF_6528	slr0752	-1.15	
ppsA	slr0301	-1.38	
gltA	sll0401	-1.26	TCA
icd	slr1289	-1.37	
frdA	slr1232	-1.31	
cmpA	slr0040	1.11	Bicarbonate uptake
cmpB	slr0041	1.02	
bicA	sll0834	1.19	
sigE	**sll1689**	**-2.38**	**Transcriptional regulation**

The downregulation of two glycogen phosphorylases (*glgP, IPF_5378*) and of the debranching enzyme isoamylase *glpX* indicate that glycogen degradation is seriously impeded in the microcystin deficient mutant. At the same time, the synthesis of the storage compound polyhydroxyalkanoate (PHA) is

downregulated in its biosynthesis genes (*phaABCE*). Furthermore, the heterotrophic-like pathways of the glycolysis and the TCA-cycle are downregulated in genes for key enzymes of these pathways. This included phosphofructokinase (*pfkA*) glyceraldehyde 3-phosphate dehydrogenase (*gap1*) and the phosphoenol-pyruvate synthase (*ppsA*) involved in the glycolytic carbohydrate degradation, whereas the affected TCA-cycle genes comprise citrate synthase (*gltA*), isocitrate-dehydrogenase (*icd*), and the succinate dehydrogenase (*frdA*).

In this respect it is noteworthy, that carbon acquisition via the uptake of bicarbonate seems to be increased by the upregulation of the two bicarbonate uptake systems *bicA* and *cmpAB*.

The above mentioned set of genes, which is strongly involved in the sugar catabolism, was shown to be positively transcriptionally regulated by the alternative sigma factor SigE (Osanai, *et al.*, 2011). *sigE* itself was strongly downregulated in the microcystin deficient mutant

3.1.7 Single Noticeable Aspects of the Transcriptional State of *ΔmcyB*

In addition to implications of the aforementioned alternative sigma factor SigE in the regulation of sugar catabolic processes, SigE was shown to have an impact on the transcription of the *hox* genes (Osanai, *et al.*, 2011) that encode for a bidirectional Ni-Fe hydrogenase. The Ni-Fe has been suggested to play a considerable part in regulation of the redox state of cyanobacterial cells (Carrieri, *et al.*, 2011). These target genes of SigE for the respective subunits of the bidirectional hydrogenase are also downregulated in the *ΔmcyB* mutant with log2 fold changes between -1.08 and -1.76.

Summarized within the topic of protein and nitrogen turnover, a few distinct genes among the DEGs stand out. The chaperone components GroEL/GroES

belong to the smaller fraction of genes that are upregulated in the microcystin deficient mutant indicating an increased need for protein folding. Glutamine and basic amino acid transporters BgtA/B were down regulated. With a lfc<-2.1 the glutamate synthase genes *gltB/D* were strongly downregulated, thus mostly stopping the reversible transformation between glutamate and glutamine.

The highest upregulation with an 18-fold higher expression in the *ΔmcyB* mutant is the *apt* gene (adenine phosphoribosyltransferase), which catalyzes the formation of AMP utilizing adenine and phosphoribosyl pyrophosphate as substrates.

3.1.8 Secondary Metabolites

The only gene cluster that was responding to an extracellular stimulus of microcystin-LR belonged to the category of secondary metabolites. The complete set of 12 genes of an orphan PKSI/III hybrid cluster (IPF_38-51) showed a significant downregulation one hour after the treatment with MC-LR. This observation in combination with earlier reports that had suggested autoinduction of microcystin as well as crosstalk between secondary metabolites (Schatz, *et al.*, 2007) has led to a closer investigation of the transcriptional reaction of the secondary metabolite gene category (Figure 3-6).

Six secondary metabolites and their respective biosynthesis gene clusters that have been described and reviewed before (Humbert, *et al.*, 2013), were in the focus of this analysis. Four of these pathways have been attributed to the production of the known metabolites microcystin, aeruginosin, cyanopeptolin, and microcyclamide.

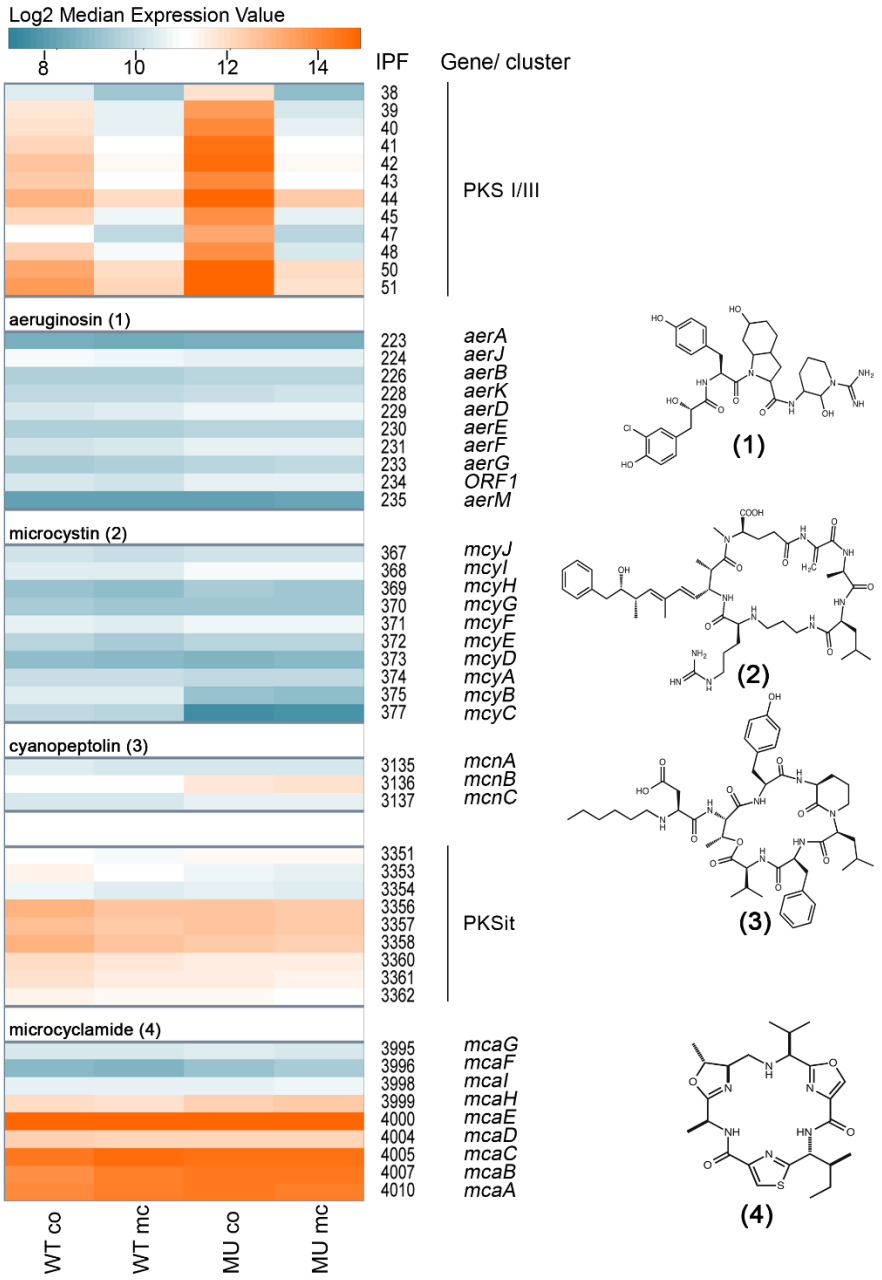

FIGURE 3-6: DIFFERENTIAL GENE EXPRESSION IN SECONDARY METABOLITE GENE CLUSTERS

Heatmap showing expression levels of secondary metabolite genes in WT PCC 7806 and the mutant *ΔmcyB* (MU) with (mc) and without (co) MC-LR treatment. Expression levels are given as median log2 values as indicated in the color code bar at the top. Gene cluster designations and genes/ IPF-numbers plus metabolite structures (aeruginosin (1), microcystin (2), cyanopeptolin (3), and microcyclamide (4) are indicated on the right. Two cryptic clusters encode polyketide synthase complexes presumably involved in the synthesis of an aromatic polyketide (PKSI/PKSII) and an enediyne type polyketide (PKSit)

The other two represent orphan gene clusters without identified metabolites. Structural predictive tools like the online platform antiSMASH (Weber*, et al.*, 2015) helped to identify putative structural characteristics. This way the before mentioned PKSI/III derived metabolite was suggested to exhibit aromatic features introduced by a chalcone type PKSIII synthase (Frangeul*, et al.*, 2008). The iterative type PKSit cluster (IPF_3351-3362) on the other hand, supposedly encodes for enzymes producing an enediyne type metabolite (Frangeul*, et al.*, 2008).

The microarray based transcriptional analysis of the biosynthesis gene clusters for these secondary metabolites showed that the only cluster responding to extracellular MC-LR under the tested conditions was the hybrid PKSI/III cluster. The expression of genes from this cluster was significantly increased in the mutant but this effect was complemented by the treatment of cultures with extracellular microcystin. The decrease of gene transcription occurred to similar final expression levels in the wild type and the mutant. Nevertheless, other gene clusters for secondary metabolites showed expression differences in the comparison between wild type and mutant. The transcription of biosynthesis genes for, aeruginosin, cyanopeptolin, and microcyclamide are slightly enhanced in *ΔmcyB*, although these differences were not significant. Interestingly, the expression levels of the precursor gene (*mcaE*) of the ribosomally produced microcyclamide was one of the highest throughout the whole transcriptomic data set.

An autoinduction of microcystin, which had been reported before, could not be confirmed under the conditions tested. The only transcriptional alterations were seen in a lower transcript abundance of the *mcyB* and *mcyC* genes in the microcystin deficient mutant. The lowered expression values most likely occur due to the genetic engineering that had introduced an antibiotic resistance cassette into the *mcyB* gene, thus either stopping transcription of both co-transcribed genes or decreasing hybridization efficiencies on the microarray.

3.1.8.1 Quantitative Expression Analysis of Secondary Metabolites in Response to Extracellular Microcystin under Three Light Conditions

After the unexpected outcome of the transcriptional data that stated a less pronounced autoinduction effected of microcystin, a comprehensive transcriptional investigation of secondary metabolites was initiated, intended to test the transcriptional response of five of the above discussed gene clusters to extracellularly applied microcystin under three different light conditions. *Microcystis* PCC 7806 wild type and *ΔmcyB* mutant cultures were grown in three replicates to the late exponential phase (OD_{750}=1.0) and then left for two days in order to acclimate to the according light conditions of either total darkness, or low light conditions of 16 µmol photons * m^{-2} * s^{-1}, or high light conditions of 70 µmol photons * m^{-2} * s^{-1}. Treatment and control samples were taken one hour after the subsequent addition of 50 ng/mL MC-LR and used for quantitative real time PCR. One gene of each cluster was chosen as representative for the production of the metabolite (microcystin: *mcyA*; cyanopeptolin: *mcnB*; microcyclamide: *mcaE*; aeruginosin: *aerJ*; PKSI/III metabolite: IPF_47).

The quantitative expression data revealed a strong impact of light intensities on the transcription of all tested secondary metabolites (Figure 3-7). Consistent with previous reports (Kaebernick, *et al.*, 2000), *mcyA* transcription increased with higher light intensities. Equal tendencies were observed for cyanopeptolin and microcyclamide, but not for aeruginosin and the unknown PKSI/III metabolite. Notably, each of the tested secondary metabolites tend to be expressed at higher levels in the microcystin deficient mutant, unless they were acclimated to darkness, when this effect appeared to be reversed. The trend of elevated secondary metabolite transcripts in the mutant was partly seen in the microarray studies as well and was confirmed by the RT-PCR results with more pronounced expression differences.

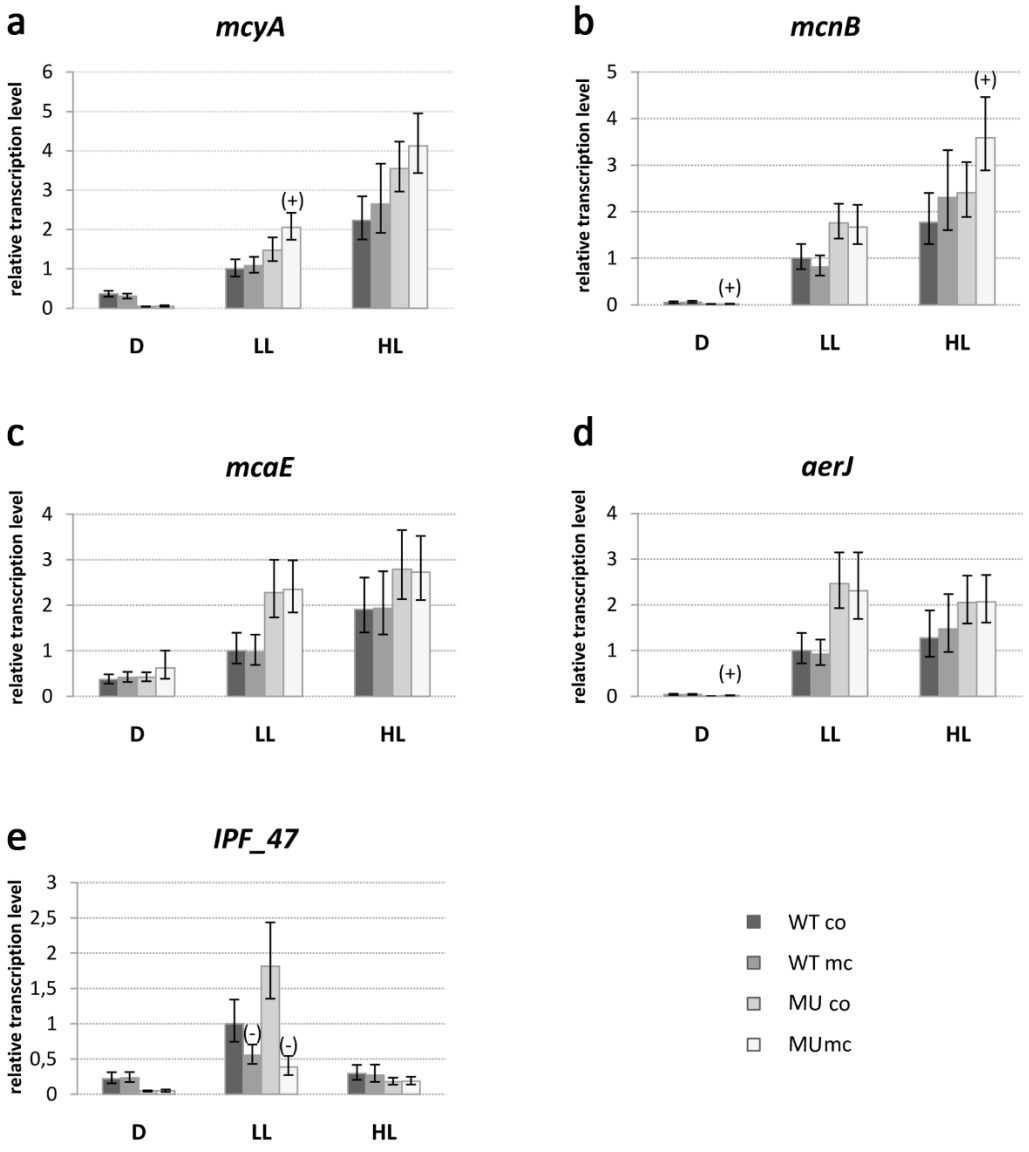

Figure 3-7: Relative Expression Levels of Secondary Metabolites under Varying Light Conditions

Results from RT-PCR showing relative expression levels of secondary metabolite biosynthesis genes *mcyA* (microcystin; a), *mcnB* (cyanopeptolin; b), *mcaE* (microcyclamide; c), *aerJ* (aeruginosin, d), and IPF47 (PKSI/PKSIII) biosynthesis in wild type (WT) and Δ*mcyB* mutant without (co) and with (mc) MC-LR treatment under conditions of darkness (D; 0 µmol photons * m^{-2} * s^{-1}), low light (LL; 16 µmol photons * m^{-2} * s^{-1}), and high light (HL; 70 µmol photons * m^{-2} * s^{-1}). Expression rates were calculated as ratios to WT-LL-co levels. Statistical testing is indicated as standard errors (error bars) with significance of MC-LR addition in relation to the control samples of the same genotype/light conditions marked on top of the bar [(+) significantly upregulated, (-) significantly downregulated].

The effect of extracellular microcystin does not show a systematic pattern. Significant inducing effects of MC-LR on the expression of *mcyA* and *mcnB* were seen only at low light conditions for *mcyA* and at high light conditions for *mcnB* and only in the *ΔmcyB* mutant (Figure 3-7 a, b).

The transcriptional pattern of the IPF_47 gene represents a clear contrast to the transcription of the four other tested secondary metabolites. Here, the highest transcription occurs during low light cultivation. Furthermore, under these light conditions microcystin addition was leading to significantly decreased transcription of the IPF_47 gene in both, wildtype and mutant cultures. Thus, this transcriptional behavior exhibits a reciprocal trend compared to *mcyA* and *mcnB* in respect to light and is in perfect agreement with data acquired in the microarray experiments.

3.2 *Microcystis* Community Interactions

In this second chapter of the experimental results, investigations regarding *Microcystis*-*Microcystis* interactions are described. This work has been carried out with axenic *Microcystis* lab strains on the one hand and with newly isolated uni-algal *Microcystis* strains from the field on the other hand. The combination of well characterized strains and *Microcystis* representatives that exhibit more original characteristics as they are found in the field, was intended to overcome a gap in current research publications. Comprehensive transcriptomic investigations of axenic lab cultures in the past have been lacking aspects of interactions while meta-transcriptomic studies from field ecosystems have not enabled the identification of bacterial community interaction partners and their distinct effects on each other.

Therefore, *Microcystis* strains were isolated from the field and characterized in regard to their morphological appearance, microcystin biosynthesis gene clusters, associated heterotrophic bacteria and genome resources. Co-habitation simulations of these field strains and well characterized lab strains and the effects of potentially released compounds on the respective other *Microcystis* strains were investigated on several levels, including phenotypic reactions and analysis of transcriptomic responses. The later were substantiated and complemented by additional physiological tests. Finally, the analysis of *Microcystis* field strain cell exudates was initiated to a preliminary level.

3.2.1 Isolation and Characterization of *Microcystis* Strains From the Field

In order to investigate inter-strain interactions within the *Microcystis* community it was reasoned to use *Microcystis* strains with a strong level of acclimation to interaction conditions as found in the field. Therefore, in this study *Microcystis* colonies from the field were isolated and transferred to

laboratory cultivation. Out of 120 freshly isolated colonies from blooms of Lake Zernsee and Lake Wannsee near Potsdam, Germany four different strains of *Microcystis* were successfully established as uni-algal batch cultures exhibiting a stable growth. These strains were designated FS2, FS10, FS66, FS77. Characterization of the four strains showed noticeable diversity concerning morphological features and microcystin toxicity. The microscopic analysis resulted in the identification of one *aeruginosa* morphotype and one *botrys* morphotype, while the other two were not further determined due to the fact that cells were taken from partial colonies only (Figure 3-8).

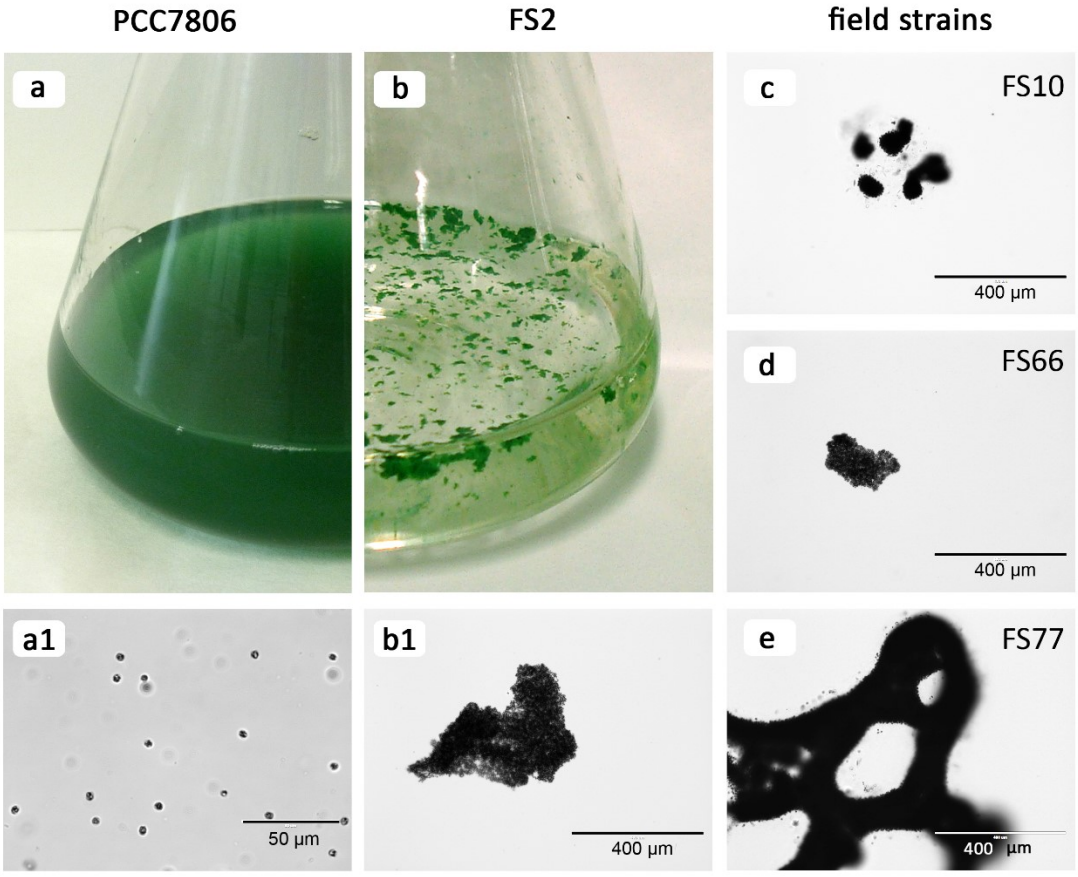

FIGURE 3-8: ISOLATED *MICROCYSTIS* FIELD STRAINS USED IN THIS STUDY

Display of strains used in this study, cell suspension of the lab strain *Microcystis aeruginosa* PCC 7806 (**a**) and according micrograph (**a1**) showing single cell appearance; **b**: colony forming field strain FS2 floating on culture surface and originally isolated FS2-colony fragment from Lake Zernsee, Germany (**b1**); further isolated *Microcystis* field colonies: **c**: FS10 (*Microcystis botrys*), **d**: FS66 (*Microcystis* spec.), **e**: FS77 (*Microcystis aeruginosa*)

PCR-analysis using specific primers for the biosynthesis gene *mcyA* showed that two of the four field strains harbor the genomic facilities to produce the hepatotoxin microcystin (Table 3-3, page 67).

Under the laboratory standard cultivation conditions, the field strain 2 (FS2) exhibited a phonotype with loose formation of colonies, which were floating on the culture surface. Highest growth rates appeared under continuous low light illumination of 16 µmol photons $* m^{-2} * s^{-1}$ without shaking or bubble aeration. The strains FS10 and FS66 kept stable colonial morphological features with position on the bottom of cultivation vessels, while the large colonies of FS77 captured varying positions in the vertical axis of the cultivation medium.

3.2.2 Analysis of the Bacterial Composition of *Microcystis* field isolate FS2

Since the FS2 *Microcystis* strain was only recently isolated from the field, it was assumed that associating bacteria were still part of the established culture. A qualitative and quantitative analysis of the putative bacterial community was initiated in order to assess the potential influence of the associates on subsequent experiments. Based on the Illumina MiSeq technology, ribosomal DNA was sequenced and taxonomically assigned to operational taxonomic units (OTUs).

The data confirmed that the established FS2 culture was uni-algal with *Microcystis* as only cyanobacterium among a solely prokaryotic community. Accounting for about 77 % of the analyzed DNA, FS2 was considered the major player in this culture. The composition of the remaining 23 % of the bacterial community showed two more major classes of associated bacteria: *Alphaproteobacteria* and *Sphingobacteria*. Remarkably, the sphingolipid producers (*Sphingobacteriales* and *Sphingomonadales*) represent 19 % of the whole bacterial consortium.

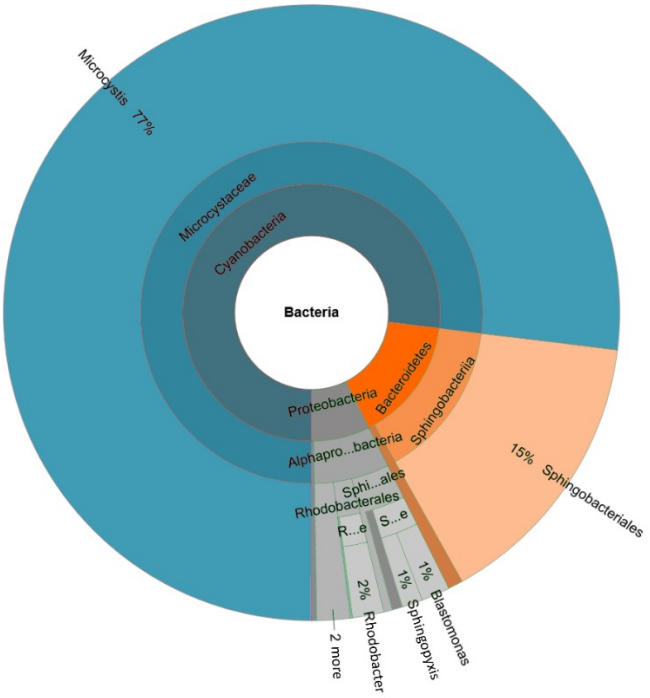

FIGURE 3-9: PHYLOGENETIC COMPOSITION OF THE BACTERIAL CULTURE OF FS2
The taxonomic classification of the bacterial community around *Microcystis* FS2 is displayed to the levels of phylum, class, order, family, and genus. For more detailed information, see data-set 5 on the supplementary disc.

3.2.3 EFFECTS OF SPENT MEDIUM OF *MICROCYSTIS* FIELD STRAINS ON ESTABLISHED LAB STRAIN

In order to investigate if *Microcystis* strains exert any visible effects on each other, co-cultivation experiments were designed that would test the bioactivity of the spent cultivation medium of each strain and its phenotypic effects on other strains. After finding that single extracellular info-chemicals, such as microcystin can exert a highly specific influence on other cells under distinct cultivation conditions, the cumulative effect of *Microcystis*-produced compounds (released into the medium) on further *Microcystis* strains was tested. Cell free cell exudates of the field strains FS2, FS10, FS66, FS77, and the lab strains PCC 7806 and Δ*mcyB* were applied to every other culture in any possible combination. From these co-cultivation experiments the field strain

FS2 emerged as uniquely influencing the other two lab strains by inducing a rapid cell aggregation after the addition of one volume of cell free FS2 exudate (Table 3-3). At the same time, PCC 7806 aggregates sank to the bottom of the cultivation vessels, unless they were mechanically set in motion.

TABLE 3-3: CHARACTERISTICS OF ISOLATED *MICROCYSTIS* FIELD STRAINS

***Microcystis* field strain**	**Morphotype**	**Toxicity**	**Cell Aggregating effect on PCC 7806 and *ΔmcyB***
FS2	*spec.*	-	++
FS10	*botrys*	MC	-
FS66	*spec.*	-	-
FS77	*aeruginosa*	MC	-

3.2.3.1 TIME COURSE EXPERIMENT OF THE PHENOTYPIC RESPONSE OF PCC 7806 AND *ΔMCYB* TO THE FS2 EXUDATE

The time frame and dynamics of this aggregation reaction were recorded in a time course experiment over 96 hours after an equal volume of FS2 exudate was applied (Figure 3-10). It shows the aggregation and disaggregation of *Microcystis* cells from 0.5 h to 48 h. Macroscopic and microscopic pictures illustrate that the microcystin deficient *ΔmcyB* mutant reacts to the external stimulus with a different aggregation pattern that leads to denser but smaller cell-clumps compared to PCC 7806. Also it appears that the mutant's reaction is slightly delayed and leads to an earlier return to a single celled state.

The occurrence of first aggregation reactions of a few cells in the lab strain cultures after 20-30 minutes exceeded regular cell division rates. Consequently, cell aggregations were assessed as result of the attachment of cells to each other. In addition to the considerable stickiness between PCC 7806 cells, an accelerated attachment of cells to the cultivation vessels was observed.

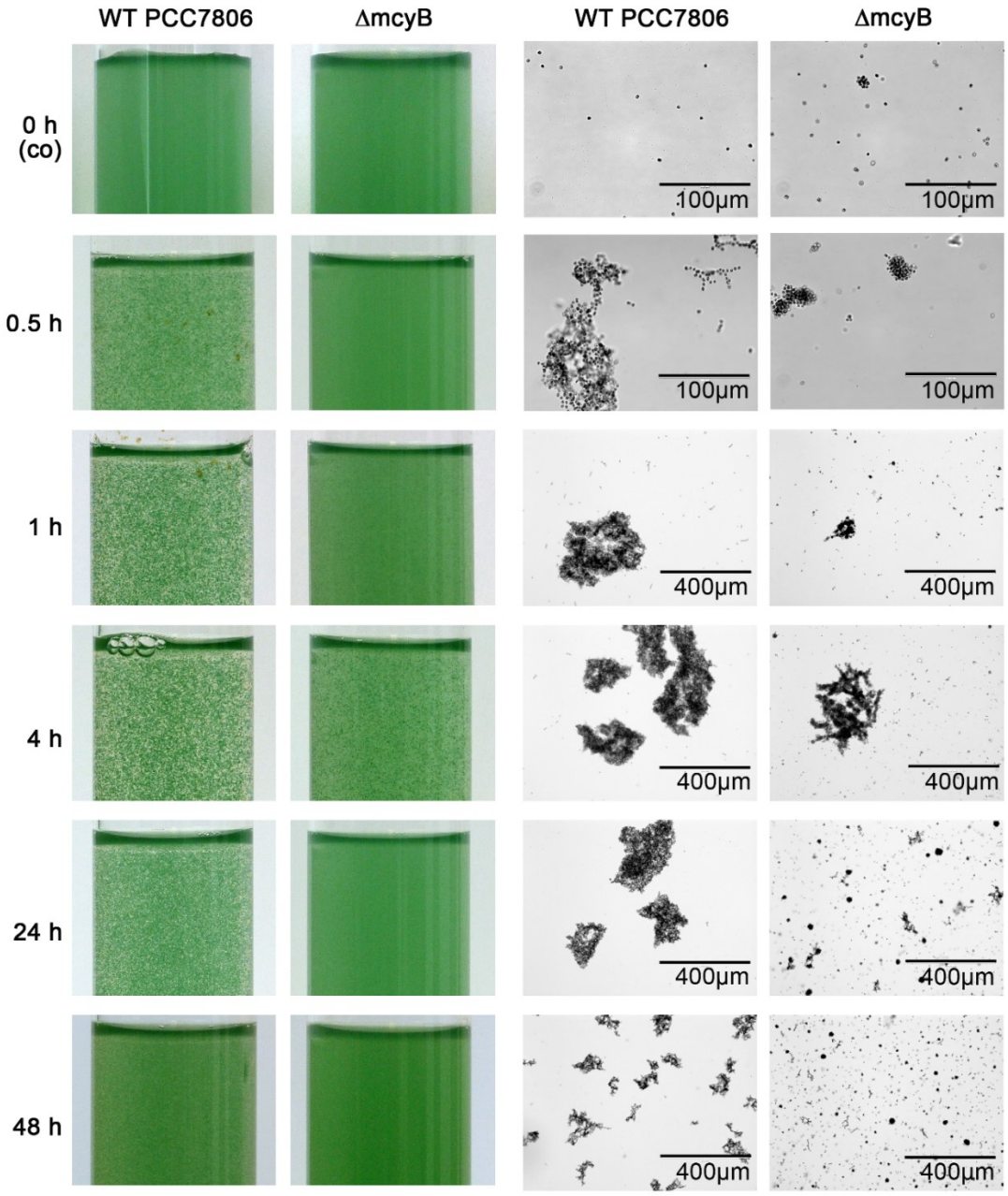

Figure 3-10: Time Course experiment Showing the Bioactivity of FS2 Exudate

The reaction of PCC 7806 and its MC-deficient mutant *ΔmcyB* to the addition of an equal volume of FS2 exudate in a time course of 96 h (only 48 h displayed) The two columns on the left side show reactions in cultivation tubes of 4 cm diameter while the according micrographs are displayed on the right.

3.2.4 Genomic Characterization of the *Microcystis* Field Strain FS2

The genomic differences between the two *Microcystis* strains PCC 7806 and FS2 were characterized in order to determine potential genes that are responsible for the observed *Microcystis* interactions. DNA comparisons of FS2-DNA and PCC 7806-DNA via microarray hybridization have identified genes, which were present in both strains and thus have resulted in similar hybridization signals on the array. Additionally, PCC 7806 specific genes were identified by the lack of an FS2 hybridization signal on the array. From these data an overlap of genomic resources of both *Microcystis* strains was determined that accounted for 87.5 % of the PCC 7806 genome. The remaining 12.5 % were analyzed regarding their gene functions (see Figure 3-11).

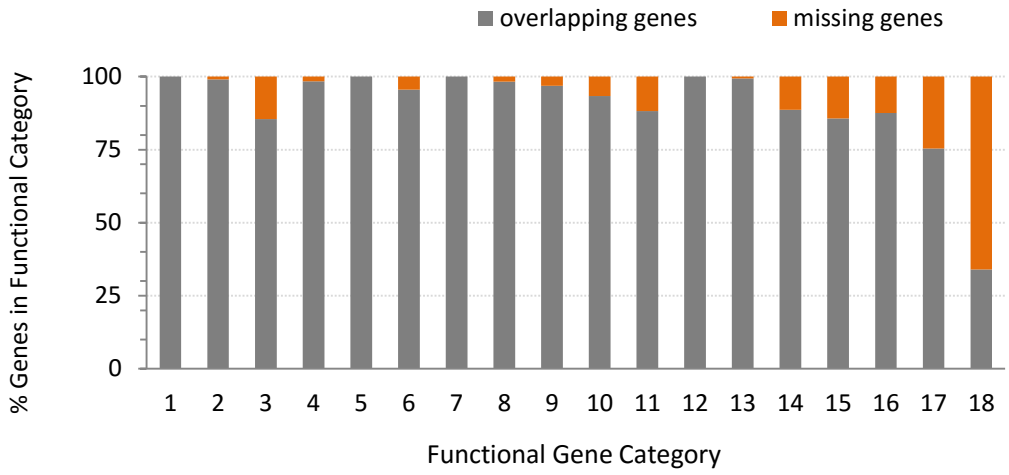

Figure 3-11: Distribution of PCC 7806 Specific Genes in Functional Gene Categories Compared to FS2

Functional Gene Categories: 1) amino acid biosynthesis; 2) biosynthesis of cofactors, etc.; 3) cell envelope; 4) cellular processes; 5) central intermediary metabolism; 6) energy metabolism; 7) fatty acid, phospholipid and sterol metabolism; 8) photosynthesis; 9) nucleotide bases, nucleosides, nucleotides; 10) regulatory functions; 11) DNA replication, DNA processing; 12) transcription; 13) translation; 14) transport and binding proteins; 15) other categories; 16) hypothetical genes; 17) unknown function; 18) secondary metabolites

Most of the genes that are specific to PCC 7806 and not present in FS2 were found in the categories **(3)** cell envelope (14.5 %, 9 genes), **(11)** DNA replication and processing (11.8 %, 9 genes), **(14)** transport and binding proteins (11.3 % 16 genes), and **(18)** secondary metabolites (66 %, 35 genes). These functional categories belong mostly to the flexible genes of the *Microcystis* genome (Humbert, *et al.*, 2013). The category of secondary metabolites was investigated more thoroughly. PCR analysis of the field strain FS2 provided a partial secondary metabolite profile summarized in Table 3-4.

TABLE 3-4: GENOMIC RESOURCES FOR SECONDARY METABOLITE PRODUCTION IN *MICROCYSTIS* PCC 7806 AND FS2

Secondary Metabolite	PCC 7806	FS2
Orphan PKSI/III cluster IPF_38 – IPF_51	+	-
Aeruginosin IPF_223 – IPF_235	+	+
Microcystin IPF_367 – IPF_377	+	-
Cyanopeptolin IPF_3131 – IPF_3137	+	-
Orphan PKS iterative cluster IPF_3351 – IPF_3362	+	+
Microcyclamide IPF_3995 – IPF_4010	+	-
Microviridin	-	+
Aeruginoguanidin	-	+
Anabaenopeptin	-	-
Microginin	-	+

3.2.4.1 Sequence Characterization of the Genomic Regions of HCO_3^- Uptake Systems

A closer look was taken at the adaptations of the investigated *Microcystis* strains to differing CO_2-conditions. The known variability of *Microcystis* genome sequences of inorganic carbon uptake systems (Sandrini, *et al.*, 2013) was explored in the field strain of FS2. Sequencing of the genomic region of FS2 around the transporter *bicA* revealed the presence of *sbtA-B*, another bicarbonate importer (Figure 3-12) that is characterized as exhibiting a high substrate affinity and low flux rate, which is believed to be advantageous at low CO_2 levels. The lower substrate affinity and higher flux rate of BicA on the other hand, is supposedly important at higher CO_2 concentrations.

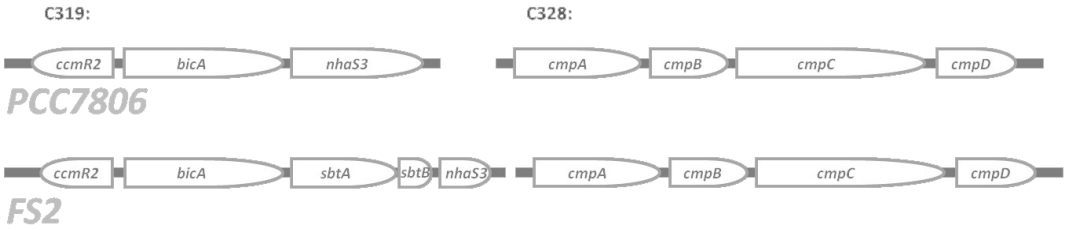

Figure 3-12: Genomic Characterization of Bicarbonate Uptake Systems in *Microcystis* PCC 7806 and FS2

Genomic regions of the bicarbonate uptake systems *bicA*, *sbtA*, and *cmpA-D* are displayed for *Microcystis* PCC 7806 and FS2 with flanking genes. For PCC 7806 the location of the discussed genes on their harboring contigs is marked (C319, C328)

3.2.5 Characterization of Sensitivities to Carbonate Supply in Mono and Co-Cultivation of *Microcystis* PCC 7806 and FS2

The *in vivo* behavior of both strains at differing CO2-conditions was tested on plate cultivation with standard BG-11 medium as well as depleted and tenfold increased carbonate sources. Two colonies of the strains on each plate were tested as mono- and co-cultures. After cultivation for three weeks, the non-toxic

Microcystis field strain showed a considerably higher sensitivity to a carbonate depleted medium while PCC 7806 only showed a minimal lower growth without bleaching and dying of the cells (Figure 3-13).

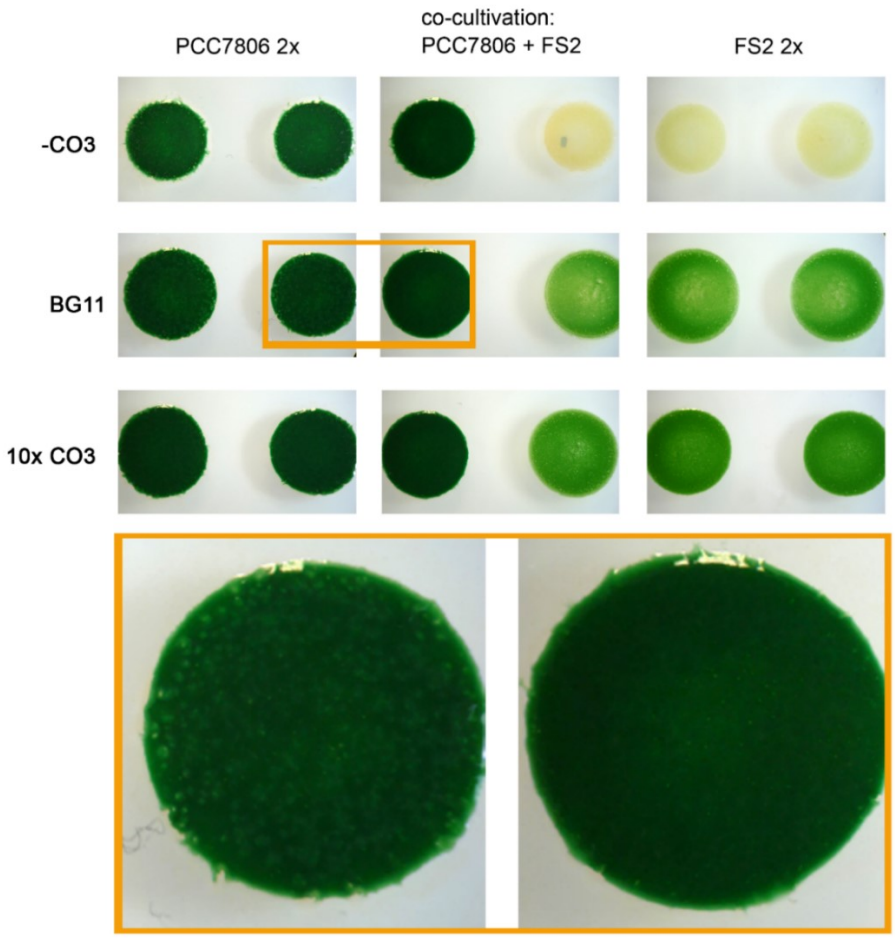

Figure 3-13: Co-Cultivation of *Microcystis* Strains at Media with Diverging Carbonate Concentrations

Photographs of colonies with according cultivation medium. Phenotypes of PCC 7806 under conditions of mono- and co-cultivation zoomed out (orange box)

In addition to the growth characteristics on different cultivation media this co-cultivation experiment has led to an altered phenotype in PCC 7806 colonies when cultivated in proximity to FS2 colonies. Similar to the bioactivity assays of the FS2 exudate (3.2.4.1, page 68) a strong visible response was triggered in PCC 7806 cells. The phenotype of the PCC 7806 in co-cultivation can be

described as smoother and containing less gaseous bubbles. The phenotypic alterations during co-cultivation on solid medium support the notion of a chemical compound excreted from FS2 that strongly affects PCC 7806 cells even after a period of three weeks.

3.2.6 MALDI Imaging Analysis of the *Microcystis* Strains PCC 7806 and FS2 in Mono- and Co-Cultivation

After previous investigations had shown altered phenotypes in *Microcystis* PCC 7806 cultures after the treatment with FS2 exudates in liquid media as well as on solid agar plates, extracellular signals were assumed to be responsible for the induced PCC 7806 reactions. A mass spectrometric MALDI imaging series was initiated that was intended to identify candidates of cyanobacterial peptides that might serve as extracellular signals. In this respect the influence of co-habitants as well as of carbon availabilities was tested as impact factors on the production and localization of these metabolites. *Microcystis* colonies (PCC 7806 and FS2) in mono- and co-culture, grown either on BG-11 agar plates or on carbonate reduced agar plates were analyzed via MALDI imaging for masses in the range of 100-2000 *m/z* with the results being displayed as false color images of the location of the detected masses (Figure 3-14).

The carbon deficiency conditions were shown to be obstructive to the production of known secondary metabolites like microcystin, cyanopeptolin, cyanobactin and most of all aeruginosin, that was not only reduced in its amounts but not detected at all under the tested conditions (Figure 3-14). Co-cultivation of PCC 7806 and FS2 was affecting secondary metabolite expression in several cases. An interesting decrease of the microcystin form MC-LR with a simultaneous increase in desmethyl-microcystin in PCC 7806 seems to indicate a shift of one form to the other during co-cultivation.

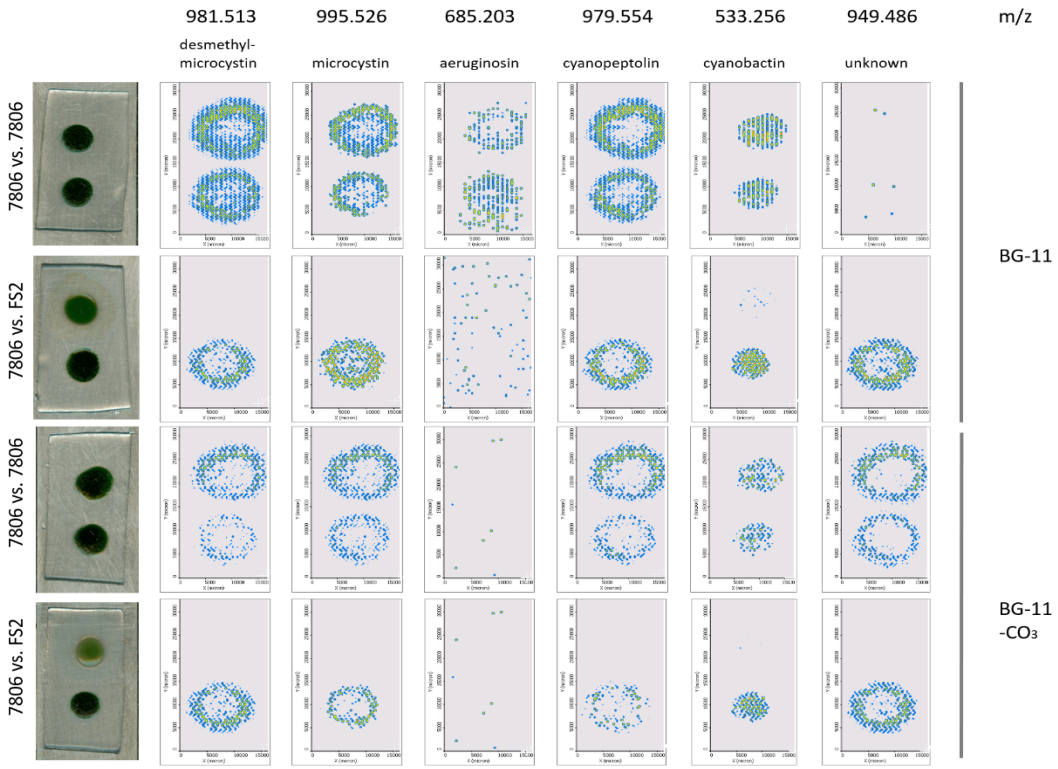

FIGURE 3-14: PRODUCTION OF SECONDARY METABOLITES UNDER CO-CULTIVATION AND CARBONATE DEPLETED CONDITIONS

Mass specific detection of metabolites according to their location within *Microcystis* colonies with cultivated on standard BG-11 agar plates and on carbonate depleted agar plates (-CO_3). The used colonies are displayed as photographs in the left column, while signals for a specific mass are displayed in false colors.

Even though the aeruginosin biosynthesis gene cluster is present in both *Microcystis* strains, the metabolite was only detected in the PCC 7806 strain and vanished in co-cultivation. In contrast, an unknown metabolite of the mass 949.486 *m/z* was only present in PCC 7806 when cultivated in proximity to FS2 or under carbonate depleted conditions. The detected metabolites that were produced by FS2 could not be attributed to known metabolites and their respective mass characteristics (data not shown). Noteworthy, cyanobactins and aeruginosins were the only metabolites showing a localization predominantly within the colonies. For the remaining metabolites displayed in Figure 3-14 an additional localization outside of the colony was confirmed indicating release of the peptides from the cells.

3.2.7 Analysis of the FS2 exudate

The spent medium of *Microcystis* FS2 was shown to considerably affect PCC 7806 cells in cultivation. In order to narrow down compounds and characteristics of the FS2 exudate that might be responsible for the observed effects, its physico-chemical features were investigated. Triplicates of the FS2 exudate treated and untreated *Microcystis* strains PCC 7806 and *ΔmcyB* were tested for their electric conductivity, pH and color appearance of the desiccated cell free FS2 medium.

Table 3-5: Physico-Chemical Characteristics of FS2-treated Media

Test parameter	**WT_sup – WT_co**	**MU_sup – MU_co**	**FS2 spent medium**
Color			Slightly yellowish to orange
pH differences	9.40 – 9.00	9.55 – 9.18	8.30
Conductivity [mS]	2.21 – 2.16	2.18 – 2.12	2.26

The electric conductivity in the treated cultures was slightly higher compared to the control cultures. That might have resulted from the dilution with the FS2 spent medium, which showed elevated values of these parameters. Interestingly, the pH values of FS2 exudate treated cultures were higher than those of the control cultures despite the fact that the pH of the freshly prepared FS2 exudate was considerably lower (Table 3-5). Therefore, it was assumed that the elevated pH resulted from cellular reactions of the treated *Microcystis* cells in response to the applied stimulus and not emerging from simple addition of alkaline compounds. The observation that the desiccated supernatant of FS2 cultures exhibited a deviating color appearance from other desiccated *Microcystis* supernatants, supports the notion of a considerably deviating

chemical composition of the cell exudates. The origin and identity of the color giving compounds however, was not further investigated.

A solid phase extraction via silica-based C18 Sep-Pak cartridges was conducted to separate hydrophobic from hydrophilic phases of the FS2 spent medium. Both phases were then tested for their bioactivity and effects on cell aggregation. Cell aggregating activity from the FS2 exudate was thereby distinctly attributed to its hydrophilic components.

3.2.8 The Transcriptional Response of PCC 7806 to the Exudate of FS2

In microarray experiments the transcriptional response of the *Microcystis* strain PCC 7806 to the FS2 exudate was measured in order to evaluate which cellular processes were involved in the specific *Microcystis* inter-strain interactions, that caused the strong observed aggregation effects. Three replicates of PCC 7806 cultures treated with FS2 exudate were compared to three replicates of the BG-11 -treated control samples. A sampling time of one hour after treatment was chosen for the transcriptomic analysis. Considering that the induced aggregation effects started occurring after 30 minutes and were strongly visible after one hour (Figure 3-10, page 68), it was assumed that differences in RNA-contents would be well detectable after one hour.

3.2.8.1 Quality Assessment of transcriptomic Microarray Data

The data analysis included an initial validation of the microarray quality. A comparison of the complete transcriptome datasets representing a) samples of the single replicates and b) the respective treatment samples, was conducted (Figure 3-15).

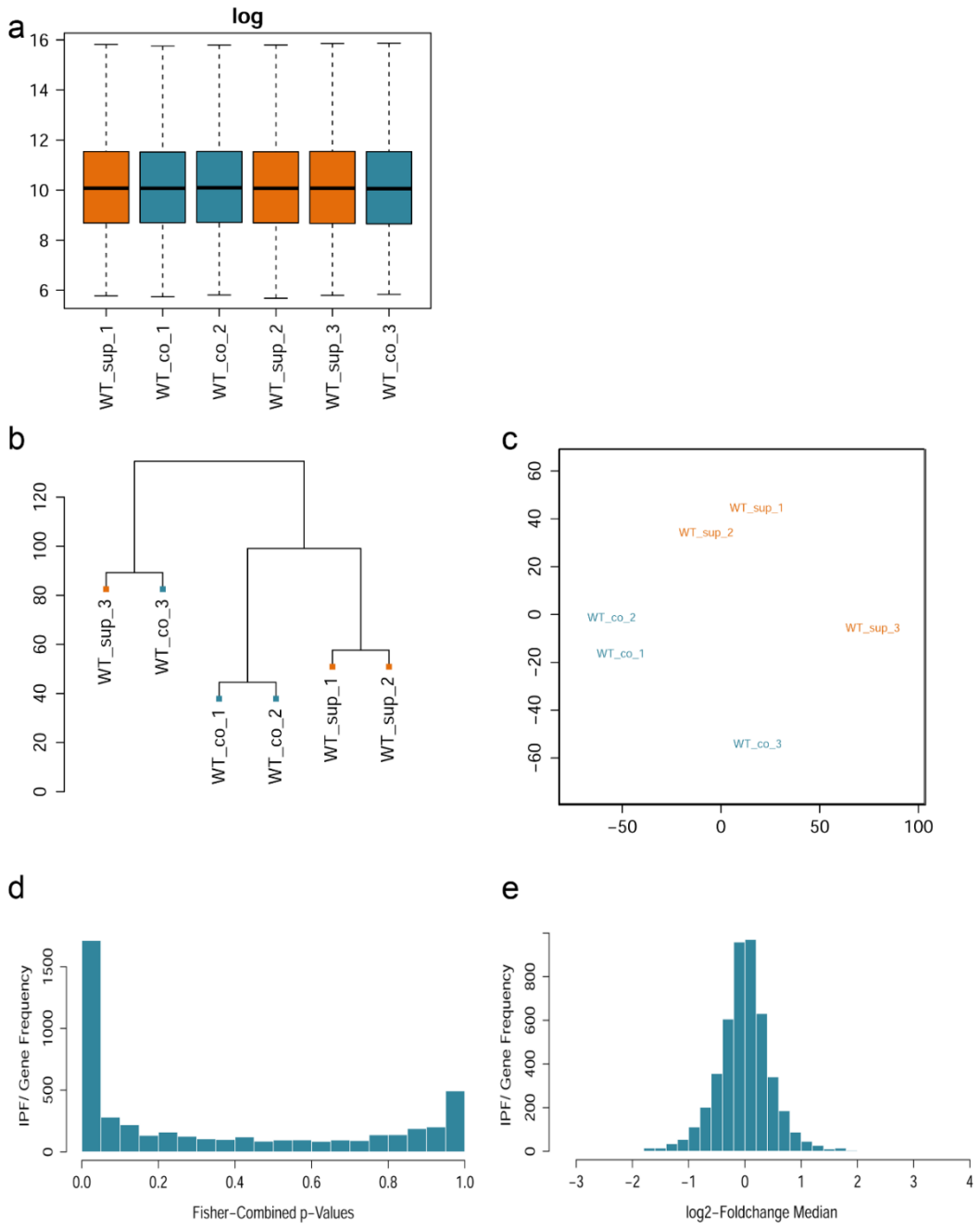

FIGURE 3-15: EVALUATION OF THE MICROARRAY DATASETS

a: overall log2-expression values of the replicate datasets of *Microcystis aeruginosa* PCC 7806 control samples (WT_co_1-3) and corresponding samples treated with *Microcystis* FS2 spent medium/exudate (WT_sup_1-3); **b**/**c**: similarities between the considered datasets, dendrogram of hierarchical clustering using the Euclidian distance matrix (**b**), Multidimensional scaling (MDS) (**c**) calculated from the results of the hierarchical clustering in (**b**). **d**: p-value distribution for the numbers of genes, **e**: distribution of log2-fold changes for according gene numbers.

The results show that the majority of log2-transformed transcription levels of the treated and untreated replicates scatter around the same value in each sample, indicating successful normalization and good comparability (Figure 3-15 a). Hierarchical clustering based on the Euclidian distance matrix was used to display the overall similarity between datasets (Figure 3-15 b). These results were further used for a multidimensional scaling analysis (MDS) (Figure 3-15 c). Both plots visualize that expression in datasets of the replicates WT_co_3 and WT_sup_3 vary from the other two pairs. The MDS plot however, indicates that control datasets are similarly distant from the respective treatment datasets and thus most likely result from similar physiological effects of the FS2-supernatant on PCC 7806 gene expression. It can be assumed that the replicates designated number 3 show a different overall expression pattern due to their measurement on a different array slide which can have enormous impact on the acquired datasets. Further statistical evaluation of the datasets confirmed robust expression data. The determined log2-fold changes exhibited a Gaussian distribution as expected with only minor deviations (Figure 3-15 e). The majority of calculated p-values was found in the range between 0-0.1 confirming a high likelihood for non-random expression results (Figure 3-15 d). Considering these preliminary analyses, the threshold for differential gene expression was set to a log2-fold change (lfc) of $1 \leq lfc \leq -1$ and p-values ≤ 0.1 which resulted in over two hundred differentially expressed genes in PCC 7806 after the addition of FS2-supernatant to the batch culture.

3.2.8.2 Differential Expression according to Functional Gene Categories

Of the 215 differentially expressed genes slightly more than 50 % were downregulated (116) while 46 % (99 genes) were upregulated after the stimulus of the FS2 exudate. The assignment of functional groups to every gene allowed to determine functional hotspots of differential gene expression.

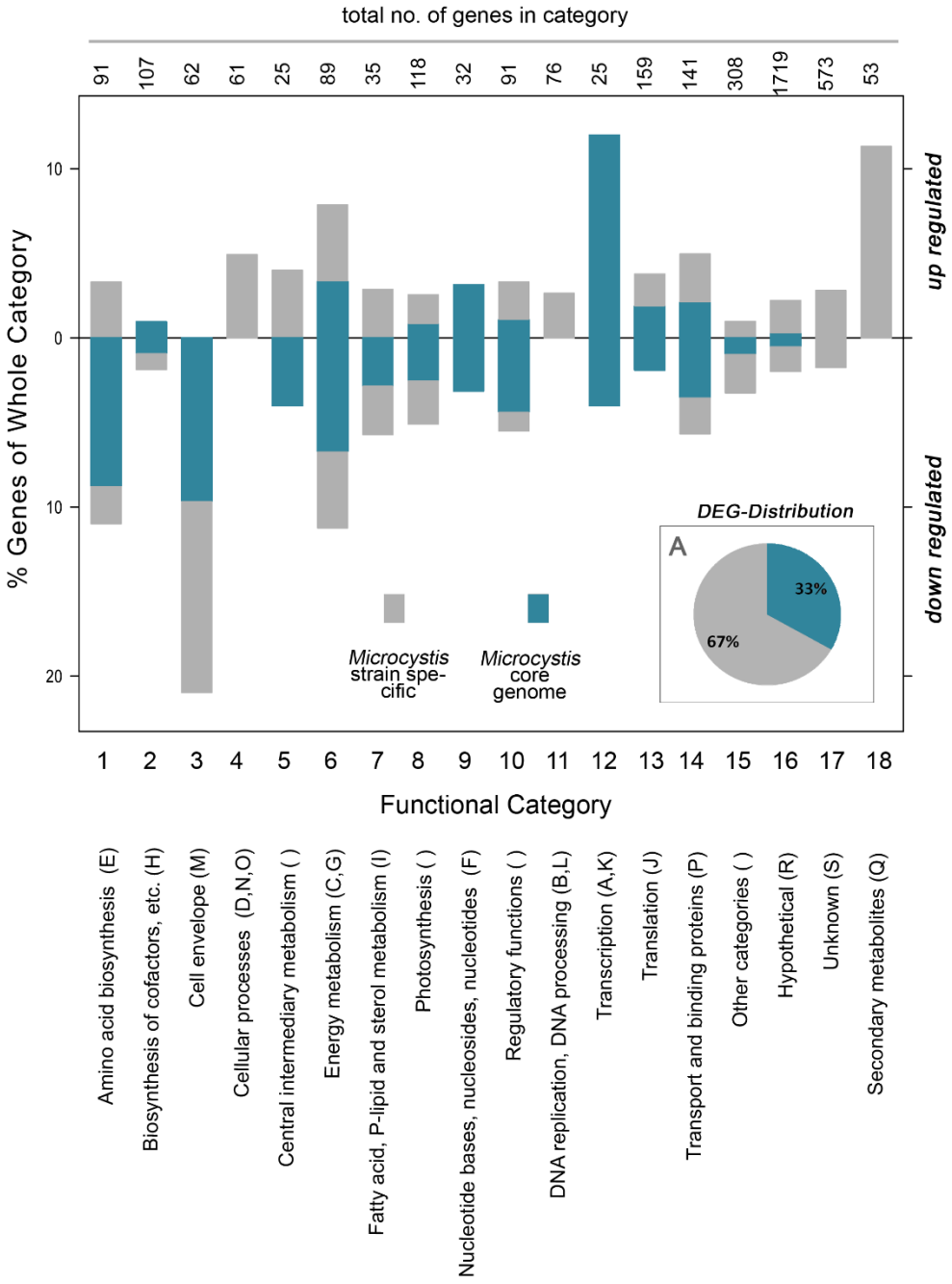

Figure 3-16: Differential Gene Expression According to Functional Gene Categories
The percentage of functional gene categories showing differential up- or downregulation with separation into genes belonging to the core genome of *Microcystis* (blue) and into strain specific genes (grey). Gene categories are obtained from CyanoBase (Kazusa genome resources; http://genome.microbedb.jp/cyanobase/) and listed with their according COG-categories (**Table 2-5**, page 42). The total number of genes belonging to one category is given on top of the bars.

Figure 3-16 shows the percentages of each assigned functional category that was up- and down-regulated. The most affected categories comprised amino acid biosynthesis, cell envelope related genes, energy metabolism, transcription, transporter genes, and secondary metabolites. This general overview illustrates that the addition of a *Microcystis* cell exudate can trigger comprehensive transcriptional changes in PCC 7806 regarding the primary as well as the secondary metabolism. Remarkably, the differentially expressed genes turned out to belong to a great part of 67 % to a set of genes that is so far considered to be strain specific to PCC 7806 and therefore are not part of the essential genes of the core genome. Consequently, the reaction of PCC 7806 to the FS2 exudate was considered highly specific and presumably is considerably different from the response of other *Microcystis* strains to the same stimulus.

3.2.8.3 Transcriptional Changes in PCC 7806 cells after FS2 Exudate Treatment in the Cellular Context

The transcriptional changes of PCC 7806 cells are displayed in regard to the involvement into metabolic processes and the cellular context (Figure 3-17, page 81). Differentially expressed genes belonging to the functional gene categories of transporters, regulators, energy metabolism, amino acid biosynthesis and cell envelope structures as well as secondary metabolites will be described in detail below.

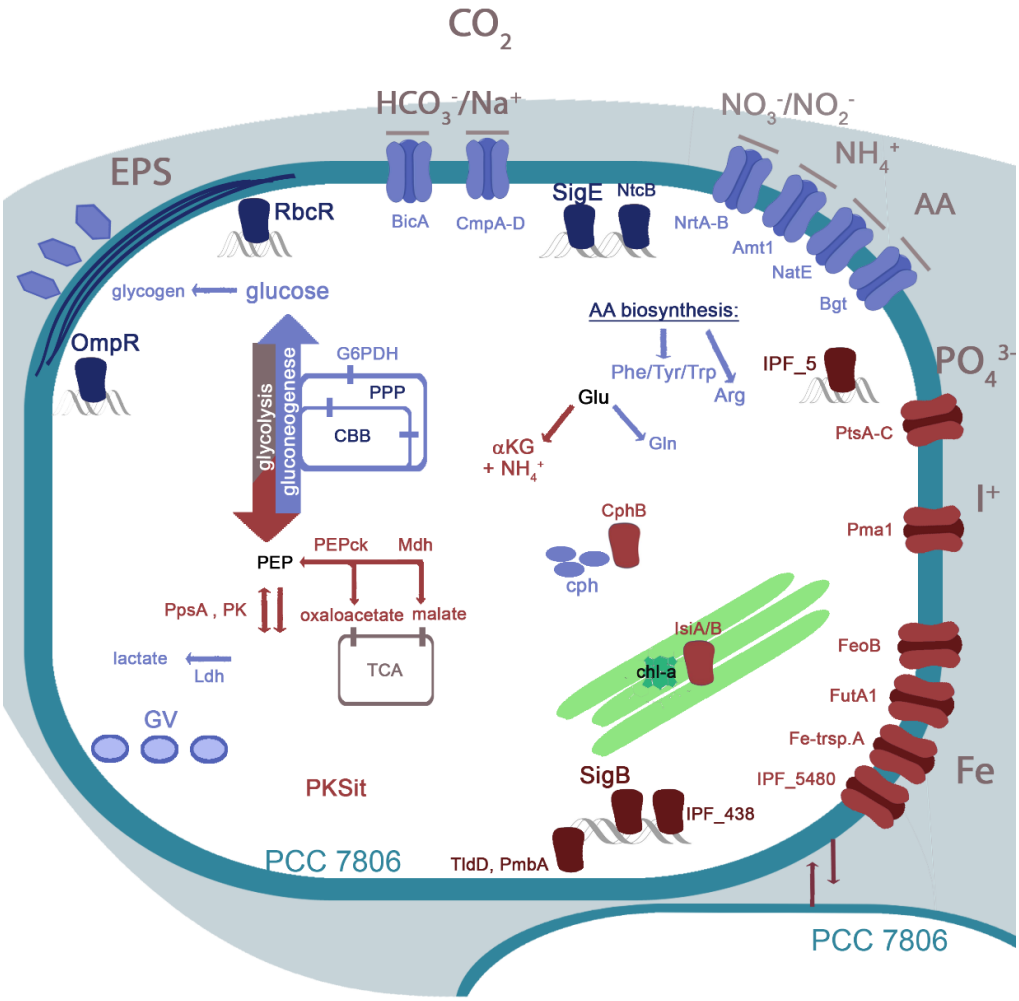

FIGURE 3-17: OVERVIEW OF THE CELLULAR AND TRANSCRIPTIONAL RESPONSES OF PCC 7806 TO THE CELL EXUDATE OF *MICROCYSTIS* FS2

Differential gene expression of cell components and proteins in PCC 7806 cells. Blue: downregulated components, red: upregulated components, grey: unchanged components. Proteins in darker/more intense colors represent transcriptional regulators. Green: thylakoids and chlorophyll (transcriptionally not altered). **EPS**: Extracellular polysaccharides, **G6PDH**: glucose-6-phosphate dehydrogenase, **PPP**: pentose phosphate pathway, **CBB**: Calvin-Benson-Bassham cycle, **PEP**: phosphoenolpyruvate, **PEPck**: phosphoenolpyruvate carboxykinase, **Mdh**: malate dehydrogenase, **TCA**: tricarboxylic acid cycle, **Ldh**: lactate dehydrogenase, **PK**: pyruvate kinase, **PpsA**: phosphoenolpyruvate synthase, **GV**: gas vesicle, **AA**: amino acid, **α-KG**: α-ketoglutarate, **cph**: cyanophycin, **IsiA/B**: iron stress induced proteins, **chl-a**: chlorophyll-a, **I+**: cations, regulators: (OmpR, RbcR, SigE, NtcB, IPF_5, SigB, TldD, PmbA)

3.2.8.4 Nutrient Homeostasis and Stress Indicators

The transcriptional data suggested that a striking, immediate change was triggered concerning the nutrient flows across the cytoplasmic membrane of the PCC 7806 cell. Several nitrogen uptake systems comprising transporters for nitrate, nitrite, ammonium as well as for several amino acids (*nrtA/B, amt1, natE, bgt*) were significantly downregulated after the FS2 exudate stimulus, while phosphate transporters were less effected with only one transporter being slightly upregulated.

3.2.8.4.1 Iron Stress Indicators

In contrast, a group of genes involved in iron homeostasis was strongly upregulated, suggesting some form of iron depletion signal. Four iron transporters (*feoB, futA1*, IPF_14, IPF_54880) were upregulated in the range of a fold change between 2.6 – 3.0 being in good accordance with the high upregulation of the two iron stress indicators *isiA* and *isiB* (iron stress induced chlorophyll binding protein A and flavodoxin). Following this strong lead of putative iron limitation induced after the addition of FS2 exudate to PCC 7806 cultures, the confirmation of iron stress was sought on the physiological level, as well. Spectral analysis of PCC 7806 cells were supposed to show on the protein level if the IsiA-binding to chlorophyll induced the typical shift of the chlorophyll absorption maximum to a lower wavelength (Andrizhiyevskaya, *et al.*, 2002).

During the time course experiment displayed in Figure 3-10 (page 68) samples were taken to analyze the absorption changes of the PCC 7806 cultures after FS2 exudate treatment. In Figure 3-18 the recorded spectra after 3 h and after 96 h after the treatment are shown for PCC 7806 and *ΔmcyB* cultures.

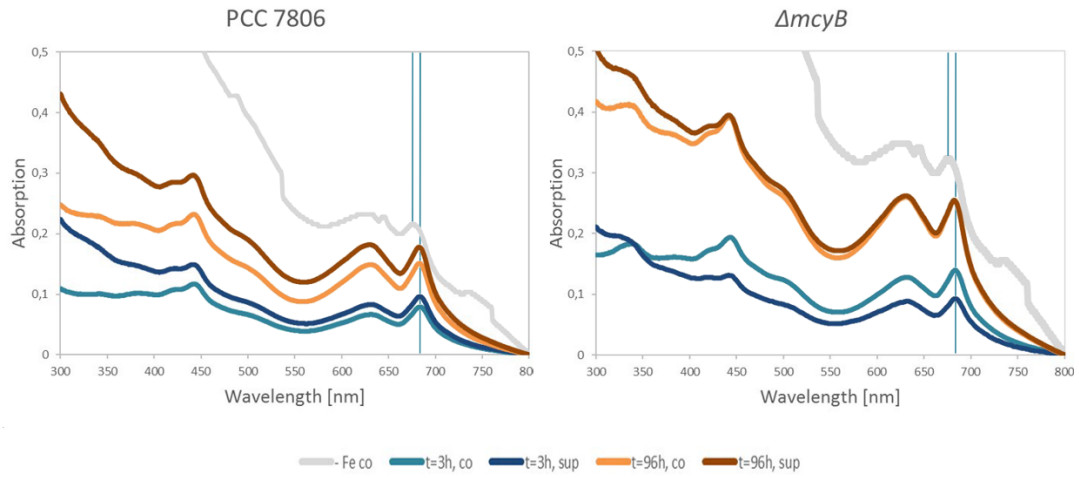

FIGURE 3-18: ABSORPTION SPECTRA OF PCC 7806 AND *ΔMCYB* CULTURES AFTER TREATMENT WITH FS2 EXUDATE

Absorption spectra were recorded after 3 and 96 h. Blue bars mark the shift of maximal chlorophyll absorption of ca. 10 nm

None of the tested cultures, exhibited a significant change in the absorption characteristics around 675 nm, which would indicate IsiA-binding to chlorophyll-a in response to iron limitation. Nevertheless, similarities to the typical absorption spectrum resulting from iron depletion within a *Microcystis* culture were detected, showing an increased absorption in the range of 300 – 400 nm. Furthermore, different acclimation dynamics of the wild type compared to the mutant were found, reflected by an inverted relation of absorption levels of control versus treated cultures in the early response (3 h). Additionally, the mutant exhibited larger differences in absorption levels after treatment and a generally higher absorption. Both, wildtype and mutant cultures showed an altered relation of absorption peaks at 630 and 675 nm. After FS2 exudate treatment, the phycocyanin amounts (absorption at 630 nm) increased in relation to those of chlorophyll (absorption at 675 nm). These changes, however, were not seen on the transcriptional level concerning biosynthesis genes of both, chlorophyll and phycocyanin.

After a potential iron stress had not shown on the protein level after FS2 exudate application, alternative causes for the transcriptional activation of iron stress related genes were tested. A decreased extracellular iron availability through the hypothetical Fe-scavenging by siderophores in the FS2 exudate and their iron complexing features were tested via the CAS-assay (Schwyn, *et al.*, 1987) for liquid media. The assay was performed for the spent medium of FS2 and compared to those of PCC 7806, *ΔmcyB* and FS66. Since the CAS assay is pH-sensitive, cell exudates were tested with an adapted pH of 5.6 and with the original pH in the range of 9.25-9.6. Neither of the tested exudates revealed significant differences in the iron complexing characteristics. A siderophore presence in the exudate of FS2 cultures of significant concentrations was hence dismissed.

3.2.8.4.2 Bicarbonate Import

Returning to the differential gene expression of transporter genes after the application of FS2 exudates to PCC 7806 cultures, two genes regarding inorganic carbon uptake showed most pronounced expression changes. The bicarbonate/sodium antiporter *bicA* and the associated sodium/proton antiporter *nhaS3* were downregulated to each 20 % and 10 % of the expression levels of control samples. Another bicarbonate uptake system *cmpA-D* was downregulated as well but to a lesser extent than *bicA*.

3.2.8.5 Stress Indicators and Regulatory Proteins

Considering that inorganic carbon uptake is essential to phototrophic life, the putative decrease of it was assumed to be implicated in cellular stress reactions. Stress indicators (*isiA, isiB*) were already found transcriptionally upregulated when investigating iron homeostasis. In addition to that, the observed aggregation of *Microcystis* cells can be found under various stress conditions

(Kehr, *et al.*, 2015; Wang, *et al.*, 2010). Differentially expressed genes were thus screened for further stress indicators and transcriptional regulators that might provide hints to the cellular processes induced by the FS2 exudate.

TABLE 3-6: TRANSCRIPTIONAL CHANGES OF STRESS MARKERS AND TRANSCRIPTIONAL REGULATORS

Gene	PCC 6803 homologue	LFC	Regulatory role (reference)
hspA (2x)	sll1514	+1,09 +1,74	general stress
ompR	slr0081	-1,13	acid stress (Tanaka, *et al.*)/ phosphate sensing
SigB	**sll0306**	**+2,49**	**high salt stress (Allen, *et al.*, 2008)/ high temperature (Tuominen, *et al.*, 2006)/ redox potential related (Imamura, *et al.*, 2003)**
IPF_438	sll0474	+1,11	osmotic stress (Milkowski, *et al.*, 1998)
pmbA	sll0887	+1,14	(metalloprotease regulating toxin-antidote systems/proliferation in *E. coli*) (Afif, *et al.*, 2001; Allali, *et al.*, 2002)
tldD	slr1322	+1,12	
fabG	sll0330	+1,28	Osmotic/ cold stress (Mikami, *et al.*, 2002)
ompR	sll1330	-1,55	Sugar catabolism (Tabei, *et al.*, 2007)
cphB	slr2001	+1,18	Supply with carbon-/nitrogen sources
SigE	sll1689	+0,76	Sugar catabolism (Osanai, *et al.*, 2011)/ nitrogen depletion
SigE/G	**slr1545**	**-1,42**	**NA**
rbcR	sll1594	-1,20	CCM activator (reviewed by (Burnap, *et al.*, 2015))
IPF_5	**sll0594**	**+1,86**	**Phosphate depletion (Kopf, *et al.*, 2015)**
IPF_1434	slr0701	-1,35	NA
IPF_3831	sll0690	+1,04	Butanol resistance (Zhu, *et al.*)

Typical stress indicators like *hspA* and *fabG* are slightly upregulated while other stress markers do not exceed the threshold, set for differential gene expression (Table 3-6). Further leads to identifying stress conditions are found among the transcriptional regulators, which are up or down regulated. Differentially expressed regulators (Table 3-6) were classified into two topics. While most of the regulators were implicated in responses to extracellular stimuli, like osmotic stress, acid stress or butanol resistance, another group of regulators was related to carbon availability, being in close correlation to the detected downregulation of bicarbonate transporters. It should be noted, that the strongest upregulation is seen for the alternative sigma factor SigB, which has been related to multiple environmental conditions (see Table 3-6).

The transcriptional response to the FS2 exudate showed only limited stress reactions and it was tested if the cultures themselves were impeded or on the contrary supported in cell division and growth. Growth rates of PCC 7806 and *ΔmcyB* cultures treated with FS2 exudate and BG-11 aliquots in control cultures were determined in a period of two weeks. The results showed only marginal growth differences, which were not significant (Table 3-7) indicating that the strong transcriptional response of PCC 7806 cells to the FS2 exudate did not coincide with a stress induced growth impediment.

TABLE 3-7: GROWTH RATES OF PCC 7806 AND *ΔMCYB* AFTER FS2 EXUDATE TREATMENT

Strain	Treatment	Growth rate / day
PCC 7806	Control	0.12 ± 0.02
	Fs2 exudate	0.11 ± 0.04
ΔmcyB	Control	0.12 ± 0.04
	FS2 exudate	0.11 ± 0.06

3.2.8.6 Energy Metabolism

As indicated before, the *bicA* HCO_3^- carbon uptake system and its associated *nhaS3* sodium/proton antiporter exhibited substantial expression differences after the FS2 exudate treatment.

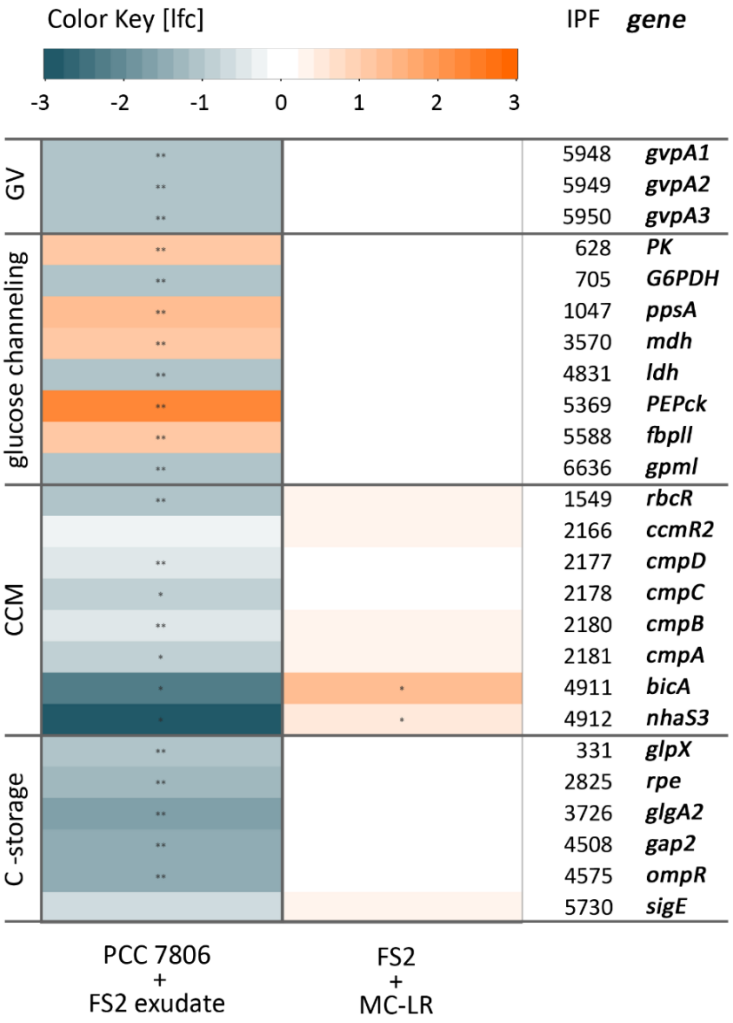

Figure 3-19: Differential Gene Expression in Energy Metabolism

Heatmap showing expression changes of carbon metabolism genes in PCC 7806 cells after FS2 exudate treatment and in FS2 cells after MC-LR treatment. Expression changes are given as median log2 fold changes (lfc) as indicated in the color code bar on top. Genes are sorted into categories of gas vesicles (GV), glucose channeling (glycolysis, pentose phosphate way gluconeogenesis and tricarboxylic acid cycle), carbon concentrating mechanism (CCM), and carbon storage related genes (C-storage). Gene designations are given as IPF numbers (individual protein file numbers) and gene abbreviations (gene).

Considering that the lack of imported inorganic carbon might affect further carbon processing pathways like carbon fixation during the Calvin Benson Bassham cycle or storage and degradation of carbon compounds, a comprehensive look was taken at affected genes belonging to the category of energy metabolism and related pathways (Figure 3-19).

All genes that showed differential expression were attributed to categories of the carbon concentrating meachnism (CCM), glucose channeling, and storage compounds. Additionally to the *bicA* uptake system, other components of the CCM were downregulated. This can be seen, for example in the downregulation of the HCO_3^- uptake system *cmpA-D*. CCM regulating genes confirm the tendency of downregulation, with the CCM activator *rbcR* being strongly downregulated while the repressing regulator *ccmR2* was only marginally affected. Other known components of the CCM regarding carboxysome synthesis or CO_2-fixation did not show significant expression changes. However, it should be noted that the CCM genes in question also showed an altered expression in FS2 cells, when treated with an external addition of 50 ng/mL microcystin-LR. Regarding the CCM genes, the non-toxic FS2 thus showed a reverse response to an external cyanobacterial peptide when compared to the reaction of the toxic PCC 7806 to the exudate of FS2.

During the analysis of carbon metabolic genes, glycolysis regulators were found slightly downregulated (*sigE*/IPF_5730 homologue to sll1689 of PCC 6803 shows lfc=-0.75; ompR/IPF_4575/homologue of sll1330: lfc=-1.55) after the FS2 exudate stimulus. The identified target genes of OmpR in glycolysis (glucokinase: *glk* [sll0593]; phosphofructokinase: *pfkA* [sll1196], fructose 1,6-bisphosphate aldolase: *fbaA* [sll0018]; phosphoglycerate mutase: *gpmB* [slr1124], and pyruvate kinase *pk* [sll0587]) (Tabei*, et al.*, 2007) were all marginally downregulated as well, with the exception of the pyruvate kinase. In fact, the PK belongs to a subcategory of glycolytic genes that showed most prominent upregulation. Among them are the phosphoenolpyruvate carboxykinase (PEPck), the pyruvate kinase (PK), and the phosphoenolpyruvate synthase (PpsA). Those represent the passage between glycolysis and tricarboxylic acid cycle (TCA) and thus might shift their reactions to one direction depending on the utilization of

their reaction products. Genes involved in the TCA hardly showed differences in expression with the exception of the malate dehydrogenase, which is upregulated under the tested conditions. Interestingly, the differentially upregulated PEPck and PK in question are not well conserved among cyanobacteria and the affected orthologues are only present in *Microcystis* and a few *Cyanothece* species. Apart from the glycolytic genes, other carbon processing channels appeared to be blocked by the downregulation of enzymes in key positions. This includes the downregulation of glucose-6-phosphate dehydrogenase as first step of the pentose phosphate pathway and downregulation of the lactate dehydrogenase (Ldh), which might decrease the reaction of pyruvate to lactate catalyzed by Ldh.

Among the genes related to carbon storage generation, a general pattern of downregulation was induced after the treatment of PCC 7806 with FS2 spent medium. This occurred for single genes on all levels that are involved in the generation of carbon storage compounds. Genes of the primary carbon fixation during the CBB (*glpX*) as well as genes of gluconeogenesis (*gap2*) (Koksharova, *et al.*, 1998) and glycogen synthesis genes (*glgA2*) are down regulated.

Due to the negative correlation between the accumulation of storage compounds as ballast freight and gas vesicle mediated buoyance in vertical migration of *Microcystis*, both parameters were compared regarding the differential regulation of involved genes. The significant downregulation of gas vesicle genes in the current transcriptional investigations was evaluated as indicator for decreased buoyancy, whereas the reduced accumulation of storage compounds would not support cell sinking tendencies. Nevertheless, PCC 7806 cells did sink to the bottom after the treatment with FS2 exudate and thus captured the opposite position to the FS2 cells, which were floating at the culture surface under standard cultivation conditions.

3.2.8.7 Amino Acid Biosynthesis Genes

The analysis of the transcriptional data of PCC 7806 cells after the stimulus of FS2 spent medium showed that genes of the amino acid biosynthesis gene category were affected in 14 % of the genes. This includes exclusively genes of the subcategories for the glutamate/nitrogen assimilation family, the serine family, and the aromatic amino acid family. In detail, the data suggest that the biosynthesis of the amino acids tryptophan, phenylalanine, and tyrosine as well as arginine and glutamine was reduced via the downregulation of the genes *aroK* (shikimate kinase), *trpC* (indole-3-glycerol phosphate synthase), *argJ* (arginine biosynthesis bifunctional), and the two glutamate ammonia ligases *glnA*, *glnN*. While all of these genes are downregulated with log2-fold changes (lfc) between -1.05 and -1.67 one gene was 5.76-fold upregulated to an lfc of 2.4 (*gdhA*). The strongly upregulated glutamate dehydrogenase catalyzes the reversible reaction of glutamate plus $NAD(P)^+$ to α-ketoglutarate + NH_4^+. Thus, its upregulation might indicate an increased utilization of the amino acid glutamate to provide α-ketoglutarate and NH_4^+.

Due to the close connection between amino acid biosynthesis and nitrogen metabolism, the down regulation of the regulator gene *ntcB* should be mentioned here. The regulator NtcB was previously reported to be responsible for nitrate assimilation in *Synechocystis* PCC 6803 (Aichi, *et al.*, 2001). Its downregulation and the downregulation of target genes like the above mentioned transporters *nrtA/B* (section 3.2.8.4, page 82), and ferredoxin-nitrite/nitrate reductase genes *nirA* and *narB* supports the notion of a decreased nitrate assimilation in PCC 7806 cells after treatment with FS2 exudate.

3.2.8.8 Cell Envelope Related Expression Changes

Over 20 % of the genes assigned to the functional category of the cell envelope were differentially downregulated after the FS2 exudate stimulus. Enzymes of the peptidoglycan biosynthesis and exopolysaccharide (EPS) biosynthesis were affected most. Downregulated key players of the cell wall synthesis included *murA* and *murC* genes as well as the D-alanine-D-alanine ligase *ddlA* and the transpeptidase (D-alanyl-D-alanine carboxypeptidase) *dacB*. A strong impact on cell division and arrest of cell growth however, was rejected, due to the fact that growth rates did not differ significantly between FS2 exudate treated and untreated PCC 7806 cultures. Production of L-rhamnose, a typical component of released polysaccharides, which can shape cell surface characteristics (Mandal, *et al.*, 2014), was transcriptionally impeded via the downregulation of the biosynthesis gene cluster *rfbABCD*.

3.2.8.9 Secondary Metabolites

Among the secondary metabolite synthesis genes that showed differential expression in response to the spent medium of FS2, genes belonging to an orphan PKS synthesis cluster designated PKSit (IPF_3353-IPF_3362) (Frangeul, *et al.*, 2008) were found. The upregulation of the whole cluster was determined in the range of a threefold higher expression (lfc=~1.65). In this respect it should be noted, that an unknown metabolite was detected in MALDI imaging approaches (949.486 *m/z,* Figure 3-14, page 74) in PCC 7806 in response to the FS2 co-cultivation stimulus. Based on the current data, this metabolite might represent a potential candidate for the unidentified PKSit-metabolite. Both strains (PCC 7806 and FS2) contain the genomic resources for the production, but FS2 did not produce the metabolite of the mass 949.486 *m/z* under the tested conditions, neither in mono-cultivation nor in co-cultivation.

4 Discussion

4.1 The Transcriptomic View into a *ΔmcyB* Mutant Cell

The microcystin deficient *ΔmcyB* of the *Microcystis aeruginosa* wild type strain PCC 7806 generated in 1997 (Dittmann, *et al.*, 1997) has been used in several comparative studies in order to gain deeper insights into the biological role of microcystin. Additionally, distinct environmental conditions that influence microcystin production such as nitrogen availability or light conditions were under extensive investigation (Harke, *et al.*, 2013; Kaebernick, *et al.*, 2000; Sevilla, *et al.*, 2010; Straub, *et al.*, 2011). Toxic and non-toxic *Microcystis* strains showed different adaptation behaviors concerning high light conditions, CO_2-levels, or the proteinaceous cell envelope composition (Kehr, *et al.*, 2006; Van de Waal, *et al.*, 2011; Zilliges, *et al.*, 2011). The transcriptomic profile of the mutant has for the first time provided a comprehensive view on gene expression patterns in the mutant, which represents complementary information to earlier proteomic and metabolomic studies (Meissner, *et al.*, 2014; Zilliges, *et al.*, 2011). Implications of microcystin within a broad variety of physiological aspects could also be found on the transcriptomic level and revealed a comprehensive reprogramming concerning central primary metabolic pathways (Figure 3-5, page 53).

In the microcystin deficient mutant cell, carbon turnover related processes seem to be diminished to a great extent. While the synthesis of the storage polyester PHA is shut down, the breakdown of glycogen is equally reduced in the mutant. Subsequent heterotrophic carbon utilization pathways to generate ATP, such as glycolysis, the TCA-cycle, and respirational oxidases show a similar downregulation. At the same time, the extreme upregulation of the adenine phosphoribosyltransferase gene (*apt*) in correlation with the upregulation of ATP synthase subunits probably indicates a high demand for AMP in the oxidative photosynthetic ATP generation. This implies an altered balance in the photosynthetic electron flows of the *ΔmcyB* mutant cells, which is further

supported by a lower ratio of PSI to PSII expression. Similar changes in PSI amounts relative to amounts of PSII were proposed in earlier comparative studies of PCC 7806 and its non-toxic mutant under low light conditions as means of stress acclimation (Hesse, *et al.*, 2001). The role of PSI portions has been strongly discussed in respect to capturing electrons that might otherwise be channeled towards the plastoquinone pool and thus, potentially facilitate photodamage (Baker, *et al.*, 1996) or be shifted towards respirational terminal oxidases, limiting CO_2-fixation in photosynthesis (Vermaas, 2001). The reduced PSI transcription found in the *ΔmcyB* mutant might therefore reflect a transcriptional program that is based on a decreased need for photoprotection and on non-occurring limitations of CO_2-fixation. A reduced need for photoprotection against oxidative stress might also be met by the downregulation of the redox-state regulating bidirectional hydrogenase (*hox* genes) found in the microcystin deficient mutant.

The transcriptional modifications within the *ΔmcyB* mutant cells appear to be controlled through the regulatory actions of four transcription factors and regulators. The major part in which is played by the alternative sigma factor SigE. The target genes of SigE have been identified in an *Synechocystis* PCC 6803 overexpression mutant (Osanai, *et al.*, 2011) and comprise most of the differentially expressed genes in the *ΔmcyB* mutant that are involved in carbon catabolism. The regulon of SigE further includes the *hox* genes and the *ycf27* regulator gene. Thus, Ycf27 is positioned downstream of SigE in the regulatory cascade and in turn affects aspects of the photosynthesis and the transfer of excitation energy from phycobilisomes to photosystem I (Ashby, *et al.*, 2002). This regulator might also be correlated with the KaiB1 expression, since a correlation between Ycf27 and circadian clock output had been recently found (Espinosa, *et al.*, 2015). It can be assumed that the fourth of the regulators, IPF_1434, which was found differentially expressed in the *ΔmcyB* mutant, is operating either upstream of SigE or is independently addressed by another regulating signal. Due to its immense downregulation, IPF_1434 is considered to play a crucial role in microcystin related matters. The distinct mechanism

that causes the differential expression of SigE and others in the absence of microcystin is so far unknown. A regulation through the covalent binding of microcystin to transcription factors as shown for the binding to RubisCO (Zilliges, *et al.*, 2011) is theoretically conceivable and will require further testing.

The transcriptomic view on a microcystin deficient cell has shown comprehensive reprogramming of genes regarding the primary metabolism. Comparable results were found in proteomic studies (Zilliges, *et al.*, 2011), where microcystin was shown to influence enzymes from the CO_2-fixation in the Calvin-Benson-Bassham cycle, like RubisCO. A metabolomic comparison of the *ΔmcyB* mutant and the PCC 7809 wild type after high light stress revealed the strongest differences in the accumulation of carbon storage and intermediate metabolites (Meissner, *et al.*, 2014). Regarding many genes, the transcripts, found differentially expressed in this study did not coincide with expression changes of the same proteins in comparative proteomic studies. These findings indicate that microcystin has independent regulating effects on both levels, influencing protein abundance by protective covalent binding, and influencing transcriptional programs through a yet unknown mechanism. While single candidates of differential transcripts, proteins and metabolites differ considerably in their regulation between the *ΔmcyB* mutant and the wild type, the majority of them is correlated with light dependent carbon channeling processes.

4.2 Discussing the Physiological Roles of Microcystin

In complementation to other comparative studies between the *ΔmcyB* mutant and the PCC 7806 wild type (Meissner, *et al.*, 2014; Zilliges, *et al.*, 2011), this transcriptomic study was intended to obtain new insights into the physiological roles of microcystin. The transcriptomic differences between the *Microcystis*

ΔmcyB mutant and the PCC 7806 wild type were clustered decisively around genes concerning carbon metabolism and related processes. Several previous studies had already stated a clear correlation between the adaptation to either high or low environmental CO_2-levels and the ability of *Microcystis* strains to produce microcystin. While toxic strains (microcystin producers) seemed well adapted to low CO_2-levels and were outcompeting their non-toxic counterparts in direct competition, the non-toxic strains dominated under conditions of high levels of dissolved CO_2 (Van de Waal, *et al.*, 2011). Interestingly, it was shown that in return the microcystin production in toxic strains increased considerably under conditions of inorganic intracellular carbon deficiency (Jähnichen, *et al.*, 2007). Based on these research findings and on the transcriptional insights into mutant and wildtype cells a model is proposed as to how microcystin may be involved in the respective adaptation to carbon availability and which cellular processes are affected in order to enable acclimation of the cells to respective environmental conditions (Figure 4-1**Fehler! Verweisquelle konnte nicht gefunden werden.**).

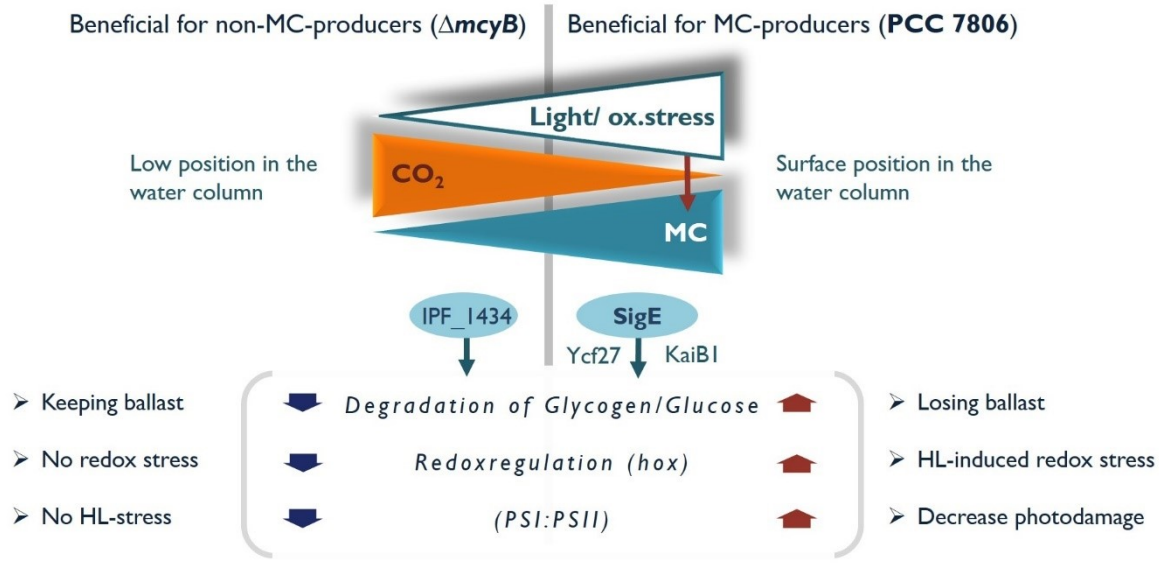

FIGURE 4-1 MODEL OF THE MICROCYSTIN EFFECTS ON CARBON METABOLIC PROCESSES AND REDOX-REGULATION

The adaptation of toxic microcystin producers to low carbon availabilities implies advantages in *Microcystis* blooms, where under high light intensities CO_2 is frequently depleted and high amounts of microcystin are produced (Kaebernick, *et al.*, 2000; Meissner, *et al.*, 2013; Talling, 1976). The high light intensities are at the same time implicated in oxidative stress and related photodamage. While these conditions predominantly occur on surface positions of aquatic habitats the opposing conditions are found in deeper water layers, where non-toxic *Microcystis* variants thrive. The transcriptional data has identified molecular processes that are underlying the preference to habitats of toxic and non-toxic *Microcystis* strains. In this respect the lower degradation of carbon storages, a decreased amount of photosystem I and a lesser expression of redox-regulating *hox*-genes in the microcystin deficient mutant are named. It might be speculated that altered mobilization of carbon storages greatly influences buoyancy regulation, since these storage compounds also represent ballast freight to the cell (Thomas, *et al.*, 1985). Maintaining ballast freight by reducing storage mobilization in the *ΔmcyB* mutant, thus, would keep the non-toxic strain within deeper water layers that exhibit the environmental conditions non-toxic *Microcystis* is suited best for. On the other hand, toxic variants would stay afloat, with less carbon ballast, also exposed to high light induced oxidative stress conditions. In this context, microcystin dependent elevated levels of the redox-regulating bidirectional hydrogenase (*hox*) probably serve the purpose of reducing redox stress. The same is true for the increased transcription of PSI that was implicated in the protection from photodamage (Baker, *et al.*, 1996).

In accordance with this proposed model, the regulation of microcystin is partly light dependent and its production is enhanced under high light exposure. While factors such as light and carbon availability influence the production of microcystin (Jähnichen, *et al.*, 2007; Kaebernick, *et al.*, 2000), the toxin itself appears to be implicated in the regulation of essential transcriptional regulators. The obtained data indicates that the alternative sigma factor SigE and its regulons capture an essential role as microcystin target in oxidative

stress acclimation and that SigE may be influenced directly or indirectly by the presence of microcystin. The suggested role of microcystin as regulating mediator in light dependent oxidative stress responses represents an addition to the protective effects that were shown in covalent protein binding as protective measures against RubisCO degradation (Zilliges, *et al.*, 2011). A role of microcystin as global regulator has been considered before (Wilhelm, *et al.*, 2011) and the transcriptional data give a first support for this hypothesis.

4.3 Cross-Talk Between Secondary Metabolites

This study has focused on the effects of multiple extracellular factors in *Microcystis* media as well as on the intra- and extracellular roles of a single secondary metabolite. The results have confirmed that secondary metabolites regularly capture roles as extracellular info-chemicals. Several of them were proposed to be part of a sophisticated communication within the water body (Kaplan, *et al.*, 2012). In this study, many known secondary metabolites were shown outside of *Microcystis* colonies in MALDI imaging approaches (Figure 3-14, page 74) and hence, might be placed in their location of action this way. A very clear indication to an extracellular function of microcystin-LR in PCC 7806 was found after the extracellular application of microcystin-LR had specifically induced the transcription of an unknown PKSI/III metabolite. While other studies had reported an additional autoinduction effect of extracellular MC-LR (Schatz, *et al.*, 2007) suggesting a form of quorum sensing, the signaling effects of microcystin were shown to be directed specifically to another metabolite under the tested conditions. The data suggests that this effect is accomplished by the extracellular perception of microcystin and signal transduction rather than by an import of microcystin, which would presumably reverse more of the transcriptional differences between the mutant and the wild type than the regulation of a single gene cluster. The significant differences in secondary metabolite transcription at different light or carbon supply conditions (Figure

3-13, page 72; Figure 3-7, page 61) illustrate that there are additional regulatory stimuli to enhance the production of the respective secondary metabolite and it can be assumed that several levels of regulation are in place. For instance, the shift of MC-LR to a desmethylated microcystin variant was found under *Microcystis* co-cultivation conditions and might have yet unidentified downstream effects. The specific control of microcystin over the PKSI/III metabolite finds parallels in similar interdependencies between secondary metabolites. On the one hand, this is indicated by reciprocal expression patterns of the metabolites cyanopeptolin, microcyclamide and aeruginosin that are increased under conditions of eliminated microcystin production (in *ΔmcyB* mutant cells) (Figure 3-7, page 61). On the other hand, the changes of metabolite amounts in response to extracellular signals from another *Microcystis* strain (Figure 3-13, page 72), (Briand*, et al.*, 2015) reflect comparable regulating patterns. The numerous interdependencies of secondary metabolite production in correlation to the particular wealth of secondary metabolites in cyanobacteria (Dittmann*, et al.*, 2015), might indicate a regulatory network and intricate cross-talk among them.

This study also showed that single secondary peptides captured a highly specific signaling role, when applied extracellularly. Under the tested conditions microcystin did not cause global changes to *Microcystis* transcriptomes and physiology. The role of distinct secondary signaling peptides as info-chemicals might be more of an accumulative nature under field conditions and other extracellular substances and stimuli potentially exert larger impacts on global metabolic transitions in *Microcystis* cells. In this respect, *Microcystis* interactions might encompass more versatile communication and signaling processes than previously assumed.

4.4 The Transcriptomic View into a PCC 7806 Cell After the Treatment with Spent Medium of *Microcystis* FS2

After simulating a co-habitation of the axenic *Microcystis* lab strain PCC 7806 and the recently isolated uncharacterized *Microcystis* field strain FS2, by incubating the lab strain with the spent medium of the field strain, it became apparent that very strong effects were exerted on the lab strain PCC 7806. These effects were visible on the phenotypic level and included a strongly elevated cell aggregation with aggregates sinking to the bottom of the water column. Furthermore, a broad transcriptional response was triggered involving 215 genes from the primary and the secondary metabolism. The transcriptional changes induced in PCC 7806 cells were summarized in Figure 3-17 (page 81), displaying the reactions in a cellular and metabolic context.

From Figure 3-17 on page 81 it can be seen that the transcriptional response to the extracellular stimulus of FS2 exudates induces a considerable reorganization of the cell envelope, which affects the cell wall as well as extracellular polysaccharides. It can be assumed that this reorganization of the cell envelope contributes to the observed "sticky" aggregating phenotype induced in PCC 7806. Cell aggregations and an altered EPS composition and mucilage production has been reported in *Microcystis* before as acclimation mechanisms to various physico-chemical stimuli and stress factors (Kehr, *et al.*, 2015; Wang, *et al.*, 2010; Xu, *et al.*, 2014).

In close connection to the altered envelope structures, an extensive shut down of nutrient uptake system was observed after the treatment with FS2 exudates. It might be speculated that both, the altered envelope structures and the downregulation of transmembrane transporters were initiated as protective measures against the added extracellular compounds from the FS2 exudates. This assumption goes hand in hand with the observation that the entire set of affected transcriptional regulators was shown to respond to extracellular chemical stimuli (Table 3-6, page 85). At the same time, the transcriptional results have shown a reduced production of the EPS compound L-rhamnose.

Considering the extensive shut down of HCO_3-import, a cellular reaction that decreases the use of carbon units for EPS-production, which were shown to function as carbon sinks (Otero, *et al.*, 2003) might be economically reasonable for the cells. A decreased extracellular presence of saccharides was also correlated to a reduced iron availability for phytoplankton (Hassler, *et al.*, 2011) due to acting as organic ligands, which might explain the strong transcriptional induction of iron stress related genes in this study.

In the light of a strongly reduced nutrient uptake of carbon and nitrogen sources, the broad transcriptional changes in carbon and amino acid metabolism probably reflected adjustments to the new nutrient supply situation. While the carbon metabolism was driven towards a more heterotrophic energy acquisition through the TCA-cycle and reduced in any other carbon processing (glycogen synthesis, pentose phosphate pathway, lactate fermentation), amino acid biosynthesis seemed to be partly reduced with a shift towards reactions that would accumulate α-ketoglutarate. Since α-ketoglutarate is metabolically positioned at the interface between carbon and nitrogen metabolism, this accumulation might have been related to the low carbon situation within the cell. Similar metabolic fluxes were found in other studies of low carbon effects (Schwarz, *et al.*, 2014), and it was proposed that α-ketoglutarate might also function as co-repressor of the CCM (Daley, *et al.*, 2012), which is in good accordance with the downregulation of CCM genes in this study.

4.5 The Ecological Niches of Two *Microcystis* Strains

In this study, the simulated co-habitation of two *Microcystis* strains has resulted in substantial alterations of the morphological characteristics and transcriptional programs in one of these strains. The genomic differences were determined to make up at least 12.5 % of their genomes, which putatively

represents the potential for producing interaction mediators/compounds. The response to the FS2-signals triggered differential gene expression mostly in the fraction of genes that are not found in the core genome of *Microcystis,* but that belong to the flexible and strain specific genes, thus, being a preferential target in terms of responding to the signals of a fellow *Microcystis* representative. Beyond the genomic differences between the two investigated strains, a few apparent differences between PCC 7806 and FS2 might be used to attribute certain ecotypes to each of them.

While the field strain FS2 captured positions at culture surface in colonial cell forms, the *Microcystis* lab strain exhibited a single-celled phenotype under standard cultivation conditions with cells being regularly dispersed throughout the water column. In simulated co-cultivation, the lab strain was seemingly forced into a deeper water layer, creating a local separation of both strains. In this respect it is tempting to interpret the immense transcriptional changes in PCC 7806, which include reprogramming of carbon utilization channels, as further positioning of each strain within their respective ecological niche. The reaction of PCC 7806 triggered a massive downregulation of gas vesicles suggesting a decreased buoyancy, which resulted in the sinking of cells, thus, occupying a position of putatively higher CO_2-availability. Simultaneously, energy acquisition was switched to the light independent more heterotrophic pathways of glycolysis and the TCA. The described sinking of the cells apparently worked without an accumulation of additional ballast glycogen, which is part of the physiological vertical migration model (Thomas*, et al.*, 1985). Both, the accumulation of ballast and the buoyancy induction by gas vesicles might be independently regulated and used with the descending of cells being supported by the enlargement of aggregates as modelled for *Microcystis* colonies (Visser*, et al.*, 1997). As a consequence of the PCC 7806 sinking, the upper water layers would be vacant for the low CO_2-adapted strain FS2. This hypothesis is supported by a genetic background of each strain with the respective suitable HCO_3^- uptake systems (Sandrini*, et al.*, 2013). Sequencing results have attributed the high substrate affinity transporter gene *sbtA* only to the FS2 strain.

Additionally, further experimental results were found that could support an acclimation reaction of PCC 7806 to deeper water layers. An increased level of phycocyanin was detected when cells were treated with FS2 exudates in this study. Elevated levels of the antenna pigments of phycocyanin would enhance photosynthetic light absorption in deeper water layers, where less light reaches the cells.

Whether the local separation of both investigated strains is intended to avoid competition or potential harm from PCC 7806 cannot be deduced from the data of this study. However, the fact that the simulated co-habitation of the two *Microcystis* strains did not result in the expression of known stress markers and did not significantly affect growth rates in PCC 7806 after the FS2 exudate treatment, suggested that both strains might not compete but rather find their respective ecological niche and co-existence. In this respect, a confirmative approach could show if one strain will outcompete the other, in case of direct co-cultivation in the same habitat.

4.6 Bioactive Compounds in the Spent Medium of *Microcystis* Field Strain 2

In this study the substantial effects of the cell exudate of one *Microcystis* strain (FS2) on another (PCC 7806) were shown. The analysis of transcriptional responses as well as other physiological reactions indicated that a reprogramming of primary metabolism occurred as well as the directed upregulation of a specific secondary metabolite. By using the undifferentiated exudate of a bacterial culture a natural situation was simulated, resembling conditions in the field. However, it must be assumed that the observed bioactivity from the used cell exudate, might originate from a mixture of multiple factors. In this respect, the transcriptional and physiological reactions are considered to be of an accumulative nature and so far, it cannot be

distinguished if the differential regulation of single genes and regulons results from several or just one factor.

In addition to that, the microbiome analysis of FS2 must be considered when discussing the bioactivity of the spent medium of FS2. With 77 % of the FS2 culture being identified as *Microcystis*, it was assumed that the bioactive factors of the spent FS2-medium originate from the *Microcystis* strain. Nevertheless, the representatives of the remaining 23 % of the bacterial community might provide a contributing effect. Most of the associating bacteria from the *Microcystis* strain FS2 have been reported in other studies concerning cyanobacterial communities before, which showed a strong diversity in the heterotrophic bacterial composition in dependency of the associated cyanobacterium (Berg*, et al.*, 2009). With 15 % of the FS2-community belonging to the order *Sphingobacteriales* and another 4 % belonging to the order *Sphingomonadales* the majority of *Microcystis* FS2 associates is made up by sphingolipid producers. Diverse roles of sphingolipids, for example in cell recognition and signaling or in cell membrane rigidity, have been identified in mammals (Brown*, et al.*, 2000; Hakomori*, et al.*, 1995). It can only be speculated that one of these functions might be captured as well for either of the partners in the community of *Microcystis* FS2 that was under investigation in this study.

The analytic data about the FS2 exudate and its bioactive fractions represents a first step towards narrowing down which compound class might have induced the strong transcriptional and physiological changes, observed in *Microcystis* PCC 7806 in this project. The preliminary characterization of the active fraction of the FS2 exudate was attributing the activity to a hydrophilic, water soluble and putatively osmotically active compound or group of compounds. Previously reported extracellular info-chemicals affecting other cyanobacteria were largely attributed to the class of secondary metabolites and peptides (Briand*, et al.*, 2015; Kaplan*, et al.*, 2012). The identified candidates from the FS2 exudate in this compound class will need further evaluation and testing.

Recent research presents another option of extracellular signal and compound transmission. The production of outer membrane vesicles (OMV) and

incorporated peptides, enzymes, saccharides, DNA and lipids can be involved in intercellular communication, transport of contents and also in horizontal gene transfer (Kulkarni, *et al.*, 2014; Kulp, *et al.*, 2010). While the implication of OMVs in the current bacterial interactions might be worth testing, it does not provide a direct lead regarding the identity and substance class of the bioactive compounds in question.

A substance class that should not be neglected as potentially active signals is constituted by polysaccharides. Numerous studies have indicated that EPS quantities are responsible for *Microcystis* aggregation processes (Li, *et al.*, 2012; Xu, *et al.*, 2014) and algal organic matter (AOM) or modified polysaccharides such as chitosan are being employed for the induced flocculation and subsequent removal of cyanobacterial bloom materials from eutrophic systems (Henderson, *et al.*, 2010; Zou, *et al.*, 2006). Beyond the application in environmental and economic concerns, a biological context and severe morphological effects have been demonstrated when *Microcystis* EPS production could be related to specific growth phases (Li, *et al.*, 2012) or were involved in species interactions with heterotrophic bacteria (Shen, *et al.*, 2011). The acquired insight into the comprehensive transcriptional responses in aggregation processes and related physiological parameters opens a new perspective on the biological and ecological implications

4.7 Limitations to this Study and Future Outlook

This study was initiated with the intention to investigate *Microcystis* interactions as well as the role of involved info-chemicals. By choosing recently isolated non-axenic *Microcystis* strains for this work, the possibility of associated bacteria influencing experimental results persisted. So far, the possibility remains that described effects in co-cultivation experiments, attributed to *Microcystis* (FS2), were originally caused by the heterotrophic

associates, and confirmative control experiments are needed. The isolation of the major players among associated heterotrophic bacteria and testing for bioactivity of their spent medium and released compounds might provide certainty in this respect. The ecological implications of two different *Microcystis* strains that exhibit very different and nearly opposing ecotypes within the same medium however, is fascinating nonetheless. A hypothetical influence originating from associated bacteria that triggers the observed comprehensive transcriptional reprogramming leading to opposing ecological niche acclimation, would indicate a closer symbiotic relation, which has not been reported before to this extent.

So far, the identification of the bioactive substance(s) in the spent medium of *Microcystis* FS2 remains on a very preliminary level. Further experiments, narrowing down the observed bioactivity to a substance class, size range and eventually the structure and the exact mass through mass spectrometric investigations will supply valuable information concerning the nature of the detected interactions. In turn, it might also provide leads to the producing organism.

Information about the FS2 genome were acquired by DNA-DNA microarrays that only provided the identity of genes present in both genomes, in PCC 7806 and in FS2. This rough comparison between the two putatively interacting *Microcystis* strains revealed most differences between PCC 7806 and FS2 among flexible genes, as could have been expected. Currently, the comprehensive genome sequencing of FS2 is being conducted. It is supposed to give a detailed characterization of the strain FS2 including the genomic resources that are only possessed by FS2 and that might be responsible for the strong effects imposed on PCC 7806.

A major part of the experimental results from this study is based on transcriptomic investigations via microarrays. The transcriptomic state was analyzed one hour after a distinct stimulus and therefore represents a snapshot of the transcriptional responses. A timeline, covering up to 24 h might have

given additional information, providing insights into early and late responses and determining the severity of the applied stimulus.

Despite these open questions, the present study has gathered new insights into *Microcystis* interactions that can occur between two strains without further biotic and abiotic influencing factors usually found in meta-transcriptomic studies. The detailed cellular processes that are involved in ecological implications and cell-cell communications were discussed in detail. A non-competitive niche acclimation strategy among *Microcystis* strains was suggested that allows for different ecotypes of *Microcystis* in the same habitats, being in good accordance with the observed diversity within *Microcystis* communities.

For the first time a comprehensive transcriptional comparison between the microcystin deficient *ΔmcyB* mutant and the microcystin producing wild type PCC 7806 was obtained, which could identify cellular processes that are affected by the intra and extracellular presence of microcystin. In that respect the essential role of the transcription factor SigE was recognized and it remains to be elucidated which molecular mechanisms are underlying the observed regulatory network which is responding to the presence and absence of microcystin.

As an unexpected byproduct, the present investigations have also delivered information about secondary metabolites that belong to orphan gene clusters with unidentified metabolite structures. The discovery of distinct conditions that lead to expression of these metabolites provides the means for their identification and structural characterization. Secondary metabolites have proven to show interesting bioactivities in many cases and their utilization in pharmaceuticals is of great interest, requiring the basic research and identification, which can be facilitated through the discovery of inducible expression conditions.

5 References

1. **Afif, H., Allali, N., Couturier, M., Van Melderen, L.**, (2001) The ratio between CcdA and CcdB modulates the transcriptional repression of the ccd poison-antidote system. *Mol Microbiol* **41**, 73-82; mmi2492 [pii]
2. **Aichi, M., Takatani, N., Omata, T.**, (2001) Role of NtcB in activation of nitrate assimilation genes in the cyanobacterium Synechocystis sp. strain PCC 6803. *J Bacteriol* **183**, 5840-5847; 10.1128/JB.183.20.5840-5847.2001
3. **Allali, N., Afif, H., Couturier, M., Van Melderen, L.**, (2002) The highly conserved TldD and TldE proteins of Escherichia coli are involved in microcin B17 processing and in CcdA degradation. *J Bacteriol* **184**, 3224-3231;
4. **Allen, J., Gantt, E., Golbeck, J., Osmond, B., Pollari, M., TyystjÃ¤rvi, T.**, in *Photosynthesis. Energy from the Sun*. (Springer Netherlands, 2008), pp. 1351-1353. 10.1007/978-1-4020-6709-9_291
5. **Andrizhiyevskaya, E. G., Schwabe, T. M., Germano, M., D'Haene, S., Kruip, J., van Grondelle, R., Dekker, J. P.**, (2002) Spectroscopic properties of PSI-IsiA supercomplexes from the cyanobacterium Synechococcus PCC 7942. *Biochim Biophys Acta* **1556**, 265-272; S0005272802003717 [pii]
6. **Ashby, M. K., Houmard, J., Mullineaux, C. W.**, (2002) The ycf27 genes from cyanobacteria and eukaryotic algae: distribution and implications for chloroplast evolution. *FEMS Microbiol Lett* **214**, 25-30; S0378109702008340 [pii]
7. **Baker, N., Andersson, B., Barber, J.**, in *Photosynthesis and the Environment*. (Springer Netherlands, 1996), vol. 5, pp. 101-121. 10.1007/0-306-48135-9_4
8. **Bar-Yosef, Y., Sukenik, A., Hadas, O., Viner-Mozzini, Y., Kaplan, A.**, (2010) Enslavement in the water body by toxic Aphanizomenon ovalisporum, inducing alkaline phosphatase in phytoplanktons. *Curr Biol* **20**, 1557-1561; S0960-9822(10)00934-6 [pii]
10.1016/j.cub.2010.07.032
9. **Beer, A.**, in *Annalen der Physik und Chemie*. (1852), vol. 86, pp. 78-88.
10. **Berg, K. A., Lyra, C., Sivonen, K., Paulin, L., Suomalainen, S., Tuomi, P., Rapala, J.**, (2009) High diversity of cultivable heterotrophic bacteria in association with cyanobacterial water blooms. *ISME J* **3**, 314-325; ismej2008110 [pii]
10.1038/ismej.2008.110
11. **Berkner, L. V., Marshall, L. C.**, (1965) On the Origin and Rise of Oxygen Concentration in the Earth's Atmosphere. *Journal of the Atmospheric Sciences* **22**, 225-261; 10.1175/1520-0469(1965)022<0225:0t0aro>2.0.c0;2
12. **Bolger, A. M., Lohse, M., Usadel, B.**, (2014) Trimmomatic: a flexible trimmer for Illumina sequence data. *Bioinformatics* **30**, 2114-2120; btu170 [pii]
10.1093/bioinformatics/btu170
13. **Briand, E., Bormans, M., Gugger, M., Dorrestein, P. C., Gerwick, W. H.**, (2015) Changes in secondary metabolic profiles of Microcystis aeruginosa

strains in response to intraspecific interactions. *Environ Microbiol*, 10.1111/1462-2920.12904

14. **Brocks, J. J., Logan, G. A., Buick, R., Summons, R. E.**, (1999) Archean molecular fossils and the early rise of eukaryotes. *Science* **285**, 1033-1036; 7752 [pii]
15. **Brown, D. A., London, E.**, (2000) Structure and function of sphingolipid- and cholesterol-rich membrane rafts. *J Biol Chem* **275**, 17221-17224; 10.1074/jbc.R000005200
R000005200 [pii]
16. **Brunberg, A.-K.**, (1999) Contribution of bacteria in the mucilage of Microcystis spp. (Cyanobacteria) to benthic and pelagic bacterial production in a hypereutrophic lake. *FEMS Microbiology Ecology* **29**, 13-22; 10.1111/j.1574-6941.1999.tb00594.x
17. **Burnap, R. L., Hagemann, M., Kaplan, A.**, (2015) Regulation of CO2 Concentrating Mechanism in Cyanobacteria. *Life (Basel)* **5**, 348-371; life5010348 [pii]
10.3390/life5010348
18. **Calteau, A., Fewer, D. P., Latifi, A., Coursin, T., Laurent, T., Jokela, J., Kerfeld, C. A., Sivonen, K., Piel, J., Gugger, M.**, (2014) Phylum-wide comparative genomics unravel the diversity of secondary metabolism in Cyanobacteria. *BMC Genomics* **15**, 977; 1471-2164-15-977 [pii]
10.1186/1471-2164-15-977
19. **Caporaso, J. G., Kuczynski, J., Stombaugh, J., Bittinger, K., Bushman, F. D., Costello, E. K., Fierer, N., Pena, A. G., Goodrich, J. K., Gordon, J. I., Huttley, G. A., Kelley, S. T., Knights, D., Koenig, J. E., Ley, R. E., Lozupone, C. A., McDonald, D., Muegge, B. D., Pirrung, M., Reeder, J., Sevinsky, J. R., Turnbaugh, P. J., Walters, W. A., Widmann, J., Yatsunenko, T., Zaneveld, J., Knight, R.**, (2010) QIIME allows analysis of high-throughput community sequencing data. *Nat Methods* **7**, 335-336; nmeth.f.303 [pii]
10.1038/nmeth.f.303
20. **Carmichael, W.**, (2008) A world overview--one-hundred-twenty-seven years of research on toxic cyanobacteria--where do we go from here? *Adv Exp Med Biol* **619**, 105-125; 10.1007/978-0-387-75865-7_4
21. **Carrieri, D., Wawrousek, K., Eckert, C., Yu, J., Maness, P. C.**, (2011) The role of the bidirectional hydrogenase in cyanobacteria. *Bioresour Technol* **102**, 8368-8377; S0960-8524(11)00462-7 [pii]
10.1016/j.biortech.2011.03.103
22. **Chaturongakul, S., Ounjai, P.**, (2014) Phage-host interplay: examples from tailed phages and Gram-negative bacterial pathogens. *Front Microbiol* **5**, 442; 10.3389/fmicb.2014.00442
23. **Chen, M., Schliep, M., Willows, R. D., Cai, Z. L., Neilan, B. A., Scheer, H.**, (2010) A red-shifted chlorophyll. *Science* **329**, 1318-1319; science.1191127 [pii]
10.1126/science.1191127

24. **Chomczynski, P., Sacchi, N.**, (1987) Single-step method of RNA isolation by acid guanidinium thiocyanate-phenol-chloroform extraction. *Anal Biochem* **162**, 156-159; 10.1006/abio.1987.9999
0003-2697(87)90021-2 [pii]
25. **Cox, M. A. A. C. a. T. F.**, *Multidimensional Scaling*. (Chapman and Hall, ed. 2, 2001),
26. **Crush, J. R., Briggs, L. R., Sprosen, J. M., Nichols, S. N.**, (2008) Effect of irrigation with lake water containing microcystins on microcystin content and growth of ryegrass, clover, rape, and lettuce. *Environ Toxicol* **23**, 246-252; 10.1002/tox.20331
27. **D'Agostino, P. M., Woodhouse, J. N., Makower, A. K., Yeung, A. C., Ongley, S. E., Micallef, M. L., Moffitt, M. C., Neilan, B. A.**, (2015) Advances in genomics, transcriptomics and proteomics of toxin-producing cyanobacteria. *Environ Microbiol Rep*, 10.1111/1758-2229.12366
28. **Daley, S. M., Kappell, A. D., Carrick, M. J., Burnap, R. L.**, (2012) Regulation of the cyanobacterial CO2-concentrating mechanism involves internal sensing of NADP+ and alpha-ketogutarate levels by transcription factor CcmR. *PLoS One* **7**, e41286; 10.1371/journal.pone.0041286
PONE-D-12-10646 [pii]
29. **Davies, J.**, (2013) Specialized microbial metabolites: functions and origins. *J Antibiot (Tokyo)* **66**, 361-364; ja201361 [pii]
10.1038/ja.2013.61
30. **Dillon, J. G., Castenholz, R. W.**, (2003) The synthesis of the UV-screening pigment, scytonemin, and photosynthetic performance in isolates from closely related natural populations of cyanobacteria (Calothrix sp.). *Environ Microbiol* **5**, 484-491; 436 [pii]
31. **Dittmann, E., Gugger, M., Sivonen, K., Fewer, D. P.**, (2015) Natural Product Biosynthetic Diversity and Comparative Genomics of the Cyanobacteria. *Trends Microbiol* **23**, 642-652; S0966-842X(15)00157-2 [pii]
10.1016/j.tim.2015.07.008
32. **Dittmann, E., Neilan, B. A., Erhard, M., von Dohren, H., Borner, T.**, (1997) Insertional mutagenesis of a peptide synthetase gene that is responsible for hepatotoxin production in the cyanobacterium Microcystis aeruginosa PCC 7806. *Mol Microbiol* **26**, 779-787;
33. **Dittmann, E., Wiegand, C.**, (2006) Cyanobacterial toxins--occurrence, biosynthesis and impact on human affairs. *Mol Nutr Food Res* **50**, 7-17; 10.1002/mnfr.200500162
34. **Edelman, M. J., Gandara, D. R., Hausner, P., Israel, V., Thornton, D., DeSanto, J., Doyle, L. A.**, (2003) Phase 2 study of cryptophycin 52 (LY355703) in patients previously treated with platinum based chemotherapy for advanced non-small cell lung cancer. *Lung Cancer* **39**, 197-199; S0169500202005111 [pii]
35. **Elser, J. J., Bracken, M. E., Cleland, E. E., Gruner, D. S., Harpole, W. S., Hillebrand, H., Ngai, J. T., Seabloom, E. W., Shurin, J. B., Smith, J. E.**, (2007) Global analysis of nitrogen and phosphorus limitation of primary

producers in freshwater, marine and terrestrial ecosystems. *Ecol Lett* **10**, 1135-1142; ELE1113 [pii]
10.1111/j.1461-0248.2007.01113.x

36. **Espinosa, J., Boyd, J. S., Cantos, R., Salinas, P., Golden, S. S., Contreras, A.**, (2015) Cross-talk and regulatory interactions between the essential response regulator RpaB and cyanobacterial circadian clock output. *Proc Natl Acad Sci U S A* **112**, 2198-2203; 1424632112 [pii]
10.1073/pnas.1424632112
37. **Fastner, J., Erhard, M., von Dohren, H.**, (2001) Determination of oligopeptide diversity within a natural population of Microcystis spp. (cyanobacteria) by typing single colonies by matrix-assisted laser desorption ionization-time of flight mass spectrometry. *Appl Environ Microbiol* **67**, 5069-5076; 10.1128/AEM.67.11.5069-5076.2001
38. **Foy, R. H., Gibson, C. E., Smith, R. V.**, (1976) The influence of daylength, light intensity and temperature on the growth rates of planktonic blue-green algae. *British Phycological Journal* **11**, 151-163; 10.1080/00071617600650181
39. **Fraenkel, G. S.**, (1959) The raison d'etre of secondary plant substances; these odd chemicals arose as a means of protecting plants from insects and now guide insects to food. *Science* **129**, 1466-1470;
40. **Frangeul, L., Quillardet, P., Castets, A. M., Humbert, J. F., Matthijs, H. C., Cortez, D., Tolonen, A., Zhang, C. C., Gribaldo, S., Kehr, J. C., Zilliges, Y., Ziemert, N., Becker, S., Talla, E., Latifi, A., Billault, A., Lepelletier, A., Dittmann, E., Bouchier, C., de Marsac, N. T.**, (2008) Highly plastic genome of Microcystis aeruginosa PCC 7806, a ubiquitous toxic freshwater cyanobacterium. *BMC Genomics* **9**, 274; 1471-2164-9-274 [pii]
10.1186/1471-2164-9-274
41. **Gan, N., Xiao, Y., Zhu, L., Wu, Z., Liu, J., Hu, C., Song, L.**, (2011) The role of microcystins in maintaining colonies of bloom-forming Microcystis spp. *Environ Microbiol* **14**, 730-742; 10.1111/j.1462-2920.2011.02624.x
42. **Garcia-Pichel, F., Belnap, J., Neuer, S., Schanz, F.**, (2003) Estimates of global cyanobacterial biomass and its distribution. *Algological Studies* **109**, 213-227;
43. **Gentleman, R. C., Carey, V. J., Bates, D. M., Bolstad, B., Dettling, M., Dudoit, S., Ellis, B., Gautier, L., Ge, Y., Gentry, J., Hornik, K., Hothorn, T., Huber, W., Iacus, S., Irizarry, R., Leisch, F., Li, C., Maechler, M., Rossini, A. J., Sawitzki, G., Smith, C., Smyth, G., Tierney, L., Yang, J. Y., Zhang, J.**, (2004) Bioconductor: open software development for computational biology and bioinformatics. *Genome Biol* **5**, R80; gb-2004-5-10-r80 [pii]
10.1186/gb-2004-5-10-r80
44. **Giovannoni, S. J., Turner, S., Olsen, G. J., Barns, S., Lane, D. J., Pace, N. R.**, (1988) Evolutionary relationships among cyanobacteria and green chloroplasts. *J Bacteriol* **170**, 3584-3592;
45. **Groth, D., Hartmann, S., Klie, S., Selbig, J.**, (2012) Principal components analysis. *Methods Mol Biol* **930**, 527-547; 10.1007/978-1-62703-059-5_22

46. **Grunewald, J., Marahiel, M. A.**, (2006) Chemoenzymatic and template-directed synthesis of bioactive macrocyclic peptides. *Microbiol Mol Biol Rev* **70**, 121-146; 70/1/121 [pii]
10.1128/MMBR.70.1.121-146.2006
47. **Gugger, M. F., Hoffmann, L.**, (2004) Polyphyly of true branching cyanobacteria (Stigonematales). *Int J Syst Evol Microbiol* **54**, 349-357; 10.1099/ijs.0.02744-0
48. **Guljamow, A., Jenke-Kodama, H., Saumweber, H., Quillardet, P., Frangeul, L., Castets, A. M., Bouchier, C., Tandeau de Marsac, N., Dittmann, E.**, (2007) Horizontal gene transfer of two cytoskeletal elements from a eukaryote to a cyanobacterium. *Curr Biol* **17**, R757-759; S0960-9822(07)01632-6 [pii]
10.1016/j.cub.2007.06.063
49. **Hakomori, S., Igarashi, Y.**, (1995) Functional role of glycosphingolipids in cell recognition and signaling. *J Biochem* **118**, 1091-1103;
50. **Hall-Stoodley, L., Costerton, J. W., Stoodley, P.**, (2004) Bacterial biofilms: from the natural environment to infectious diseases. *Nat Rev Microbiol* **2**, 95-108; 10.1038/nrmicro821
51. **Harel, M., Weiss, G., Lieman-Hurwitz, J., Gun, J., Lev, O., Lebendiker, M., Temper, V., Block, C., Sukenik, A., Zohary, T., Braun, S., Carmeli, S., Kaplan, A.**, (2013) Interactions between Scenedesmus and Microcystis may be used to clarify the role of secondary metabolites. *Environ Microbiol Rep* **5**, 97-104; 10.1111/j.1758-2229.2012.00366.x
52. **Harke, M. J., Gobler, C. J.**, (2013) Global transcriptional responses of the toxic cyanobacterium, Microcystis aeruginosa, to nitrogen stress, phosphorus stress, and growth on organic matter. *PLoS One* **8**, e69834; 10.1371/journal.pone.0069834
PONE-D-13-10764 [pii]
53. **Hassler, C. S., Schoemann, V., Nichols, C. M., Butler, E. C., Boyd, P. W.**, (2011) Saccharides enhance iron bioavailability to Southern Ocean phytoplankton. *Proc Natl Acad Sci U S A* **108**, 1076-1081; 1010963108 [pii]
10.1073/pnas.1010963108
54. **Henderson, R. K., Parsons, S. A., Jefferson, B.**, (2010) The impact of differing cell and algogenic organic matter (AOM) characteristics on the coagulation and flotation of algae. *Water Res* **44**, 3617-3624; S0043-1354(10)00256-3 [pii]
10.1016/j.watres.2010.04.016
55. **Hesse, K., Dittmann, E., BÃ¶rner, T.**, (2001) Consequences of impaired microcystin production for light-dependent growth and pigmentation of Microcystis aeruginosa PCC 7806. *FEMS Microbiology Ecology* **37**, 39-43; http://dx.doi.org/10.1016/S0168-6496(01)00142-8
56. **Hisbergues, M., Christiansen, G., Rouhiainen, L., Sivonen, K., Borner, T.**, (2003) PCR-based identification of microcystin-producing genotypes of different cyanobacterial genera. *Arch Microbiol* **180**, 402-410; 10.1007/s00203-003-0605-9

57. **Huang, X., Madan, A.**, (1999) CAP3: A DNA sequence assembly program. *Genome Res* **9**, 868-877;
58. **Hudnell, H. K., Boyer, G.**, in *Cyanobacterial Harmful Algal Blooms: State of the Science and Research Needs*. (Springer New York, 2008), vol. 619, pp. 153-165. 10.1007/978-0-387-75865-7_7
59. **Humbert, J. F., Barbe, V., Latifi, A., Gugger, M., Calteau, A., Coursin, T., Lajus, A., Castelli, V., Oztas, S., Samson, G., Longin, C., Medigue, C., de Marsac, N. T.**, (2013) A tribute to disorder in the genome of the bloom-forming freshwater cyanobacterium Microcystis aeruginosa. *PLoS One* **8**, e70747; 10.1371/journal.pone.0070747
PONE-D-13-09234 [pii]
60. **Imamura, S., Asayama, M., Takahashi, H., Tanaka, K., Shirai, M.**, (2003) Antagonistic dark/light-induced SigB/SigD, group 2 sigma factors, expression through redox potential and their roles in cyanobacteria. *FEBS Lett* **554**, 357-362; S0014579303011888 [pii]
61. **Ishida, K., Matsuda, H., Murakami, M., Yamaguchi, K.**, (1997) Kawaguchipeptin B, an antibacterial cyclic undecapeptide from the cyanobacterium Microcystis aeruginosa. *J Nat Prod* **60**, 724-726; 10.1021/np970146k
np970146k [pii]
62. **Ishitsuka, M. O., Kusumi, T., Kakisawa, H., Kaya, K., Watanabe, M. M.**, (1990) Microviridin. A novel tricyclic depsipeptide from the toxic cyanobacterium Microcystis viridis. *Journal of the American Chemical Society* **112**, 8180-8182; 10.1021/ja00178a060
63. **Jähnichen, S., Ihle, T., Petzoldt, T., Benndorf, J.**, (2007) Impact of inorganic carbon availability on microcystin production by Microcystis aeruginosa PCC 7806. *Appl Environ Microbiol* **73**, 6994-7002; AEM.01253-07 [pii]
10.1128/AEM.01253-07
64. **Kaebernick, M., Neilan, B. A., Borner, T., Dittmann, E.**, (2000) Light and the transcriptional response of the microcystin biosynthesis gene cluster. *Appl Environ Microbiol* **66**, 3387-3392;
65. **Kaplan, A., Harel, M., Kaplan-Levy, R. N., Hadas, O., Sukenik, A., Dittmann, E.**, (2012) The languages spoken in the water body (or the biological role of cyanobacterial toxins). *Front Microbiol* **3**, 138; 10.3389/fmicb.2012.00138
66. **Karlsson, B., Vaara, T., Lounatmaa, K., Gyllenberg, H.**, (1983) Three-dimensional structure of the regularly constructed surface layer from Synechocystis sp. strain CLII. *J Bacteriol* **156**, 1338-1343;
67. **Kehr, J. C., Dittmann, E.**, (2015) Biosynthesis and function of extracellular glycans in cyanobacteria. *Life (Basel)* **5**, 164-180; life5010164 [pii]
10.3390/life5010164
68. **Kehr, J. C., Gatte Picchi, D., Dittmann, E.**, (2011) Natural product biosyntheses in cyanobacteria: A treasure trove of unique enzymes. *Beilstein J Org Chem* **7**, 1622-1635; 10.3762/bjoc.7.191

69. **Kehr, J. C., Zilliges, Y., Springer, A., Disney, M. D., Ratner, D. D., Bouchier, C., Seeberger, P. H., de Marsac, N. T., Dittmann, E.**, (2006) A mannan binding lectin is involved in cell-cell attachment in a toxic strain of Microcystis aeruginosa. *Mol Microbiol* **59**, 893-906; MMI5001 [pii] 10.1111/j.1365-2958.2005.05001.x
70. **Kessel, M., Eloff, J.**, (1975) The ultrastructure and development of the colonial sheath of Microcystis marginata. *Archives of Microbiology* **106**, 209-214; 10.1007/bf00446525
71. **Koksharova, O., Schubert, M., Shestakov, S., Cerff, R.**, (1998) Genetic and biochemical evidence for distinct key functions of two highly divergent GAPDH genes in catabolic and anabolic carbon flow of the cyanobacterium Synechocystis sp. PCC 6803. *Plant Mol Biol* **36**, 183-194;
72. **Komárek, J.**, *Suesswasserflora von Mitteleuropa Bd. 19/1: Cyanoprokaryota I. Chroococcales*. (Spektrum Akademischer Verlag, 1998),
73. **Kopf, M., Klahn, S., Scholz, I., Hess, W. R., Voss, B.**, (2015) Variations in the non-coding transcriptome as a driver of inter-strain divergence and physiological adaptation in bacteria. *Sci Rep* **5**, 9560; srep09560 [pii] 10.1038/srep09560
74. **Koressaar, T., Remm, M.**, (2007) Enhancements and modifications of primer design program Primer3. *Bioinformatics* **23**, 1289-1291; btm091 [pii] 10.1093/bioinformatics/btm091
75. **Kulkarni, H. M., Jagannadham, M. V.**, (2014) Biogenesis and multifaceted roles of outer membrane vesicles from Gram-negative bacteria. *Microbiology* **160**, 2109-2121; mic.0.079400-0 [pii] 10.1099/mic.0.079400-0
76. **Kulp, A., Kuehn, M. J.**, (2010) Biological functions and biogenesis of secreted bacterial outer membrane vesicles. *Annu Rev Microbiol* **64**, 163-184; 10.1146/annurev.micro.091208.073413
77. **Labrie, S. J., Samson, J. E., Moineau, S.**, (2010) Bacteriophage resistance mechanisms. *Nat Rev Microbiol* **8**, 317-327; nrmicro2315 [pii] 10.1038/nrmicro2315
78. **Larsen, L. K., Moore, R. E., Patterson, G. M.**, (1994) beta-Carbolines from the blue-green alga Dichothrix baueriana. *J Nat Prod* **57**, 419-421;
79. **Li, M., Zhu, W., Gao, L., Lu, L.**, (2012) Changes in extracellular polysaccharide content and morphology of Microcystis aeruginosa at different specific growth rates. *Journal of Applied Phycology* **25**, 1023-1030; 10.1007/s10811-012-9937-7
80. **Makower, A. K., Schuurmans, J. M., Groth, D., Zilliges, Y., Matthijs, H. C., Dittmann, E.**, (2014) Transcriptomics-aided dissection of the intracellular and extracellular roles of microcystin in Microcystis aeruginosa PCC 7806. *Appl Environ Microbiol* **81**, 544-554; AEM.02601-14 [pii] 10.1128/AEM.02601-14
81. **Mandal, S., Rath, J.**, *Extremophilic Cyanobacteria For Novel Drug Development*. (Springer International Publishing, 2014),
82. **Martin, M.**, (2011) Cutadapt removes adapter sequences from high-throughput sequencing reads. *EMBnet.journal* **17**, 10.14806/ej.17.1.200

pp. 10-12
83. **Meeks, J. C., Castenholz, R. W.**, (1971) Growth and photosynthesis in an extreme thermophile, Synechococcus lividus (Cyanophyta). *Arch Mikrobiol* **78**, 25-41;
84. **Meissner, S., Fastner, J., Dittmann, E.**, (2013) Microcystin production revisited: conjugate formation makes a major contribution. *Environ Microbiol* **15**, 1810-1820; 10.1111/1462-2920.12072
85. **Meissner, S., Steinhauser, D., Dittmann, E.**, (2014) Metabolomic analysis indicates a pivotal role of the hepatotoxin microcystin in high light adaptation of Microcystis. *Environ Microbiol*, 10.1111/1462-2920.12565
86. **Mikami, K., Kanesaki, Y., Suzuki, I., Murata, N.**, (2002) The histidine kinase Hik33 perceives osmotic stress and cold stress in Synechocystis sp PCC 6803. *Mol Microbiol* **46**, 905-915; 3202 [pii]
87. **Milkowski, C., Quinones, A., Hagemann, M.**, (1998) A DNA fragment from the cyanobacterium Synechocystis sp. PCC 6803 mediates gene expression inducible by osmotic stress in E. coli. *Curr Microbiol* **37**, 108-116;
88. **Miller, T. R., Beversdorf, L., Chaston, S. D., McMahon, K. D.**, (2013) Spatiotemporal molecular analysis of cyanobacteria blooms reveals Microcystis--Aphanizomenon interactions. *PLoS One* **8**, e74933; 10.1371/journal.pone.0074933
PONE-D-13-18487 [pii]
89. **Mosteller, F. a. F., R. A.**, (1948) Questions and Answers. *The American Statistician* **2**, pp. 30-31; 10.2307/2681650
90. **Neilan, B. A., Pearson, L. A., Muenchhoff, J., Moffitt, M. C., Dittmann, E.**, (2012) Environmental conditions that influence toxin biosynthesis in cyanobacteria. *Environ Microbiol* **15**, 1239-1253; 10.1111/j.1462-2920.2012.02729.x
91. **Neuhof, T., Schmieder, P., Preussel, K., Dieckmann, R., Pham, H., Bartl, F., von Dohren, H.**, (2005) Hassallidin A, a glycosylated lipopeptide with antifungal activity from the cyanobacterium Hassallia sp. *J Nat Prod* **68**, 695-700; 10.1021/np049671r
92. **Omata, T., Price, G. D., Badger, M. R., Okamura, M., Gohta, S., Ogawa, T.**, (1999) Identification of an ATP-binding cassette transporter involved in bicarbonate uptake in the cyanobacterium Synechococcus sp. strain PCC 7942. *Proc Natl Acad Sci U S A* **96**, 13571-13576;
93. **Osanai, T., Oikawa, A., Azuma, M., Tanaka, K., Saito, K., Hirai, M. Y., Ikeuchi, M.**, (2011) Genetic engineering of group 2 sigma factor SigE widely activates expressions of sugar catabolic genes in Synechocystis species PCC 6803. *J Biol Chem* **286**, 30962-30971; M111.231183 [pii]
10.1074/jbc.M111.231183
94. **Otero, A., Vincenzini, M.**, (2003) Extracellular polysaccharide synthesis by Nostoc strains as affected by N source and light intensity. *J Biotechnol* **102**, 143-152; S0168165603000221 [pii]
95. **Otsuka, S., Suda, S., Shibata, S., Oyaizu, H., Matsumoto, S., Watanabe, M. M.**, (2001) A proposal for the unification of five species of the cyanobacterial genus Microcystis Kutzing ex Lemmermann 1907 under the

rules of the Bacteriological Code. *Int J Syst Evol Microbiol* **51**, 873-879; 10.1099/00207713-51-3-873

96. **Otten, T. G., Paerl, H. W.**, (2011) Phylogenetic inference of colony isolates comprising seasonal Microcystis blooms in Lake Taihu, China. *Microb Ecol* **62**, 907-918; 10.1007/s00248-011-9884-x
97. **Ozaki, K., Ohta, A., Iwata, C., Horikawa, A., Tsuji, K., Ito, E., Ikai, Y., Harada, K.**, (2008) Lysis of cyanobacteria with volatile organic compounds. *Chemosphere* **71**, 1531-1538; S0045-6535(07)01494-4 [pii] 10.1016/j.chemosphere.2007.11.052
98. **Paerl, H. W.**, (2014) Mitigating harmful cyanobacterial blooms in a human- and climatically-impacted world. *Life (Basel)* **4**, 988-1012; life4040988 [pii] 10.3390/life4040988
99. **Paerl, H. W., Otten, T. G.**, (2013) Harmful cyanobacterial blooms: causes, consequences, and controls. *Microb Ecol* **65**, 995-1010; 10.1007/s00248-012-0159-y
100. **Pankratova, E. M., Vakhrushev, A. S.**, (1969) [Utilization by higher plants of nitrogen fixed from the atmosphere by blue-green algae]. *Mikrobiologiia* **38**, 1080-1084;
101. **Parveen, B., Ravet, V., Djediat, C., Mary, I., Quiblier, C., Debroas, D., Humbert, J. F.**, (2013) Bacterial communities associated with Microcystis colonies differ from free-living communities living in the same ecosystem. *Environ Microbiol Rep* **5**, 716-724; 10.1111/1758-2229.12071
102. **Penn, K., Wang, J., Fernando, S. C., Thompson, J. R.**, (2014) Secondary metabolite gene expression and interplay of bacterial functions in a tropical freshwater cyanobacterial bloom. *ISME J* **8**, 1866-1878; ismej201427 [pii] 10.1038/ismej.2014.27
103. **Peuthert, A., Chakrabarti, S., Pflugmacher, S.**, (2007) Uptake of microcystins-LR and -LF (cyanobacterial toxins) in seedlings of several important agricultural plant species and the correlation with cellular damage (lipid peroxidation). *Environ Toxicol* **22**, 436-442; 10.1002/tox.20266
104. **Pfaffl, M. W.**, (2001) A new mathematical model for relative quantification in real-time RT-PCR. *Nucleic Acids Res* **29**, e45;
105. **Price, G. D., Shelden, M. C., Howitt, S. M.**, (2011) Membrane topology of the cyanobacterial bicarbonate transporter, SbtA, and identification of potential regulatory loops. *Mol Membr Biol* **28**, 265-275; 10.3109/09687688.2011.593049
106. **Price, G. D., Woodger, F. J., Badger, M. R., Howitt, S. M., Tucker, L.**, (2004) Identification of a SulP-type bicarbonate transporter in marine cyanobacteria. *Proc Natl Acad Sci U S A* **101**, 18228-18233; 0405211101 [pii] 10.1073/pnas.0405211101
107. **R Core Team, R. F. f. S. C.**, (2013) R: A Language and Environment for Statistical Computing.
108. **Rabouille, S., Thebault, J. M., Salencon, M. J.**, (2003) Simulation of carbon reserve dynamics in Microcystis and its influence on vertical migration with Yoyo model. *C R Biol* **326**, 349-361;

109. **Rasmussen, B., Fletcher, I. R., Brocks, J. J., Kilburn, M. R.**, (2008) Reassessing the first appearance of eukaryotes and cyanobacteria. *Nature* **455**, 1101-1104; nature07381 [pii]
10.1038/nature07381

110. **Rippka, R., Deruelles, J., Waterbury, J. B., Herdman, M., Stanier, R. Y.**, (1979) Generic Assignments, Strain Histories and Properties of Pure Cultures of Cyanobacteria. *J Gen Microbiol* **111**, 1-61; 10.1099/00221287-111-1-1

111. **Robarts, R. D., Zohary, T.**, (1987) Temperature effects on photosynthetic capacity, respiration, and growth rates of bloomâ€forming cyanobacteria. *New Zealand Journal of Marine and Freshwater Research* **21**, 391-399; 10.1080/00288330.1987.9516235

112. **Sambrook, J. F., E. F. (Edward F.); Maniatis, Tom; Cold Spring Harbor Laboratory**, *Molecular cloning : a laboratory manual*. (Cold Spring Harbor Laboratory Press, New York, ed. 2nd, 1989),

113. **Sandrini, G., Matthijs, H. C., Verspagen, J. M., Muyzer, G., Huisman, J.**, (2013) Genetic diversity of inorganic carbon uptake systems causes variation in CO2 response of the cyanobacterium Microcystis. *ISME J* **8**, 589-600; ismej2013179 [pii]
10.1038/ismej.2013.179

114. **Saqrane, S., Oudra, B.**, (2009) CyanoHAB occurrence and water irrigation cyanotoxin contamination: ecological impacts and potential health risks. *Toxins (Basel)* **1**, 113-122; 10.3390/toxins1020113
toxins-01-00113 [pii]

115. **Schatz, D., Keren, Y., Vardi, A., Sukenik, A., Carmeli, S., Borner, T., Dittmann, E., Kaplan, A.**, (2007) Towards clarification of the biological role of microcystins, a family of cyanobacterial toxins. *Environ Microbiol* **9**, 965-970; EMI1218 [pii]
10.1111/j.1462-2920.2006.01218.x

116. **Schwarz, D., Orf, I., Kopka, J., Hagemann, M.**, (2014) Effects of Inorganic Carbon Limitation on the Metabolome of the Synechocystis sp. PCC 6803 Mutant Defective in glnB Encoding the Central Regulator PII of Cyanobacterial C/N Acclimation. *Metabolites* **4**, 232-247; metab04020232 [pii]
10.3390/metab04020232

117. **Schwyn, B., Neilands, J. B.**, (1987) Universal chemical assay for the detection and determination of siderophores. *Anal Biochem* **160**, 47-56; 0003-2697(87)90612-9 [pii]

118. **Seckbach, J.**, *Algae and Cyanobacteria in Extreme Environments*. (Springer Netherlands, 2007),

119. **Sevilla, E., Martin-Luna, B., Vela, L., Bes, M. T., Peleato, M. L., Fillat, M. F.**, (2010) Microcystin-LR synthesis as response to nitrogen: transcriptional analysis of the mcyD gene in Microcystis aeruginosa PCC7806. *Ecotoxicology* **19**, 1167-1173; 10.1007/s10646-010-0500-5

120. **Shen, H., Niu, Y., Xie, P., Tao, M. I. N., Yang, X. I.**, (2011) Morphological and physiological changes in Microcystis aeruginosa as a result of interactions with heterotrophic bacteria. *Freshwater Biology* **56**, 1065-1080; 10.1111/j.1365-2427.2010.02551.x

121. **Shibata, M., Katoh, H., Sonoda, M., Ohkawa, H., Shimoyama, M., Fukuzawa, H., Kaplan, A., Ogawa, T.**, (2002) Genes essential to sodium-dependent bicarbonate transport in cyanobacteria: function and phylogenetic analysis. *J Biol Chem* **277**, 18658-18664; 10.1074/jbc.M112468200 M112468200 [pii]

122. **Shibata, M., Ohkawa, H., Kaneko, T., Fukuzawa, H., Tabata, S., Kaplan, A., Ogawa, T.**, (2001) Distinct constitutive and low-CO_2-induced CO_2 uptake systems in cyanobacteria: genes involved and their phylogenetic relationship with homologous genes in other organisms. *Proc Natl Acad Sci U S A* **98**, 11789-11794; 10.1073/pnas.191258298 191258298 [pii]

123. **Shin, H. J., Matsuda, H., Murakami, M., Yamaguchi, K.**, (1997) Aeruginosins 205A and -B, Serine Protease Inhibitory Glycopeptides from the Cyanobacterium Oscillatoria agardhii (NIES-205). *The Journal of Organic Chemistry* **62**, 1810-1813; 10.1021/jo961902e

124. **Silhavy, T. J., Kahne, D., Walker, S.**, (2010) The bacterial cell envelope. *Cold Spring Harb Perspect Biol* **2**, a000414; cshperspect.a000414 [pii] 10.1101/cshperspect.a000414

125. **Sivonen, K., Leikoski, N., Fewer, D. P., Jokela, J.**, (2010) Cyanobactins-ribosomal cyclic peptides produced by cyanobacteria. *Appl Microbiol Biotechnol* **86**, 1213-1225; 10.1007/s00253-010-2482-x

126. **Smyth, G. K., Speed, T.**, (2003) Normalization of cDNA microarray data. *Methods* **31**, 265-273; S1046202303001555 [pii]

127. **Steffen, M. M., Belisle, B. S., Watson, S. B., Boyer, G. L., Bourbonniere, R. A., Wilhelm, S. W.**, (2015) Metatranscriptomic evidence for co-occurring top-down and bottom-up controls on toxic cyanobacterial communities. *Appl Environ Microbiol* **81**, 3268-3276; AEM.04101-14 [pii] 10.1128/AEM.04101-14

128. **Straub, C., Quillardet, P., Vergalli, J., de Marsac, N. T., Humbert, J. F.**, (2011) A day in the life of microcystis aeruginosa strain PCC 7806 as revealed by a transcriptomic analysis. *PLoS One* **6**, e16208; 10.1371/journal.pone.0016208

129. **Tabei, Y., Okada, K., Tsuzuki, M.**, (2007) Sll1330 controls the expression of glycolytic genes in Synechocystis sp. PCC 6803. *Biochem Biophys Res Commun* **355**, 1045-1050; S0006-291X(07)00354-3 [pii] 10.1016/j.bbrc.2007.02.065

130. **Talling, J. F.**, (1976) The Depletion of Carbon Dioxide from Lake Water by Phytoplankton. *Journal of Ecology* **64**, 79-121; 10.2307/2258685

131. **Tanaka, Y., Kimura, M., Moriyama, A., Kubo, Y., Sambe, M., Uchiyama, J., Ohta, H.**, in *Photosynthesis Research for Food, Fuel and the Future*. (Springer Berlin Heidelberg), pp. 593-595. 10.1007/978-3-642-32034-7_128

132. **Thomas, R. H., Walsby, A. E.**, (1985) Buoyancy Regulation in a Strain of Microcystis. *Microbiology* **131**, 799-809; doi:10.1099/00221287-131-4-799

133. **Tillett, D., Dittmann, E., Erhard, M., von Dohren, H., Borner, T., Neilan, B. A.**, (2000) Structural organization of microcystin biosynthesis in Microcystis aeruginosa PCC7806: an integrated peptide-polyketide synthetase system. *Chem Biol* **7**, 753-764; S1074-5521(00)00021-1 [pii]

134. **Tuominen, I., Pollari, M., Tyystjarvi, E., Tyystjarvi, T.**, (2006) The SigB sigma factor mediates high-temperature responses in the cyanobacterium Synechocystis sp. PCC6803. *FEBS Lett* **580**, 319-323; S0014-5793(05)01471-7 [pii] 10.1016/j.febslet.2005.11.082

135. **Untergasser, A., Cutcutache, I., Koressaar, T., Ye, J., Faircloth, B. C., Remm, M., Rozen, S. G.**, (2012) Primer3--new capabilities and interfaces. *Nucleic Acids Res* **40**, e115; gks596 [pii] 10.1093/nar/gks596

136. **Van de Waal, D. B., Verspagen, J. M., Finke, J. F., Vournazou, V., Immers, A. K., Kardinaal, W. E., Tonk, L., Becker, S., Van Donk, E., Visser, P. M., Huisman, J.**, (2011) Reversal in competitive dominance of a toxic versus non-toxic cyanobacterium in response to rising CO2. *ISME J* **5**, 1438-1450; ismej201128 [pii] 10.1038/ismej.2011.28

137. **Vermaas, W. F. J.**, in *eLS*. (John Wiley & Sons, Ltd, 2001). 10.1038/npg.els.0001670

138. **Via-Ordorika, L., Fastner, J., Kurmayer, R., Hisbergues, M., Dittmann, E., Komarek, J., Erhard, M., Chorus, I.**, (2004) Distribution of microcystin-producing and non-microcystin-producing Microcystis sp. in European freshwater bodies: detection of microcystins and microcystin genes in individual colonies. *Syst Appl Microbiol* **27**, 592-602; S0723-2020(05)70298-8 [pii] 10.1078/07232020041748163

139. **Visser, P., Passarge, J., Mur, L.**, (1997) Modelling vertical migration of the cyanobacterium Microcystis. *Hydrobiologia* **349**, 99-109; 10.1023/a:1003001713560

140. **Walsby, A. E.**, (1972) Gas-filled structures providing buoyancy in photosynthetic organisms. *Symp Soc Exp Biol* **26**, 233-250;

141. **Wang, Y. W., Zhao, J., Li, J. H., Li, S. S., Zhang, L. H., Wu, M.**, (2010) Effects of calcium levels on colonial aggregation and buoyancy of Microcystis aeruginosa. *Curr Microbiol* **62**, 679-683; 10.1007/s00284-010-9762-7

142. **Weber, T., Blin, K., Duddela, S., Krug, D., Kim, H. U., Bruccoleri, R., Lee, S. Y., Fischbach, M. A., Muller, R., Wohlleben, W., Breitling, R., Takano, E., Medema, M. H.**, (2015) antiSMASH 3.0-a comprehensive resource for the genome mining of biosynthetic gene clusters. *Nucleic Acids Res* **43**, W237-243; gkv437 [pii] 10.1093/nar/gkv437

143. **Weiz, A. R., Ishida, K., Makower, K., Ziemert, N., Hertweck, C., Dittmann, E.**, (2011) Leader peptide and a membrane protein scaffold guide the biosynthesis of the tricyclic peptide microviridin. *Chem Biol* **18**, 1413-1421; S1074-5521(11)00352-8 [pii] 10.1016/j.chembiol.2011.09.011

144. **Welker, M., Brunke, M., Preussel, K., Lippert, I., von Dohren, H.**, (2004) Diversity and distribution of Microcystis (Cyanobacteria) oligopeptide chemotypes from natural communities studied by single-colony mass spectrometry. *Microbiology* **150**, 1785-1796; 10.1099/mic.0.26947-0

150/6/1785 [pii]

145. **Welker, M., von Dohren, H.**, (2006) Cyanobacterial peptides - nature's own combinatorial biosynthesis. *FEMS Microbiol Rev* **30**, 530-563; FMR022 [pii] 10.1111/j.1574-6976.2006.00022.x

146. **Werz, D. B., Ranzinger, R., Herget, S., Adibekian, A., von der Lieth, C. W., Seeberger, P. H.**, (2007) Exploring the structural diversity of mammalian carbohydrates ("glycospace") by statistical databank analysis. *ACS Chem Biol* **2**, 685-691; 10.1021/cb700178s

147. **Whitton, B., Potts, M., Vincent, W.**, in *The Ecology of Cyanobacteria*. (Springer Netherlands, 2002), pp. 321-340. 10.1007/0-306-46855-7_12

148. **Wiedner, C., Visser, P. M., Fastner, J., Metcalf, J. S., Codd, G. A., Mur, L. R.**, (2003) Effects of light on the microcystin content of Microcystis strain PCC 7806. *Appl Environ Microbiol* **69**, 1475-1481;

149. **Wilhelm, S. W., Boyer, G. L.**, (2011) Ecology: Healthy competition. *Nature Clim. Change* **1**, 300-301;

150. **Woodhouse, J. N., Kinsela, A. S., Collins, R. N., Bowling, L. C., Honeyman, G. L., Holliday, J. K., Neilan, B. A.**, (2015) Microbial communities reflect temporal changes in cyanobacterial composition in a shallow ephemeral freshwater lake. *ISME J*, ismej2015218 [pii] 10.1038/ismej.2015.218

151. **Xu, H., Jiang, H., Yu, G., Yang, L.**, (2014) Towards understanding the role of extracellular polymeric substances in cyanobacterial Microcystis aggregation and mucilaginous bloom formation. *Chemosphere* **117**, 815-822; S0045-6535(14)01246-6 [pii] 10.1016/j.chemosphere.2014.10.061

152. **Xu, H., Paerl, H. W., Qin, B., Zhu, G., Gaoa, G.**, (2010) Nitrogen and phosphorus inputs control phytoplankton growth in eutrophic Lake Taihu, China. *Limnology and Oceanography* **55**, 420-432; 10.4319/lo.2010.55.1.0420

153. **Yang, J. Y., Phelan, V. V., Simkovsky, R., Watrous, J. D., Trial, R. M., Fleming, T. C., Wenter, R., Moore, B. S., Golden, S. S., Pogliano, K., Dorrestein, P. C.**, (2012) Primer on agar-based microbial imaging mass spectrometry. *J Bacteriol* **194**, 6023-6028; JB.00823-12 [pii] 10.1128/JB.00823-12

154. **Yang, Z., Kong, F., Shi, X., Zhang, M., Xing, P., Cao, H.**, (2008) CHANGES IN THE MORPHOLOGY AND POLYSACCHARIDE CONTENT OF MICROCYSTIS AERUGINOSA (CYANOBACTERIA) DURING FLAGELLATE GRAZING1. *Journal of Phycology* **44**, 716-720; 10.1111/j.1529-8817.2008.00502.x

155. **Yoshida, T., Makita, Y., Nagata, S., Tsutsumi, T., Yoshida, F., Sekijima, M., Tamura, S., Ueno, Y.**, (1997) Acute oral toxicity of microcystin-LR, a cyanobacterial hepatotoxin, in mice. *Nat Toxins* **5**, 91-95; 10.1002/1522-7189(1997)5:3<91::AID-NT1>3.0.CO;2-H

156. **Zhai, C., Zhang, P., Shen, F., Zhou, C., Liu, C.**, (2012) Does Microcystis aeruginosa have quorum sensing? *FEMS Microbiol Lett* **336**, 38-44; 10.1111/j.1574-6968.2012.02650.x

157. **Zhang, J., Kobert, K., Flouri, T., Stamatakis, A.**, (2014) PEAR: a fast and accurate Illumina Paired-End reAd mergeR. *Bioinformatics* **30**, 614-620; btt593 [pii]
10.1093/bioinformatics/btt593

158. **Zhu, H., Ren, X., Wang, J., Song, Z., Shi, M., Qiao, J., Tian, X., Liu, J., Chen, L., Zhang, W.**, Integrated OMICS guided engineering of biofuel butanol-tolerance in photosynthetic Synechocystis sp. PCC 6803. *Biotechnol Biofuels* **6**, 106; 1754-6834-6-106 [pii]
10.1186/1754-6834-6-106

159. **Zilliges, Y., Kehr, J. C., Meissner, S., Ishida, K., Mikkat, S., Hagemann, M., Kaplan, A., Borner, T., Dittmann, E.**, (2011) The cyanobacterial hepatotoxin microcystin binds to proteins and increases the fitness of microcystis under oxidative stress conditions. *PLoS One* **6**, e17615; 10.1371/journal.pone.0017615

160. **Zilliges, Y., Kehr, J. C., Mikkat, S., Bouchier, C., de Marsac, N. T., Borner, T., Dittmann, E.**, (2008) An extracellular glycoprotein is implicated in cell-cell contacts in the toxic cyanobacterium Microcystis aeruginosa PCC 7806. *J Bacteriol* **190**, 2871-2879; JB.01867-07 [pii]
10.1128/JB.01867-07

161. **Zou, H., Pan, G., Chen, H., Yuan, X.**, (2006) Removal of cyanobacterial blooms in Taihu Lake using local soils. II. Effective removal of Microcystis aeruginosa using local soils and sediments modified by chitosan. *Environ Pollut* **141**, 201-205; S0269-7491(05)00446-X [pii]
10.1016/j.envpol.2005.08.042

6 Acknowledgements

Many people have contributed to this study and provided great support. First and foremost, Elke Dittmann has provided scientific guidance, optimism and creativity, has opened opportunities, chances and the scientific world.

During several cooperations I have encountered supporting people who took the time for teaching and who provided their invaluable knowhow. Hans Matthijs, Merijn Schuurmans, and Wim Ensink have introduced me into the world of microarrays, and haven given me a friendly welcome in Amsterdam.

Detlef Groth's support and teaching in questions of bioinformatics and statistics created the groundwork for this study. Eric Helfrich has enthusiastically carried out MALDI imaging experiments at the ETH Zurich and supplied his great expertise. I also thank Fabian Horn from the GFZ Potsdam for his professional analysis of acquired microbiome data.

A big thanks goes to the Neilan-Lab in Sydney and all lab members who warmly welcomed me and shared their knowledge, equipment and, most of all, their time with me.

This thesis has grown and evolved through the help, the input and new perspective after proofreading. Thanks for your priceless help: Sven, Sarah, Jason, and Jenny.

Starting this paragraph brings a smile to my face, because the thankyou to my lab buddies from the whole Dittmann-Group makes me remember the help, time, laughter, friendship, parties, cakes, mensa-mensa-mensa, and inspiration in any aspect of life (Annika, Anne, Arthur, Chen-Lin, Douglas, Emmanuel, Eva, Jan, Katrin, Niklas, Sabine, Sandra, Sophie, Sven)

The following people shall be thanked for being the rocks and eternal loves of my private life: Mom and Dad, the Hallelujahs Toni, Cindy, Jenny and many more, whose friendship makes each and every one of my days.

7 Appendix

7.1 Datasets

Data-set 1: File: "data-set 1_PCC7806_All_probes_indexfile"

Detailed Information on hybridization probes used in PCC 7806-specific microarrays

Data-set 2: File: "data-set 2_FS2-related_microarray_data"

Expression values, log2-foldchenges, and p-values obtained from microarrays with related gene information regarding comparisons between the *Microcystis ΔmcyB* mutant and the wild type PCC 7806 and externally applied microcystin-LR

Data-set 3: File: "data-set 3_microcystin-related_microarray_data"

Expression values, log2-foldchenges, and p-values obtained from microarrays with related gene information regarding comparisons between FS2-exudate treated and control samples of PCC 7806, as well as MC-treated FS2 materials, and FS2-DNA hybridization data

Data-set 4: File: "data-set 4_mcyB-mutant_DNA_hybridization_check"

Microarray data from DNA DNA hybridization of the *ΔmcyB* mutan, listing deviations between *ΔmcyB* and PCC 7806

Data-set 5: File: "data-set 5_microbiome_FS2"

OTU counts and taxonomic composition of the bacterial community in the Culture of Microcystis sp. FS2

7.2 List of figures

7.3 List of Tables

7.4 Publications

1) (Weiz, *et al.*, 2011)

   Weiz, A. R., Ishida, K., Makower, K., Ziemert, N., Hertweck, C., Dittmann, E., (2011) Leader peptide and a membrane protein scaffold guide the biosynthesis of the tricyclic peptide microviridin. *Chem Biol* **18**, 1413-1421; S1074-5521(11)00352-8 [pii]

2) (Makower, *et al.*, 2014)

   Makower, A. K., Schuurmans, J. M., Groth, D., Zilliges, Y., Matthijs, H. C., Dittmann, E., (2014) Transcriptomics-aided dissection of the intracellular and extracellular roles of microcystin in Microcystis aeruginosa PCC 7806. *Appl Environ Microbiol* **81**, 544-554; AEM.02601-14 [pii]

3) (D'Agostino, *et al.*, 2015)

   D'Agostino, P. M., Woodhouse, J. N., Makower, A. K., Yeung, A. C., Ongley, S. E., Micallef, M. L., Moffitt, M. C., Neilan, B. A., (2015) Advances in genomics, transcriptomics and proteomics of toxin-producing cyanobacteria. *Environ Microbiol Rep*, 10.1111/1758-2229.12366

4) A manuscript titled “Multifaceted Interactions between a toxic and a non-toxic Microcystis strain” is shortly to be submitted.

5) Other:

   Audio contribution to DLF radio report on cyanobacterial toxins: http://bit.ly/1KOekVR

6) Contributions in Conferences:

Date	Conference	Contribution
2016	**ISPP** 15th International Symposium on Phototrophic Prokaryotes	Poster presentation: *"The* Microcystis *Network - Multifaceted roles of intercellular communication in* Microcystis*"*
2014	**VAAM workshop** *"Biology of natural products-producing microorganisms"*	Talk: *"Transcriptomic Dissection of the Intracellular and the Extracellular role of Microcystin in* M. aeruginosa *PCC 7806"*
2013	**ESF-EMBO Symposium** *"Molecular Bioenergetics Of Cyanobacteria: Shaping The Environment"*	Poster presentation: *"Communication and Heterogeneity among* Microcystis *colonies"*
2011	8th European Workshop on Molecular Biology of Cyanobacteria	Poster presentation: *"Understanding* Microcystis *Colony Formation Regarding Molecular and Ecological Aspects"*
2011	**ESF-EMBO Symposium** *Molecular Bioenergetics of Cyanobacteria: From Cell to Community*	Poster presentation: *"Secondary Metabolite Expression-Regulatory Aspects of the Depsipeptide Microviridin"*